3225
6-19-62

MASTER

ORNL-3290
UC-10 – Chemical Separations Processes
for Plutonium and Uranium
TID-4500 (17th ed.)

TRANSURANIUM QUARTERLY PROGRESS REPORT FOR PERIOD ENDING FEBRUARY 28, 1962

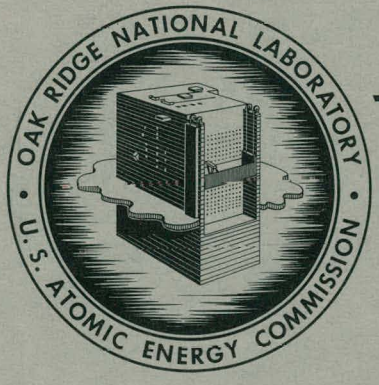

OAK RIDGE NATIONAL LABORATORY
operated by
UNION CARBIDE CORPORATION
for the
U.S. ATOMIC ENERGY COMMISSION

DISCLAIMER

Printed in USA. Price $2.00 Available from the

Office of Technical Services
U. S. Department of Commerce
Washington 25, D. C.

ORNL-3290

Contract No. W-7405-eng-26

CHEMICAL TECHNOLOGY DIVISION
METALS AND CERAMICS DIVISION
ENGINEERING AND MAINTENANCE DIVISION
REACTOR CHEMISTRY DIVISION
PLANT ENGINEERING, ORGDP

TRANSURANIUM QUARTERLY PROGRESS REPORT FOR PERIOD ENDING FEBRUARY 28, 1962

Compiled by
D. E. Ferguson

DATE ISSUED

JUN 13 1962

OAK RIDGE NATIONAL LABORATORY
Oak Ridge, Tennessee
operated by
UNION CARBIDE CORPORATION
for the
U.S. ATOMIC ENERGY COMMISSION

1.0 ABSTRACT

The development of separation processes for the transuranium elements, process equipment development, HFIR target fabrication development, design of the TRU facility, design of development facilities, corrosion studies, analytical research and development, and the preparation of U-232 samples for research are reported here. Work done by the Chemical Technology, Metallurgy, Engineering and Maintenance, and Reactor Chemistry Divisions of Oak Ridge National Laboratory and Design Group at Oak Ridge Gaseous Diffusion Plant in the Transuranium Element Processing Program is included.

Process Development. The aluminum in HFIR targets will be transmuted to silicon at the rate of 2% per year. The rate of dissolution of aluminum in HCl solution was proportional to the cube of the HCl concentration, doubled for every 8-9°C rise in temperature, and was inversely proportional to the silicon content in the range 0.1 to 3% silicon.

The tertiary amine solvent extraction process for separating the transuranium elements from the lanthanides was successfully tested on a laboratory scale. In a batch countercurrent test, americium recovery was >99%, with a decontamination factor of $>10^4$ from rare earths. Of the other expected contaminants, only Ti^{4+} followed the transuranium elements through the process. Separation of americium and curium from the transcurium elements by 2-ethylhexylphenylphosphonic acid was also demonstrated on a laboratory scale, with a californium recovery of >99% and <0.1% of the americium carried along in a seven-stage countercurrent extraction.

An anion exchange process for recovering americium and curium from plutonium process waste was developed and successfully tested on a laboratory scale. The americium, curium, and rare earth fission products are sorbed on an anion exchange resin from 2.3 M $Al(NO_3)_3$, eluted with dilute HNO_3, converted to a chloride solution by extracting the nitrate with a tertiary amine after addition of LiCl, and isolation of the americium and curium by amine extraction. The overall recovery of americium was >99%, with less than 0.1% of rare earths following the product.

Remote piping disconnects made by an area seal leaked less than 10^{-8} cc/sec of helium after 10 makes and breaks. Small misalignments and marks in the seating area did not cause excess leakage. A mixer-settler was adapted to permit the use of very low flow rates and phases with small density differences. The change consisted in adding submerged weirs between the settlers and mixers to prevent solvent back-mixing. An improved mixing impeller was demonstrated, and a pressurized-water fire-extinguishing system for solvent fires in gloveboxes was devised and successfully tested.

HFIR Target Fabrication Process Development. Blending of actinide oxide and

aluminum powder for pressing into pellets was successfully demonstrated with small rods in the blending vessel to prevent agglomeration. Pellets with pressed densities 91% of theoretical were obtained at 33 tsi. In tests of end-closure tube welding, direct current-fusion welding of a butt-joint design appeared satisfactory, although there were areas of nonfusion in the leaktight welds. Tube collapse onto the pellets could be obtained at an isostatic pressure of about 13,000 psi, but intimate contact between tube and pellets at all points was not obtained in these initial tests. Preliminary studies indicated that radiography could be used to inspect the end-closure welds. The remotely operable fabrication equipment for the TRU facility is being designed and some items are being fabricated or bought for future testing.

Transuranium Facility Design. Conceptual design of the TRU facility by Catalytic Construction Company is complete and Title I design is in progress. Process design studies were made on HFIR target dissolution, the solvent extraction steps, and the preparation of actinide oxides. Conceptual design of process equipment and in-cell layouts were largely completed, and equipment flowsheets and processing schedules were developed. Shielding calculations indicated that 54 in. of magnetite concrete satisfies the dose rate criteria. Experiments with shielding window configurations indicated that an oil-glass laminated window would match the 54 in. of concrete. Maximum permissible concentrations of the various transuranium nuclides were calculated and the hazards evaluated. Conceptual design of the development facilities to be installed in cells 3 and 4 of Bldg. 4507 was completed, and detailed design and procurement were initiated.

Corrosion Studies. In exploratory corrosion tests to select materials of construction for handling chloride solutions in the TRU facility, six potential materials were selected: Hastelloys B and C, niobium, tantalum, titanium, and Zircaloy-2. The results of subsequent tests eliminated Hastelloy B and titanium and indicated a possible hydrogen embrittlement problem with tantalum and niobium and severe corrosion of Hastelloy C in heat-effect zones. Heat-treated Hastelloy C appeared satisfactory for most components, but either tantalum or Zircaloy-2 must be used in some corrosive situations. The effect of alpha activity at the level of 2 watts/liter on corrosion of the above materials in chloride solutions was determined to be the same as that produced by H_2O_2 addition.

Analytical Radiochemical Methods Development. Eight radiochemical methods were developed and tested. All use alpha counting as the basic measurement. Preliminary work indicates that the method of Peppard can be adapted for berkelium determination.

Uranium-232 Preparation. Process flowsheets for isolating U-232 from irradiated Pa-231 were tested and successfully demonstrated by isolating 5 mg of U-232 from 8 g of irradiated Pa-231. Final purification methods for the U-232 were developed and tested.

CONTENTS

2.0 INTRODUCTION

Gram quantities of transuranium elements for research uses are to be produced in the High Flux Isotope Reactor, HFIR, and Transuranium Processing Facility, TRU, being built at Oak Ridge National Laboratory. Production of these elements in quantity will simplify research with them and make it possible to enlarge our knowledge of their chemistry, the solid state physics, and metallurgy. Target material will be provided for production of still heavier and unknown elements.

Isotopes of curium, berkelium, californium, einsteinium, and fermium will result from irradiation in the HFIR of Pu-242 and of a mixture of Am-242 with Cm-244. These feed materials are being produced by long-term irradiation of 10-kg batches of Pu-239 in a Savannah River reactor. The irradiated Pu-239 will be processed at Savannah River to recover the Pu-242 as decontaminated PuO_2 and the americium-curium as a solution containing about 3 kg of rare earth fission products. The rare earths will be removed from the americium-curium and the actinide oxides fabricated into HFIR targets in the TRU Facility. Also in the TRU Facility the irradiated HFIR targets will be processed to recover the heavy elements for research uses and the recovered curium isotopes will be refabricated into HFIR targets.

3.0 PROCESS DEVELOPMENT

3.1 Chemical Development (R. E. Leuze, R. D. Baybarz, M. H. Lloyd)

Methods for recovering transuranium elements from irradiated HFIR targets and for recovering americium and curium from plutonium process waste are being developed. Aluminum-silicon dissolution in hydrochloric acid, actinide-lanthanide separation by tertiary amine extraction, californium-americium separation by phosphonate extraction, americium-curium-rare earth concentration from nitrate waste by anion exchange, and conversion from nitrate to chloride by amine extraction have been studied.

Aluminum-Silicon Alloy Dissolution in Hydrochloric Acid. When aluminum is irradiated in a nuclear reactor, some of the aluminum is converted to silicon. It was calculated that approximately 3% of the aluminum in HFIR targets will be converted to silicon during an 18-month irradiation. Since the proposed process calls for target dissolution in hydrochloric acid, the effect of the silicon content on the dissolution rate is being studied. Preliminary investigation into the hydrochloric acid dissolution of aluminum alloys containing various amounts of silicon have been made with three alloys: X-8001 containing ~0.1% Si, an 1100 series alloy containing ~0.3% Si, and a specially prepared alloy containing 97% Al and 3% Si.

In the hydrochloric acid concentration range 1-6 M, the dissolution rate of all three alloys was proportional to the cube of the acid concentration (Fig. 3.1a). For a given acidity, the dissolution rate was inversely proportional to the silicon content of the alloy. The dissolution rate of the 1100 series alloy, which contains ~0.3% Si, was approximately 10 times that of aluminum containing 3% Si, and the dissolution rate of X-8001 aluminum, which contains ~0.1% Si, was about 4 times that of the 1100 series aluminum. The dissolution rate of 97% Al-3% Si alloy in 6 M HCl in the temperature range 25-70°C doubled for every 8-9°C increase in temperature (Fig. 3.1b).

Separation of Transuranium Elements from Rare Earths by Tertiary Amine Extraction. A tertiary amine solvent extraction system for separating the transuranium elements from the lanthanides was developed and tested on a laboratory scale (1). Extraction of the transuranium elements with tertiary amines from concentrated LiCl solutions gives a separation factor of about 100. After dissolution of HFIR targets in hydrochloric acid, feed for the amine extraction step can be prepared by adding LiCl and distilling off the excess acid.

The transuranium elements are extracted from 11 M LiCl containing only a trace of acid by Alamine 336 (a mixture of octyl and decyl tertiary amines) diluted

---

(1) R. D. Baybarz and Boyd Weaver, "Separation of Transplutoniums from Lanthanides by Tertiary Amine Extraction," ORNL-3185, Dec. 4, 1961.

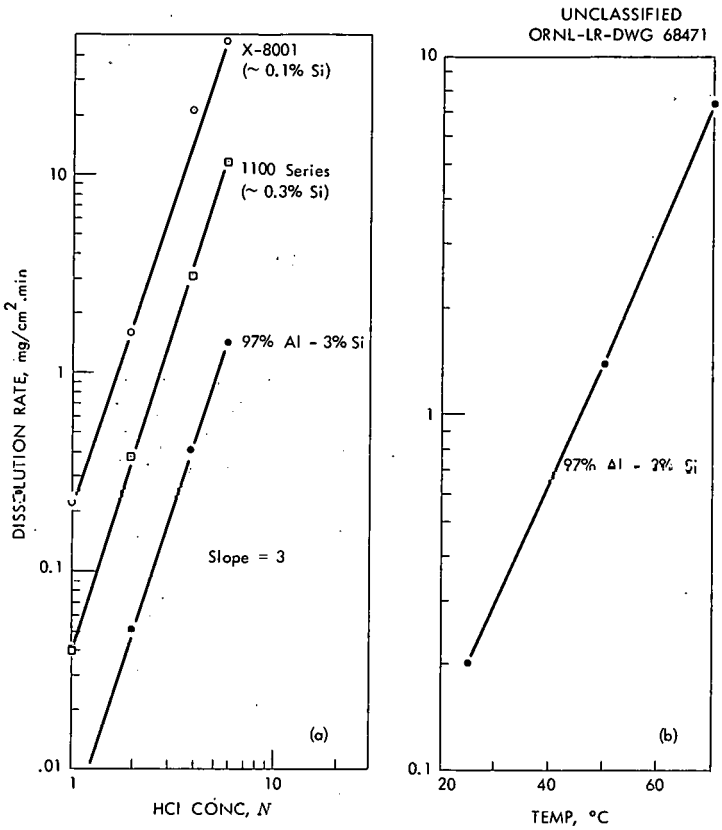

Fig. 3.1. Effect of (a) acid concentration at 50°C and (b) temperature with 6 *M* HCl on rate of dissolution of aluminum alloys in hydrochloric acid.

with diethyl benzene (Fig. 3.2). The scrub solution is 11 M LiCl-0.02 M HCl, and the uranium elements are stripped with 5 M HCl. In laboratory-scale tests, with 6 scrub and 6 extraction stages americium recovery was 99.99% with a decontamination factor from rare earths of $>10^4$. Difficulties were encountered in slow phase separation and slow approach to equilibrium.

The relative extraction positions of the individual elements of both groups, normalized to curium, are shown in Fig. 3.3 for the tertiary amine chloride in hydrocarbon diluent vs 11 M LiCl. In this system the order of extractability of the transuranium elements is Cf > Bk > Am $\geq$ Cm and Cf > Fm > Es, with Cm the least extractable. The lanthanide group is much less extractable than the transuranium elements, but the differences between elements within the group are small. Of the lanthanides tested, europium is the most extractable. The separation factor between the least extractable transplutonium, curium, and the most extractable lanthanide, europium, is of the order of 100. Over the ranges studied, the extraction coefficients of elements of both groups were dependent directly on the 17th power of the LiCl concentration, inversely on the 1.5 power of the acid concentration, and directly on the square of the amine concentration. Contaminant ions that were extracted with the transuranium elements were Cd^{2+}, Hg^{2+}, Pd^{2+}, Fe^{3+}, Co^{2+}, Mn^{2+}, Ti^{4+}, Cu^{2+}, Sn^{4+}, Sn^{2+}, Zr^{4+}, and Ru^{3+} (2). Of the elements extracted, only Ti^{4+} will be

(2) R. D. Baybarz and H. B. Kinser, "Separation of Transplutoniums from Lanthanides by Tertiary Amine Extraction. II. Contaminant Ions," ORNL-3244, Feb. 20, 1962.

stripped with the transuranium elements by 5 M HCl. The remaining contaminants will stay in the organic phase.

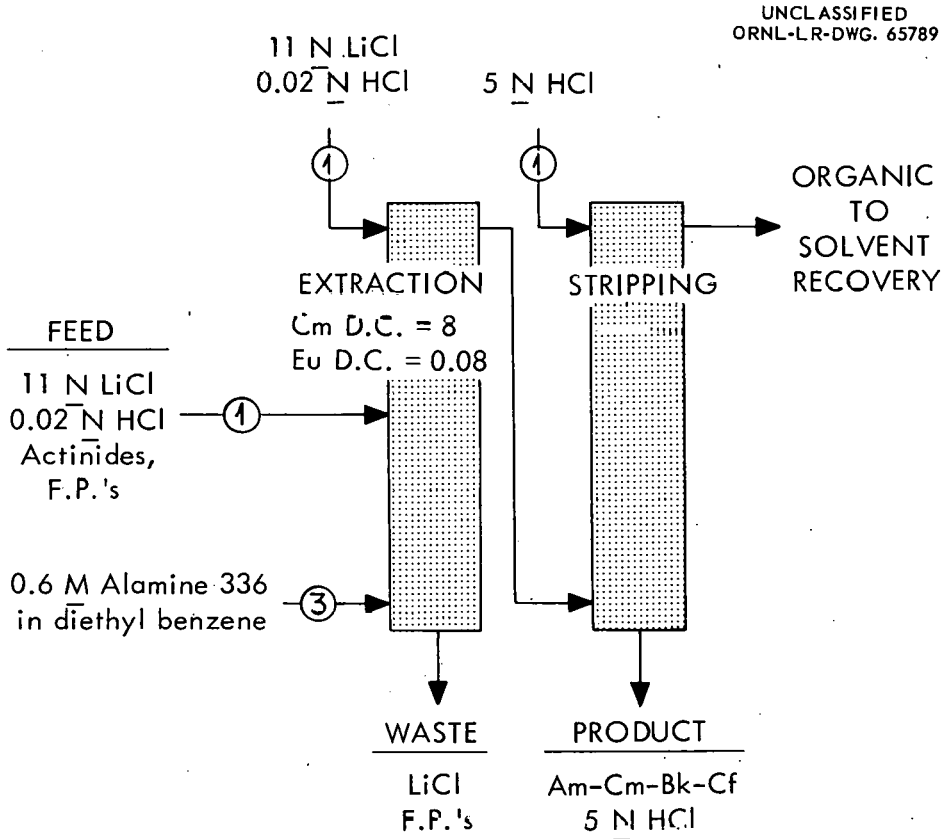

Fig. 3.2. Actinide-lanthanide separation flowsheet.

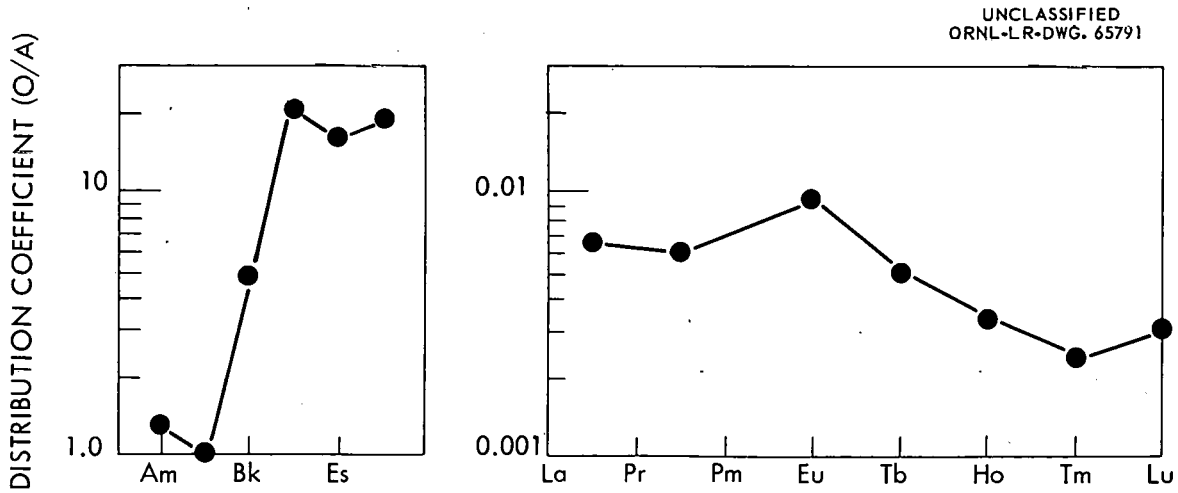

Fig. 3.3. Relative extractability of actinides and lanthanides.

Separation of Transuranium Elements by Phosphonate Extraction. When irradiated HFIR targets are processed, the product from the tertiary amine extraction will contain americium, curium, berkelium, einsteinium, and fermium in dilute hydrochloric acid. In a solvent extraction process for separating berkelium, californium, and einsteinium from americium and curium developed and tested on a laboratory scale (3), the solvent, 2-ethylhexylphenylphosphonic acid (2-EH(ØP)A) in diethyl benzene (DEB), extracts the heavier transuranium elements from 1.25 M HCl. The separation factor between californium and curium is 100 (4).

The transcurium elements are extracted by 1.0 M 2-EH(ØP)A in DEB. The feed solution is 1 M HCl (Fig. 3.4) and the scrub solution 1.5 M HCl, and the extracted transcurium elements are stripped with 4 M HCl. In a 7-stage countercurrent extraction, californium was 99.9% recovered, with an americium removal of >99.9%, giving an overall separation factor of 10^6. The conditions were: feed 1.4 M HCl; scrub 1.8 M HCl; extractant 1.0 M 2-EH(ØP)A in DEB with a flow ratio of 1/1/2. Under the conditions used in this test berkelium would remain with the americium-curium. In the flowsheet recommended above the berkelium will follow the californium. In this system the extractability of the transuranium elements increases

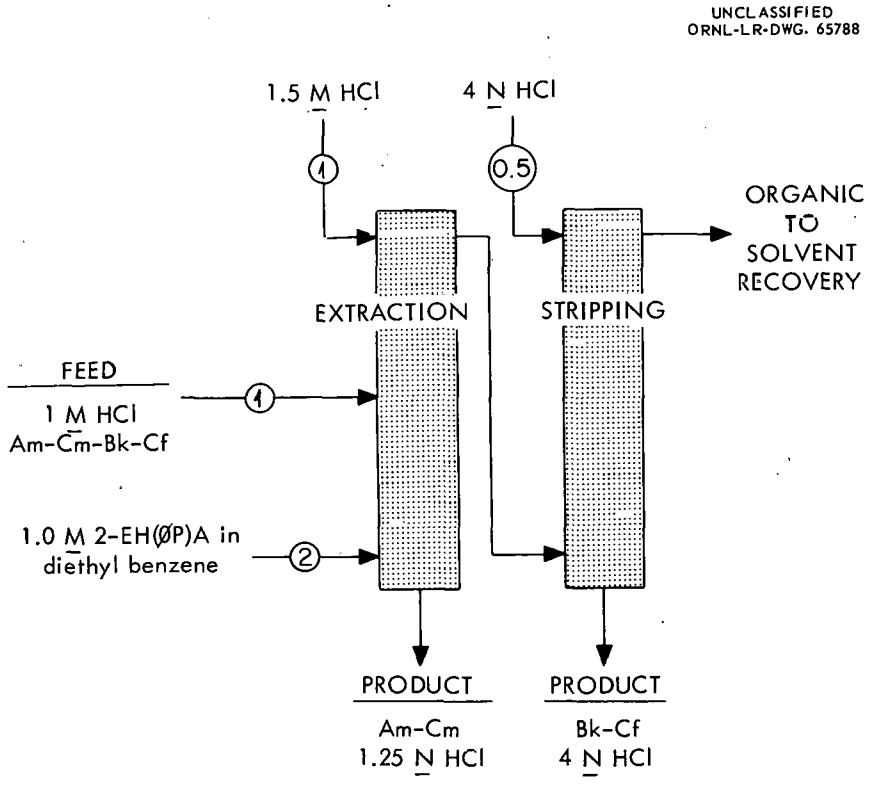

Fig. 3.4. Transuranium element separation flowsheet.

(3) R. D. Baybarz, "Separation of Transplutonium Elements by Phosphonate Extraction," ORNL-3273, in press.

with increasing number (Fig. 3.5) but not with an orderly progression as with the lanthanides (4) where the separation factor between adjacent rare earths is 2.5.

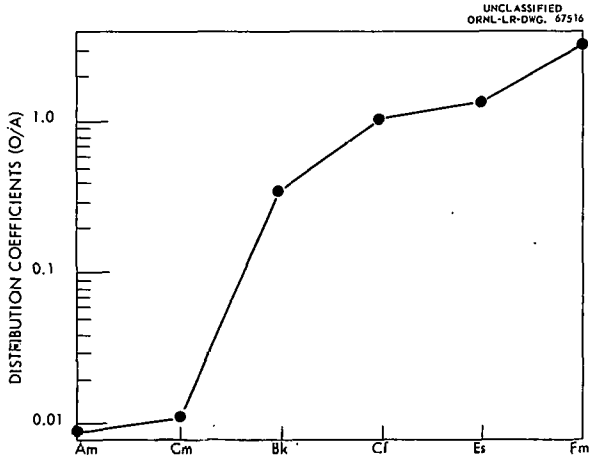

Fig. 3.5. Relative extractability of transuranium elements from 2 N HCl by 1.0 M 2-EH(ØP)A in diethyl benzene.

The separation factors between adjacent transuranium elements were: Cm/Am = 1.4; Bk/Cm = 30; Cf/Bk = 3.3; Es/Cf = 1.3; and Fm/Es = 2.5. The extraction coefficients of the transuranium elements were dependent inversely on the cube of the hydrogen ion concentration and directly on the cube of the phosphonic acid concentration in the solvent. The extractability also depended on the acid used, in the order $HClO_4 > HCl > HNO_3$. Contaminant ions extracted with californium were Zr^{4+}, Ti^{3+}, Fe^{3+}, Sn^{2+}, MoO_4^{2-}, UO_2^{2+}, and Pu^{4+}. Of these, Zr^{4+}, MoO_4^{2-}, UO_2^{2+}, and Pu^{4+} remained in the solvent while Ti^{3+}, Fe^{3+}, and Sn^{2+} followed the californium in stripping. The elements that were not extracted were Sr^{2+}, Ru^{3+}, Fe^{2+}, Cu^{2+}, Zn^{2+}, Al^{3+}, Cd^{2+}, Ni^{2+}, Cr^{3+}, Co^{3+}, and Mn^{2+}.

Americium-Curium Recovery. Americium and curium in plutonium process waste can be recovered by sorbing the americium-curium and rare earth fission products on anion exchange resin from 2.3 M $Al(NO_3)_3$ and eluting with dilute HNO_3, converting the eluate to chloride solution by extracting the HNO_3 into a tertiary amine from mixed HCl-HNO_3, and selectively extracting the americium-curium into tertiary amine from 11 M LiCl-0.02 M HCl. Highly irradiated plutonium-aluminum alloy will be processed in cell 1 of Bldg. 4507 for recovery of plutonium and preparation of a nitrate solution concentrate of americium-curium-rare earths. The concentrate will be processed in cell 4 for isolation of the americium-curium.

The anion exchange step (Fig. 3.6) has been developed and tested on a laboratory scale (5). Acid-free aluminum nitrate feed is prepared by heating the plutonium

(4) D. F. Peppard, G. W. Mason, I. Hacher, "Acidic Esters of Phosphonic Acid as Selective Extractants for Metallic Cations: Selected M(III) Tracer Studies," J. Inorg. Nucl. Chem. 18: 245 (1961).

(5) M. H. Lloyd, "Anion Exchange Recovery of Americium and Curium from Plutonium Process Waste," ORNL-3291, to be issued.

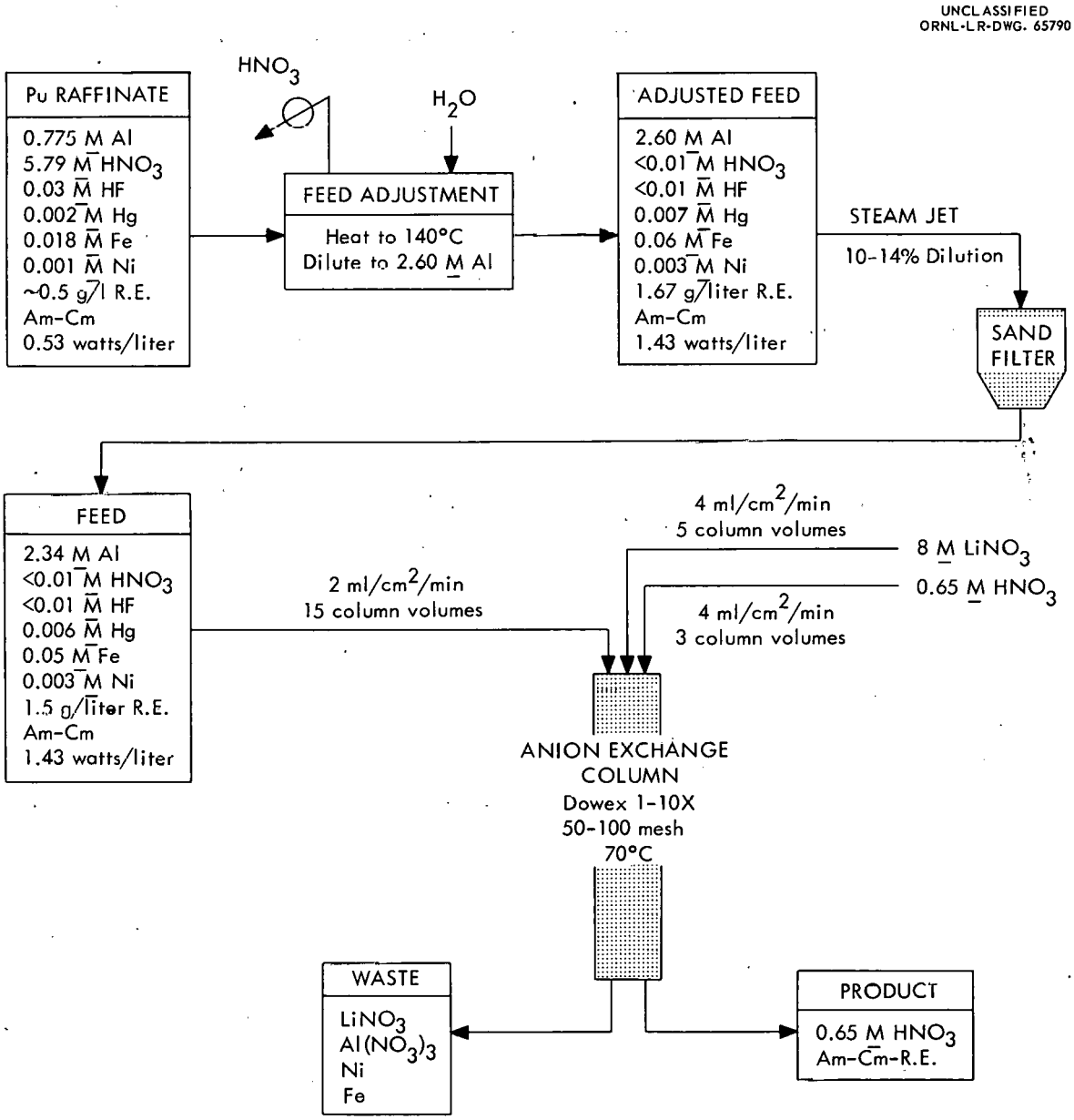

Fig. 3.6. Flowsheet for recovery of americium and curium from plutonium process waste.

raffinate to 140°C and then diluting with water to an aluminum concentration of 2.6 M. The solution will be transferred by a steam jet, which results in a minimum feed dilution, 10%. Fifteen column displacement volumes of feed are pumped through the column, which is packed with 50-100 mesh Dowex 1-10X resin at 70°C. Aluminum and iron are washed from the column with 5 column volumes of 8 M $LiNO_3$, and the product is eluted with 3 column volumes of 0.65 M HNO_3. In laboratory demonstrations, products containing 8.5 g of rare earths per liter were obtained in which the aluminum concentration was decreased from 3.34 M to 0.05 M. No americium losses were detectable and decontamination from iron was essentially complete.

The effects on sorption of resin particle size, feed flow rates, aluminum concentration, resin cross linkage, and temperature were investigated. Americium losses with 27 column volumes of feed and Dowex 1-10X resin were <1% for 50-100 mesh resin, 2.3% for 50-60 mesh, and 35% for 10-50 mesh. Decreasing the resin cross linkage from 10% to 4% increased americium losses from 0.9% to 11.21% for 27 column volumes of feed. In experiments with europium tracer, losses increased from 0.1% to 23% for 15 column volumes of feed when the flow rate was increased from 2 to 4 $ml/cm^2/min$; and were of the order of 0.12, 0.27, 2.2, and 16.2% when aluminum feed concentrations were 2.7, 2.3, 2.0, and 1.8 M, respectively. Column temperature does not appear to be critical; results were satisfactory in the temperature range 60-85°C. Results with coarse Permutit SK resin were comparable to those with Dowex 1-10X; fine mesh Permutit was not available for comparison.

The chemical flowsheet for processing the americium-curium concentrate is being tested in laboratory-scale experiments with synthetic solutions containing tracers. The nitrate removal step was demonstrated with a synthetic feed containing 1 M HNO_3, 4 M HCl, 5 g/liter rare earths, and 0.5 g/liter ruthenium with Ru^{106} and Am^{241} tracers. The feed was contacted with 2.5 vol of 0.6 M Alamine 336 in DEB. The 16-stage mixer-settler was operated as an extraction section only and no scrub was used. Most of the nitrate and ruthenium were extracted. The aqueous product contained 99.95% of the americium, <10% of the ruthenium, and <0.01 M HNO_3.

Product from the nitrate removal step was converted to 11.4 M LiCl containing only 0.005 M HCl by adding LiCl and evaporating to a pot temperature of 135°C, and was adjusted to 11 M LiCl-0.01 M HCl. Americium was extracted from this feed with 0.67 M Alamine 336 hydrochloride in DEB, and rare earths were scrubbed from the extract with 9 M LiCl-0.33 M $AlCl_3$. Extraction conditions were 8 scrub and 8 extraction mechanical stages at a temperature of 50-55°C. Flow rates for the scrub, feed, and extractant were 5, 5, and 10 ml/min, respectively. Stage efficiencies were only about 50% because of back-mixing. The extracted product contained 99.9% of the americium and <0.1% of the rare earths. Americium was stripped from the solvent with 5 M HCl. Overall americium recovery was >99.8%.

3.2 Process Equipment Development (P. A. Haas, A. D. Ryon, F. L. Daley, T. S. Mackey)

Disconnects. In tests to select a disconnect design for use in the TRU processing cells, an area seal between a female half of 20° included angle and a male half of 18° angle appeared superior to the line contact seal obtained with lower seating forces. The area seals leaked less than 10^{-8} cc of helium per second after 10 makes and breaks. Leak-tight closures were also obtained for interchanged halves, for up to 0.5° misalignment, for 2- to 4-mils-deep center punch marks to simulate mechanical damage, and for dimensional variations exceeding those necessary for economical manufacture. A continuous scratch across the sealing surface did result in leakage. In accelerated corrosion tests with aqua regia, the 1/16-in.-thick wall tubing was completely penetrated by the acid without any leakage at the disconnect seal.

Solvent Extraction Contactor Development. A mixer-settler for use in the TRU chemical processing work was adapted from one of Belgian* design by installing a submerged weir between each settler and its downstream mixer (Fig. 3.7). There is an organic recycle passage between each mixer-settler pair. A McCabe-Thiele plot of earlier run data had showed extensive backmixing of the organic phase, resulting in poor stage efficiency, with the unmodified extractor. The purpose of the weir was to balance the static head in the settler with an equal head on the downstream side of the weir to maintain the aqueous-organic interface independent of mixer speed.

In evaluation tests the weir adequately held the aqueous-organic interface in the settler, preventing organic backmixing (Fig. 3.8), over a wide range of conditions (Table 3.1). Aqueous solutions used ranged in specific gravity (25°C) from 1.0053 to 1.2420 and viscosity (30°C) from 0.8074 to 5.958 centipoises, while the specific gravities of the organic solutions ranged from 0.7648 to 0.9547 and viscosities from 0.924 to 6.05. In each test a mixing speed to give a good dispersion was chosen, and the maximum throughput without flooding was determined. Flooding was due to dispersion and was not in any case caused by inadequate pumping. The aqueous flow was then stopped and the mixer speed required to pump out the aqueous-organic interface determined. As the specific gravity difference between the aqueous and organic phases increased, the mixer speed required to make a good dispersion and the mixer speed required to pump out the aqueous-organic interface also increased.

The throughput was proportional to $\mu^{-0.7}$ (viscosity) (Fig. 3.9), and the maximum throughput, at the mixer speed required to give a good dispersion, decreased as the viscosity of the continuous organic phase increased. The viscosity of the dispersed aqueous phase seemed to have little effect on mixer-settler throughput.

Because of evidence of poor mixing by the pump impellers used in earlier

*ORNL drawings D-34200, 34201, 34202, 34203, and 34205.

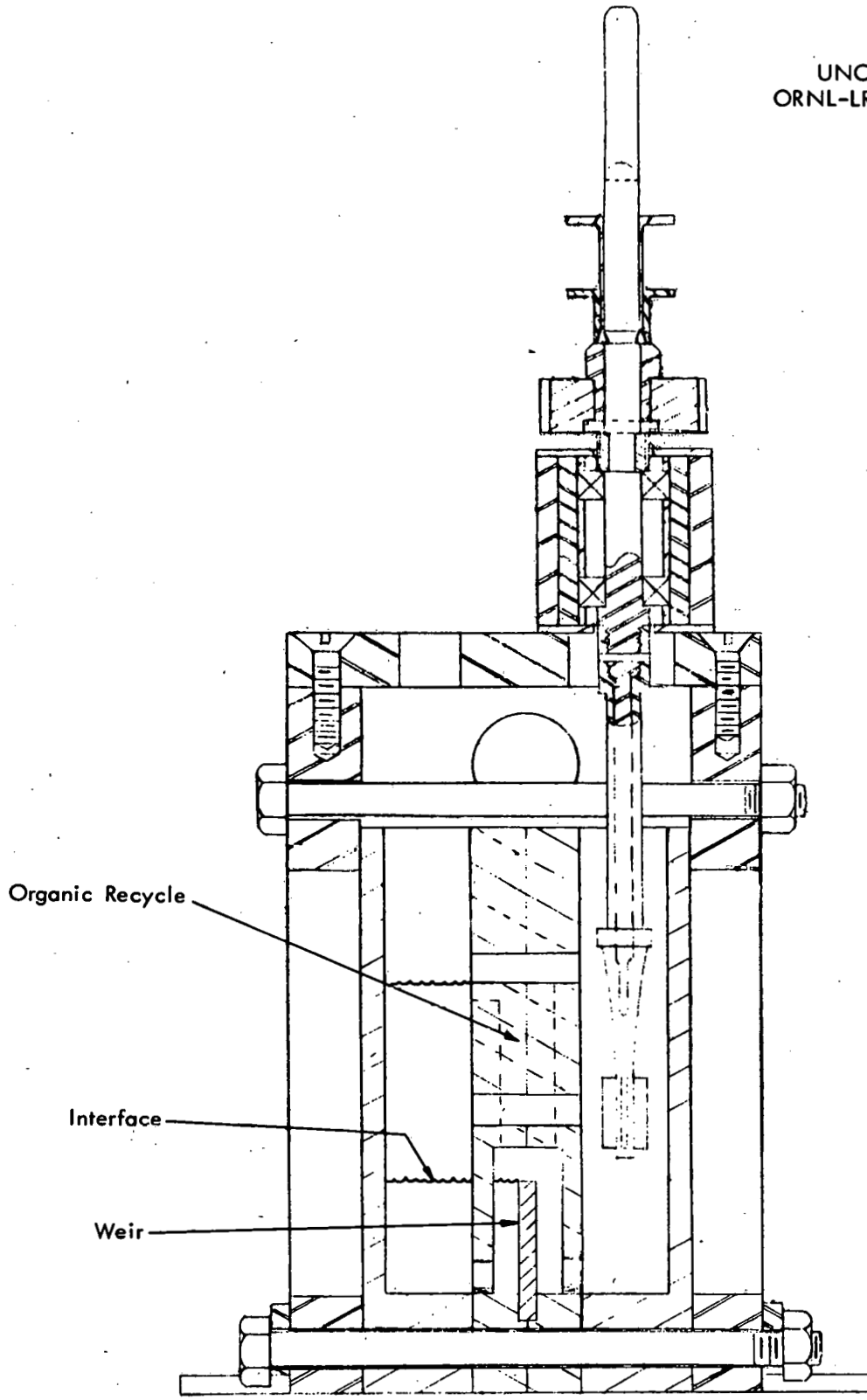

Fig. 3.7. Sectional view of modified mixer-settler.

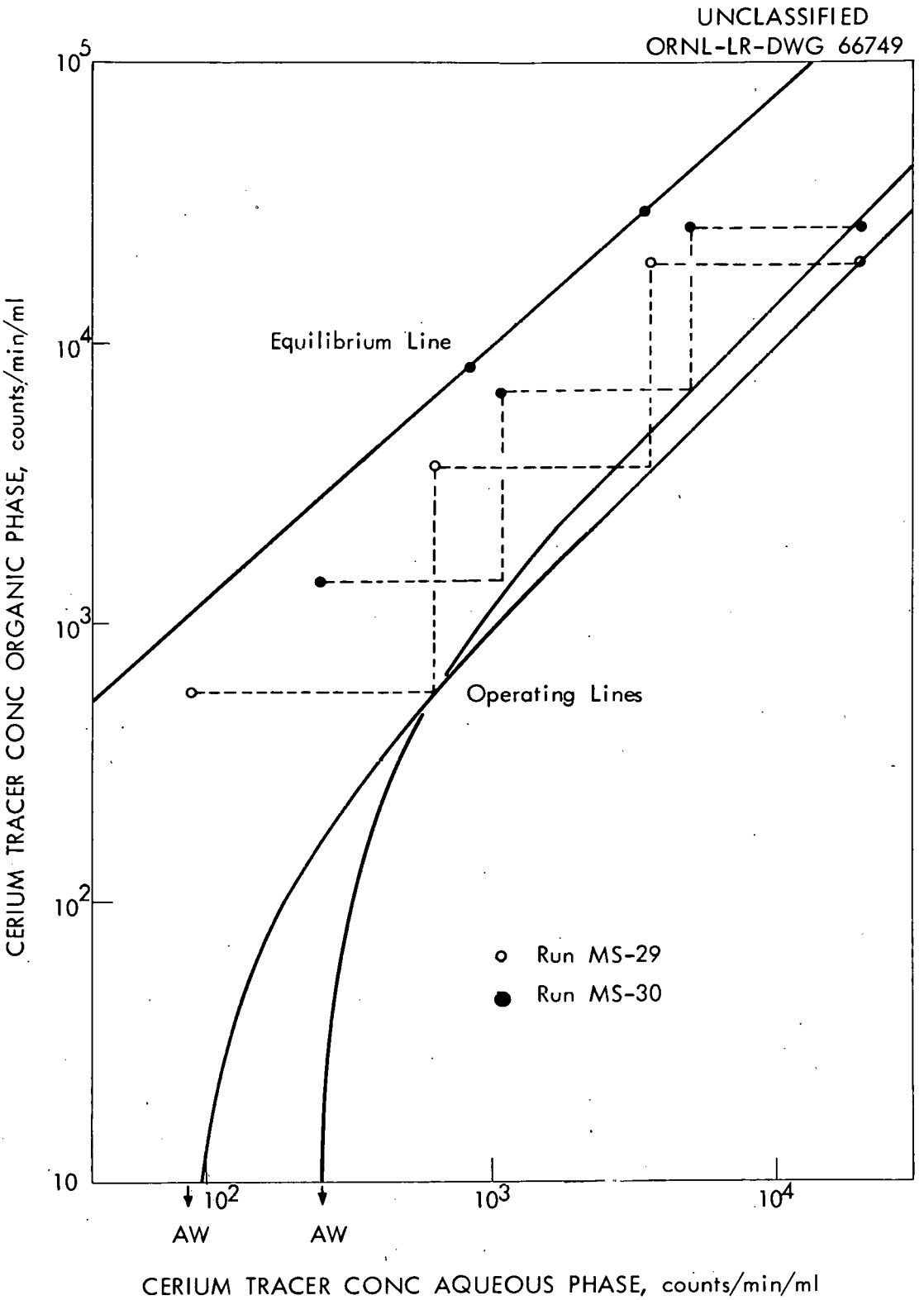

Fig. 3.8. McCabe-Thiele plot for extraction Runs MS-29, MS-30.

Table 3.1. Weir Hydraulic Data

Test Solutions	Specific Gravity (25°C)	Specific Gravity Difference Aq-Org	Viscosity (30°C), centipoises	Maximum[a] Flow Rate, ml/min	Required Mixer Speed, rpm	
					For Good Dispersion	To Pump Out Interface at No Aq Flow
1 wt % HNO_3	1.0053		0.807	20		
85% TBP in Amsco	0.9547	0.0506	3.31	20	1000	>1000
10 wt % HNO_3	1.0335		0.826	20		
85% TBP in Amsco	0.9547	0.0788	3.31	20	1000	>1000
1.5 M HCl	1.0168		0.872	10		
30% Alamine 336 in DEB	0.8713	0.1455	6.05	10	1300	1400
1.5 M HCl	1.0168		0.873	35		
Diethyl Benzene	0.8603	0.1565	0.924	35	1300	1700
				10		
				60	1500	1700
1 wt % HNO_3	1.0053		0.807	20		
5% TBP in Amsco	0.7648	0.2405	1.26	30	1850	2150
11 M LiCl	1.2420		5.96	8		
30% Alamine 336 in DEB	0.8713	0.3707	6.05	8	1600	>2000
11 M LiCl	1.2420		5.96	20		
5% TBP in Amsco	0.7648	0.4772	1.26	30	2770[b]	>2770

[a] At mixer speed required to give good dispersion.
[b] Poor dispersion.

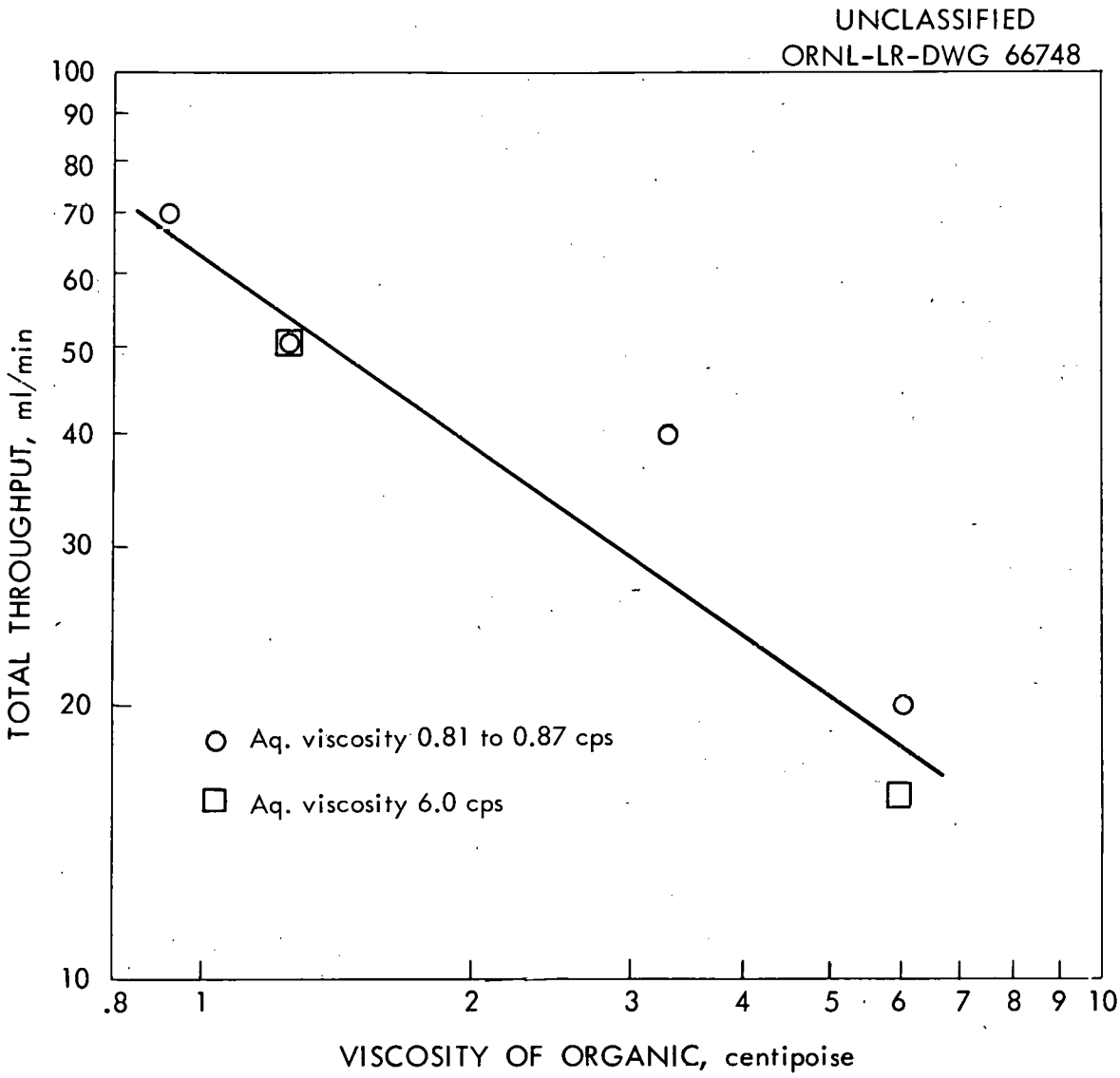

Fig. 3.9. Effect of viscosity on throughput.

runs, four-blade stainless steel and Teflon impellers* were tested in the Belgian mixer-settler. The four-blade Teflon impeller increased the average stage efficiency for cerium extraction over the 59% at 1800 rpm with the pump impeller to 93% at 1725 rpm (Table 3.2). With the four-blade stainless steel impeller, the average stage efficiency was 90% at 1400 rpm.

The phase ratio (aqueous flow/organic flow) at which the Belgian mixer-settler was operated had a marked effect on the cerium extraction stage efficiency for the TBP-$Al(NO_3)_3$ flowsheet. As the phase ratio approached 1 from 3.4, the stage efficiency of the mixer-settler was increased from 45% to 93%.

TRU Glovebox Fire Test Results. Fire tests conducted in the proposed TRU glovebox demonstrated the necessity for promptly extinguishing the fire to prevent loss of containment due to possible burnthrough of the rubber gloves and to prevent heating of the glovebox floor, which in each test produced an explosive mixture due to the increased evaporation rate of the solvent (6). Explosion tests demonstrated the necessity for preventing explosive concentrations in the glovebox since the ignition of an ortho-xylene air mixture just inside the explosive range produced pressure sufficient to rupture the box seals.

Tests of fire extinguishing system components indicated what is felt to be the optimum protection system. This system would consist of a standard commercially available water spray nozzle with a small reservoir containing 2 to 3 gal of water under a reliable pressure force such as a spring or dead weight.

4.0 HFIR TARGET FABRICATION PROCESS DEVELOPMENT
(W. C. Thurber)

4.1 Target Fabrication Development (E. E. Barton, R. G. Gilliland, D. M. Hewette, R. W. McClung)

The target rod for the HFIR reactor is envisioned as a six-finned tube of X-8001 aluminum containing a 20-in.-long column of pellets composed of an actinide oxide dispersed in aluminum (Fig. 4.1). Plenums at each end of the rod will accommodate any fission gases released during operation. The finned tube is inserted in a hexagonal can, which provides a controlled passage for cooling water through the target region of the reactor.

---

*Four blades 1/2 by 3/16 in., spaced at 90° on a 1/8-in. shaft.

(6) T. S. Mackey, "TRU Glovebox Fire Test Results," ORNL Central Files Memo No. 61-12-51.

Table 3.2. Cerium Extraction Runs MS-29 and 30 Data

Feed: 1.4 M $Al(NO_3)_3$
0.5 g/liter RE
Ce tracer 19,400 γ counts/min·ml

Organic: 30% TBP in Amsco

Impeller: four-blade Teflon

Extraction Stage No.	Ce γ, counts/min·ml				Stage[a] Efficiency, %
	Flowing Streams		Equilibrated Samples		
	Aq	Org	Aq	Org	
Run MS-29, aq flow 20 ml/min, org flow 20 ml/min, mixing speed 1725 rpm					
1	3,580	19,300	3,460	29,800	92
2	634	3,640	837	8,340	93
3	87	576	-	-	95
Run MS-30, aq flow 8.1 ml/min, org flow 5.5 ml/min, mixing speed 2160 rpm					
1	4,860	26,700	3,460	29,800	88
2	1,060	6,880	837	8,340	93
3	250	1,450	-	-	90

[a]Murphee efficiency based on aqueous phase calculated by use of a McCabe-Thiele plot.

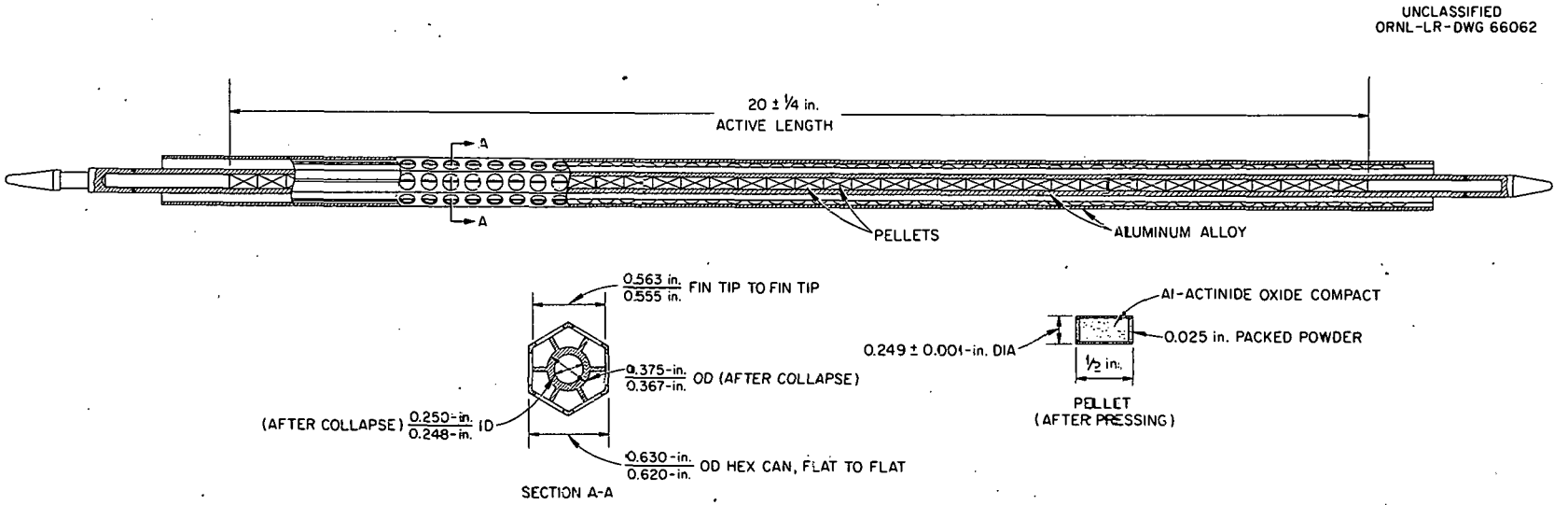

Fig. 4.1. HFIR target rod.

The fabrication process tentatively selected consists of the following basic operations: (1) weighing and blending a suitable mixture of aluminum and actinide oxide powders; (2) metering a charge of this mix into a thin-walled aluminum sleeve capped on each end with aluminum powder; (3) pressing the powder-filled sleeve into a green pellet with a density approaching 90% of the theoretical value; (4) inserting these pellets into a finned aluminum tube and closing the ends by fusion welding; (5) isostatically pressing the finned tube onto the pellet column; and (6) inspecting and cleaning the assembled rod.

4.1.1 Pellet Preparation

Characterization of Actinide Oxides. The conceptual target rod design incorporates a 20-in.-long stack of pellets, each ~0.25 in. dia by ~0.5 in. long, made of actinide oxide dispersed in aluminum powder. Because of the radiological hazards in handling and the limited supply of actinide oxides, rare earth oxides have been used for the development work. The cerium and gadolinium oxides used were prepared by techniques similar to those planned for use in the TRU Facility, i.e., by calcination of either hydroxides or oxalates, which have size fractions such that they disperse into the air during pouring or shaking. Surface areas vary from 5 to 10 m^2/g. Lindsay Mix, a mixture of rare earth oxides, was purchased.

The reference oxide content for a Pu-242-bearing rod is 18 vol %.

Blending Experiments. In experiments with an oblique blender, with 4-oz wide-mouth bottles as containers, 1 hr was sufficient to blend mixtures of 10, 15, 20, and 25 vol % oxide in quantities approximating those required for a single target. The use of -325 mesh (44 μ) aluminum powders prevented gross segregation. To decrease the possible explosion hazard and handling problems associated with fine aluminum powders, removal of the <4-μ material from the -325 mesh aluminum powder may be necessary.

Agglomeration of the oxide, which was noted in many cases (Fig. 4.2a), was prevented (Fig. 4.2b) by inserting small rods into the blending container, combining an effect analogous to rod milling with the blending operation. Since the blending hopper is also to be used as the calcining vessel, any light caking of the oxide that might occur during calcining will also be broken up by the action of the rods.

The blended oxide mixtures had pour densities 25-35% of theoretical, with a scatter of ±10% when the amount was of the order of that required for one pellet. After being pressed at 33 tsi, the compacts had a density 91% of theoretical for the 25 vol % mixture.

A mockup of the proposed combined blending and metering device was assembled and shown to be feasible. The parts for a more complete mockup, which will also include the rod milling operation, have been received, and the proposed pro-

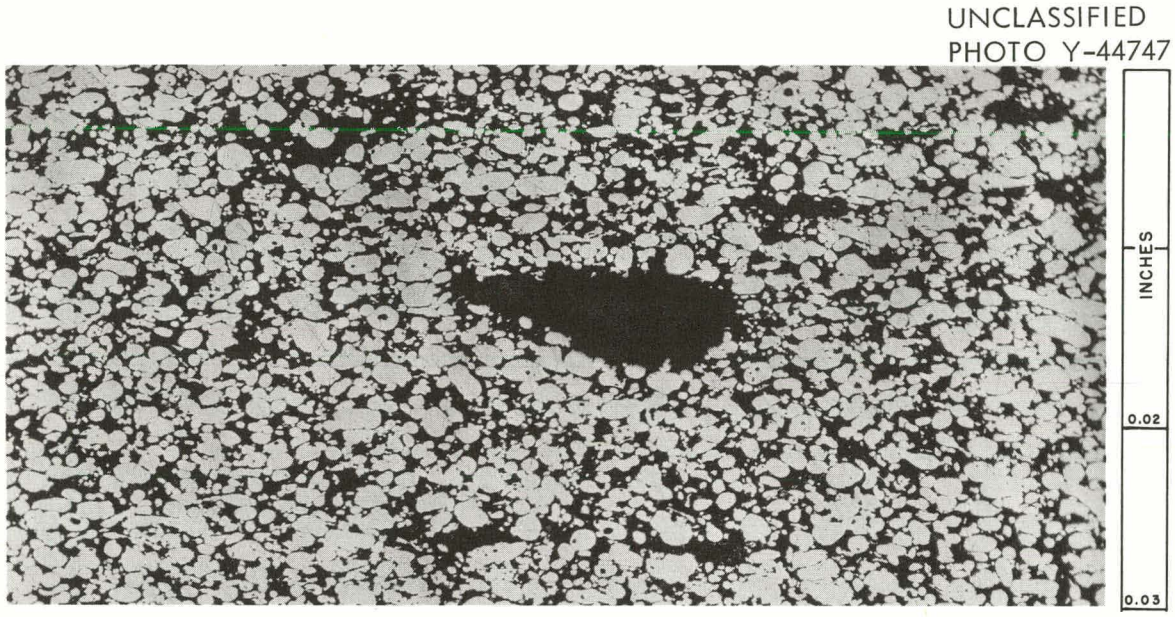

(a)

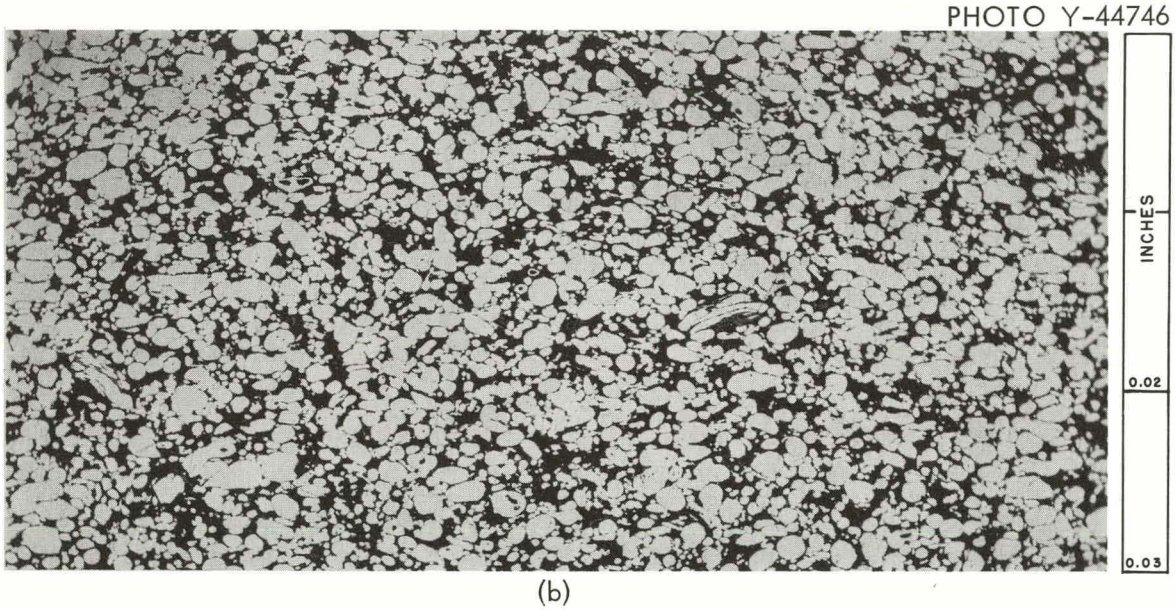

(b)

Fig. 4.2. Longitudinal section of pressed pellets showing (a) agglomerates of oxide (black material) and (b) absence of oxide agglomeration. The mixture of 21 vol % oxide in aluminum was blended 1 hr prior to pressing at 33 tsi to 88% of theoretical density. As polished.

cedure will be evaluated from the calcining to the metering operation.

Pressing Experiments. Current fabrication procedures specify pressing the pellets in thin-walled aluminum sleeves with an aluminum powder cover on each end to provide a primary source of containment for the actinide materials. Aluminum sleeves of 15 mils wall thickness were selected. Experimental pressings, with a 2 to 1 compression ratio at 33 tsi, of pellets in 15-mil-wall cups, gave a more satisfactory collapse pattern (Fig. 4.3a) than did pressings in 5- or 10-mil-wall cups. The 10-mil-wall cups occasionally folded, and the 5-mil-wall cups folded and buckled extensively (Fig. 4.3b). This extreme collapse could entrap die lubricant or particulate contamination, rupture the wall, or adversely affect heat transfer in the target rod. The use of wall thicknesses >15 mils was not considered, since with thicker walls the volume available for the oxides would be less. The diametrical clearance between cup and die cavity must be 1 mil or less to prevent folding of the wall.

In a longitudinal section of the pressed cup, the oxide-aluminum powder mixture (light-gray area in Fig. 4.3a) has a dovetail appearance. As a result of the pressing, the wall thickness increases except at the base, where the cup bottom offers resistance, producing a possible weak spot in the pellet wall and nonuniform loading of the target oxides. This was prevented by using aluminum powder covers at both ends (Fig. 4.3c). Leak tests with helium, to simulate the fission product gases xenon and krypton, showed that such powder plugs, with their connecting porosity, readily allow passage of released fission gas from the pellet. This design is in keeping with the provision of void spaces in the ends of the target rod for accumulation of released fission gas.

To further decrease the possibility of spreading contamination, the reference concept calls for the use of drill bushings as disposable pressing dies. These bushings have a surface finish of around 20 μin. and can be supplied with a $\pm$0.0003-in.-i.d. tolerance. Powder pressings in such dies were satisfactory with pressures up to 40 tsi, but some bushings failed with pressures >40 tsi.

In all the pressing experiments reported, stearic acid dissolved in acetone was used as a die lubricant, and the pressed pellet will be cleaned to remove residual lubricant and ensure a contamination-free surface. Cleaning procedures examined thus far have incorporated either organic solvents, a commercial decontaminant (Turco 4513), or dilute sodium hydroxide solutions used in conjunction with various combinations of thermal treatments. The most promising cleaning method appears to be one using dilute sodium hydroxide solution.

4.1.2 End Closure Welding

Experiments were started to devise techniques for remote automatic welding of closures for type 1100 aluminum tubes. These fusion welds are being made with

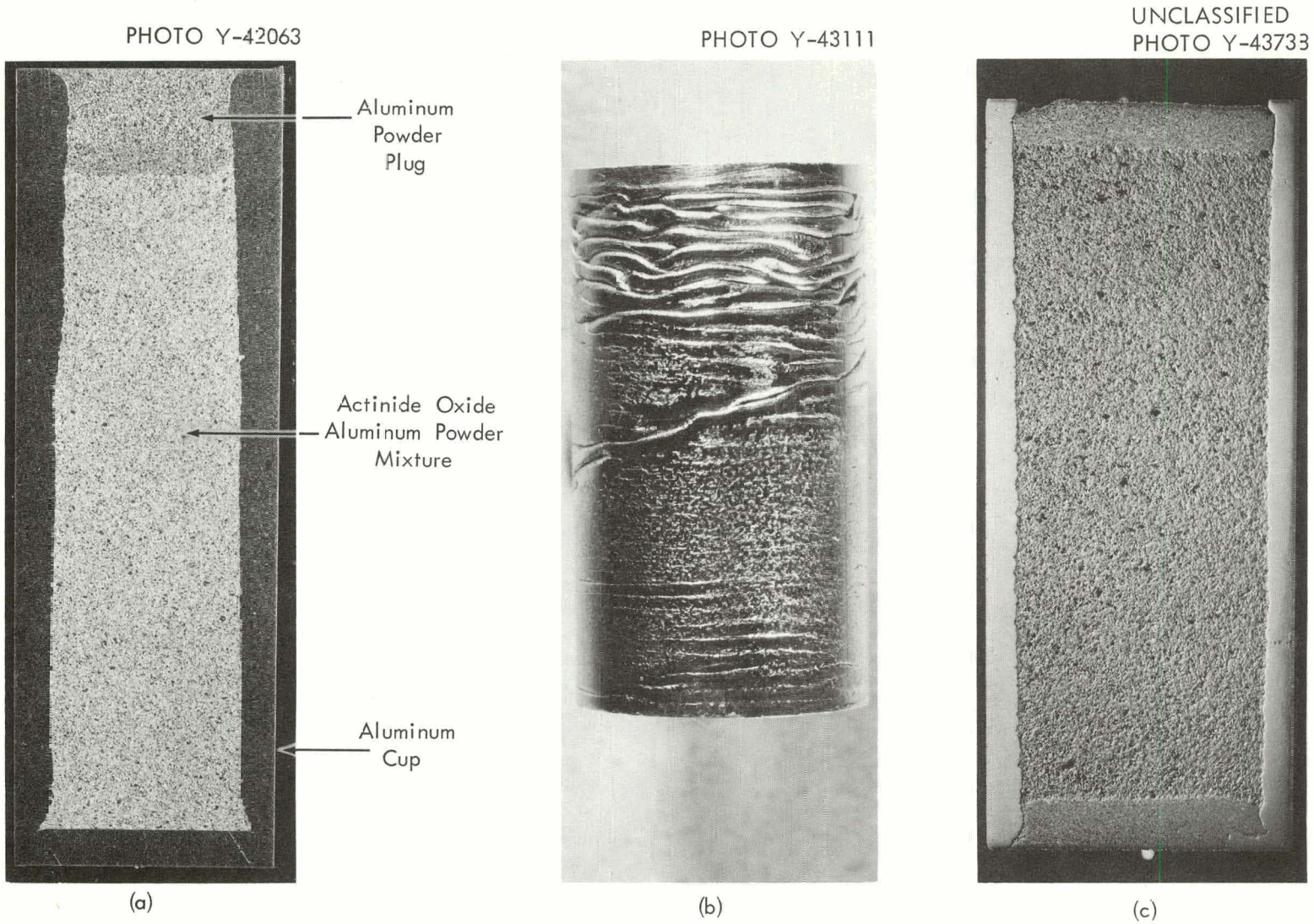

Fig. 4.3. Pressed pellets in aluminum cups. (a) 15-mil-wall cup, longitudinal section; (b) 5-mil-wall cup; (c) powder plugs at both ends.

a butt-joint design on 3/8-in.-o.d. by 0.060-in.-wall tubing. Preliminary results indicate that direct current is better than alternating. With alternating current the weld metal became more porous and the welds had only about half the penetration of those made with direct current.

Because of the extremely high heat capacity of aluminum, localized nonfusion in the weld area is a problem. Currently, welds that are leaktight but still contain nonfused areas are being made by direct current. Leaktight welds with and without nonfusion areas (Fig. 4.4) are made with welding currents of 45-60 amp, welding speeds of 10-15 in./min, and helium as the inert cover gas.

Studies are also under way to investigate the welding of other aluminum alloys, e.g. X-8001, which may be used in the target rods. Efforts will be made to reduce the very broad weld beads of the type shown in Fig. 4.4. General refinements in welding techniques, as well as modified joint designs, are also planned to further ensure overall joint integrity in remotely produced welds.

4.1.3 Tube Collapse Studies

To improve heat transfer in target rods, the finned outer tube will be isostatically collapsed around the target pellets. In initial experiments with 3/8-in.-o.d. 1100 aluminum tubing loaded with pellets and end caps welded in place, ~12,000 psi was required to collapse the tubing to the extent that further changes in diameter were not noted. This stabilization of diameter was assumed to indicate contact between the pellets and the tube. At the same time, the tube length, limited to 13 in. by the capacity of the autoclave, decreased ~15 mils. Mineral oil at room temperatures was used as the hydraulic fluid.

The results of the most recent collapse experiment with a finned 1100 aluminum tube machined from bar stock, although not conclusive, suggest a collapse pressure of ~13,000 psi. The void spaces collapsed in a two-lobe failure at ~15,000 psi (Fig. 4.5). Radiographs and destructive examination indicate that the target rod was not in intimate contact with the pellets at all points even after an applied pressure of 16,000 psi. The cross section of this tube approximated the cross section of the proposed target rod. A liner, 1-5/16 in. long, 0.023 in. wall, in each end simulated the fission-gas void space. Pellets were of solid 1100 aluminum cylinders coined in drill bushing dies to control the surface finish. The diametrical clearance between the pellet and inside diameter of the tube was 6 mils, a value selected as the minimum that would permit remote loading. The pressure was applied in increments, and diameter and length measurements were made between increments.

4.1.4 End-closure Inspection

The results of a preliminary study to determine the feasibility of remotely radiographing the target rod end-plug welds indicated that radiation from plutonium

UNCLASSIFIED
PHOTO Y-44867

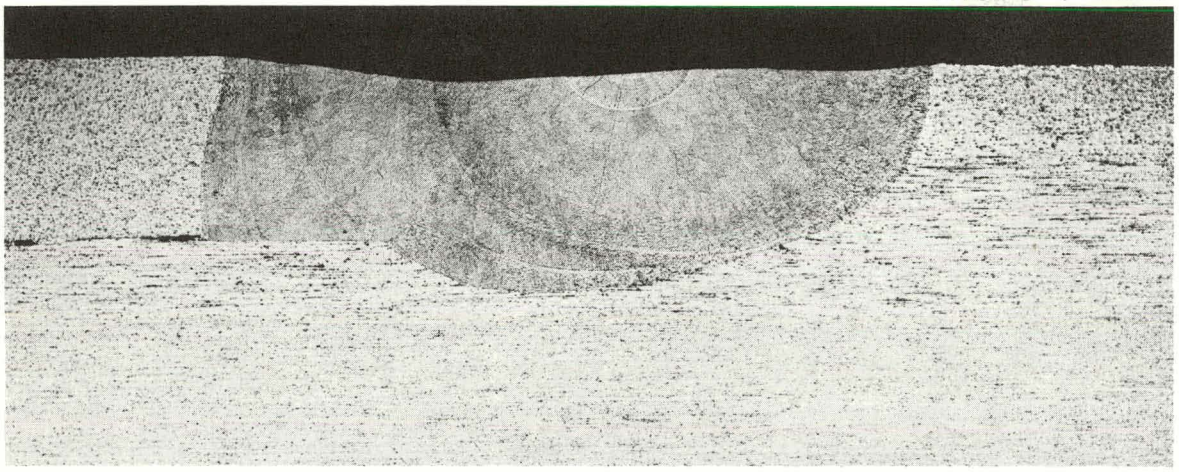

(a)

PHOTO Y-44868

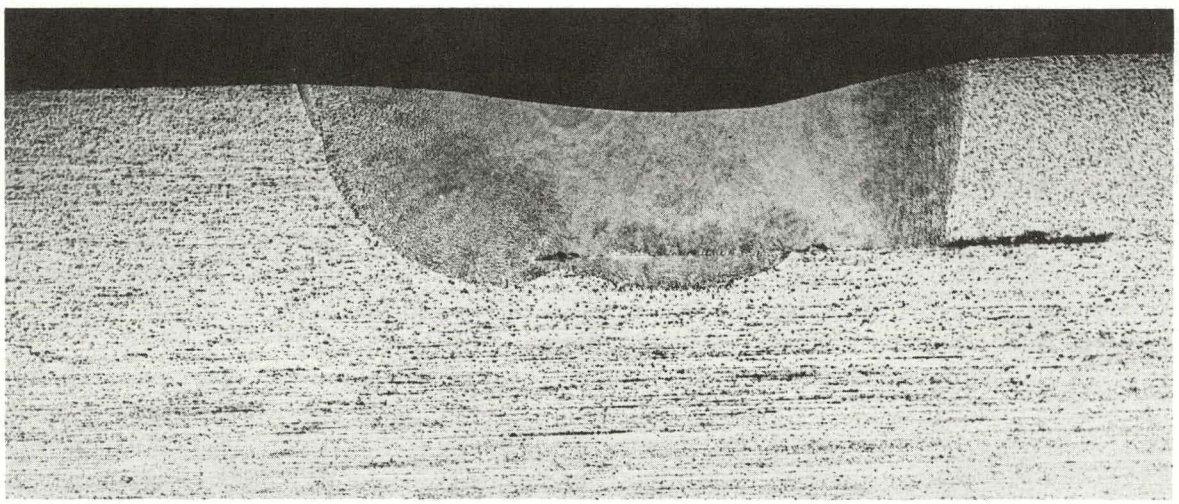

(b)

Fig. 4.4. Composite of fusion-welded end closure in type 1100 aluminum tubing. (a) sound leak-tight area; (b) lead-tight area with zone of nonfusion. Etchant: 97% H_2O, 1% HF, 1% HNO_3, 1% HCl.

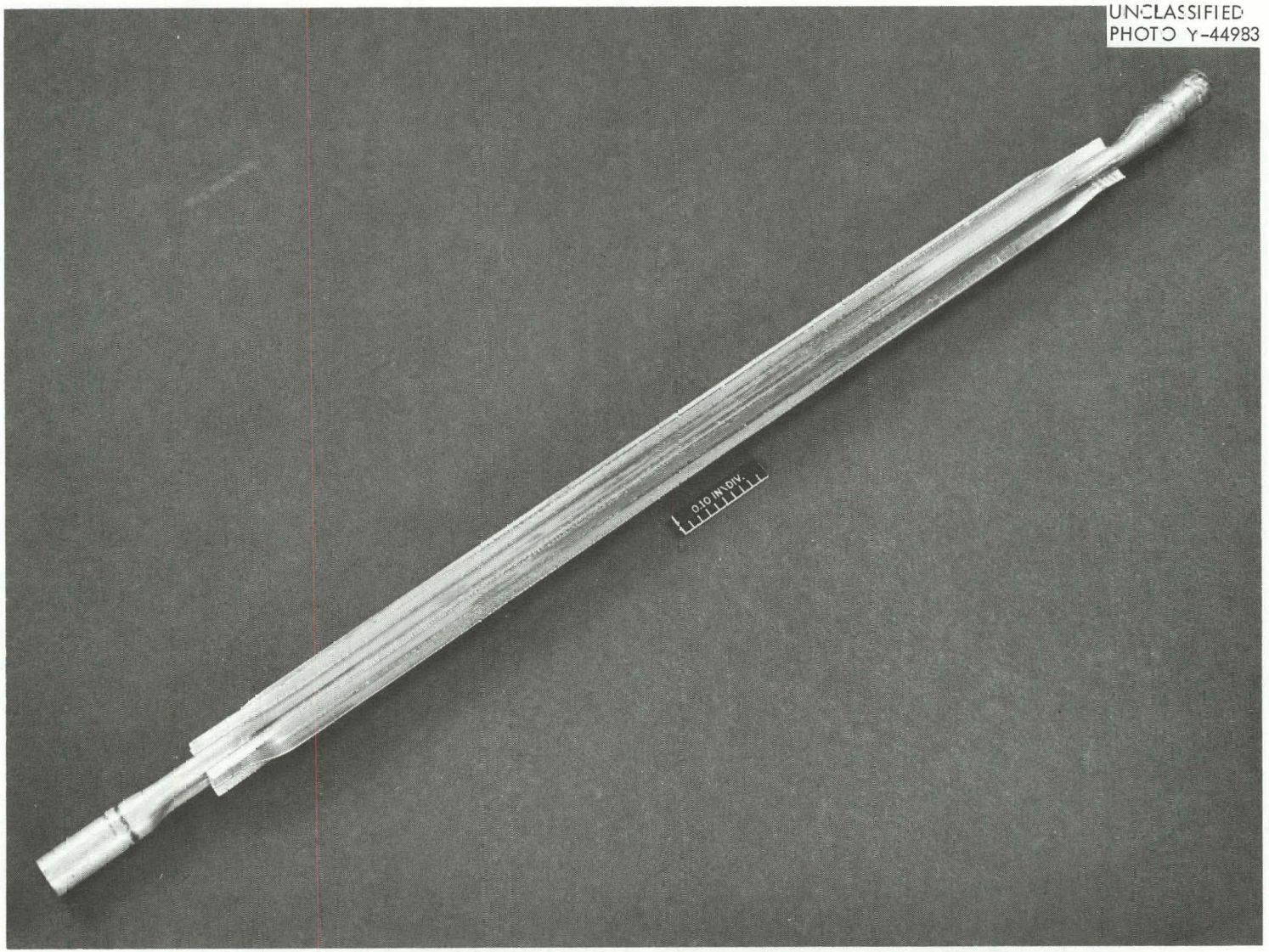

Fig. 4.5. Simulated target rod after collapse at 16,000 psi. Note nonuniform collapse over end plenums.

will not interfere with the test. The predicted irradiation backgrounds were 0.05 rad/hr of 0.1-Mev γ radiation from Pu-242 targets and ~300 rad/hr of the same energy for Am-243, Cm-244, and curium recycle targets. The neutron background has very little effect on the radiographic film.

A sample closure weld radiographed at 48 kvp for 8 sec gave a reasonable radiograph of better than 2% sensitivity. Duplicate films subjected to varying exposures of 100-kvcp x irradiation, to superimpose the anticipated fogging from background radiation on the image of the weld, showed that ~1 r of such irradiation may be tolerated without serious degradation of the image quality. If the total exposure time of the film to the background can be maintained very nearly that of the image-forming exposure, useful radiography may be performed on the americium and curium targets. The exposure time may be limited by loading the film in a shielded container with a movable shutter. A considerable advantage could be realized by placing the target rod in a shielded sleeve with only the weld area exposed for inspection, thus removing most of the background radiation from the radiographic film.

4.2 Equipment Development (M. K. Preston, A. L. Lotts, R. I. Deaderick)

Three cells are now allotted in the Transuranium Processing Plant for fabrication and inspection of HFIR target elements. The four-cell space originally assigned was found to be excessive after study of preliminary equipment designs and elimination of some of the earlier proposed operations. The phases planned for the equipment development program are, in sequence: (1) design of remotely operated equipment; (2) procurement and construction of equipment; (3) individual equipment testing; (4) equipment testing in cell mockups; (5) redesign and reconstruction of equipment where necessary; (6) installation and cold operation of the equipment in the Transuranium Processing Plant; and (7) operation of the equipment to fabricate actual HFIR target elements. The project is now in the design phase.

The basic criteria established for the target rod fabrication process are that operations should be simple, reliable, and capable of producing elements to the specified tolerances, and that the equipment should be small, require minimum maintenance, be well advanced technologically, and resistant to damage by β, γ, and neutron irradiation. The system must be designed to minimize the spread of contamination, and components must be easily repaired or replaced. Therefore transfer arms and other special devices will be used to move target rod components between steps in the process, and all equipment will be designed to operate semi-automatically, without manipulators. Manipulators will be used only for maintenance and for transfer of components to and from the intercell conveyor. Wherever possible, sensitive parts of equipment will be small enough for charging to or discharging from the cubicle via the intercell conveyor. All equipment will be demountable with the use of an impact wrench and small enough for removal through the 36- by 18-in. hatch in the cell roof. Auxiliary enclosures will be used to further minimize the spread of contamination.

4.2.1 Process Flowsheets and Equipment Layouts

The powder-metallurgical, welding, chemical, and inspection operations have been assigned to a cell according to the degree of contamination expected from them. Generally, operations with loose powders will be performed in cell 3; those with pellets in unsealed tubes in cell 2; and those with sealed target rods in cell 1.

Cell 3 (Figs. 4.6 and 4.7)

All materials will be transported to cell 3 by the intercell conveyor and to the individual process steps by the manipulator. Solid waste will be removed by the same devices.

Calcination. A container bearing the actinide hydroxide will be taken to cell 3 from cell 4 by the intercell conveyor and to the calciner by the manipulator. Present planning calls for a special container so that all operations through blending may be done without transfer of the actinide oxide.

Weighing. The container bearing the oxide will be transferred to the scale by the manipulator. The weight of the oxide batch will be determined so that the proper charge of aluminum may be introduced, and the container will then be taken to the blender by the transfer arm. En route, the charge of aluminum powder, prepared outside the cell, will be admitted to the container.

Blending, Weight Dispensing, and Die Loading. The mixture will be blended and dispensed to the die, which will rest on a scale located immediately below the blender. The blender and scale will be interlocked so that when the desired weight of powder is reached, dispensing will cease. The blender will continue to mix the remaining material until the next die is ready to be charged. The dies will be prepared outside the cell, and the aluminum tube and bottom powder cap will be in place when they are introduced into the cell. The die loaded with actinide oxide and aluminum powder will be conveyed via the transfer arm to the cap-powder loader, where sufficient aluminum powder to cover the actinide oxide will be volumetrically dispensed, and thence to the press, also by the transfer arm.

Pressing. The die will be positioned in the press and a top punch from a magazine loaded. Tentatively the pressing will be done to a fixed height (0.500 in.) at a pressure of 33 tsi. The bottom punch and pellet will be ejected from the press and routed automatically to separate containers. The top punch and die will be removed by the transfer arm to a waste container. To minimize pellet contamination, die components, which are inexpensive, will be discarded after one pellet has been pressed. The container holding the pressed pellets will be transferred to the dewaxing furnace by the manipulator.

Thermal Treatment. The pellets will be held at ~450°C for 1 hr to remove die lubricant and relieve stresses. Again in a container, the pellets will be trans-

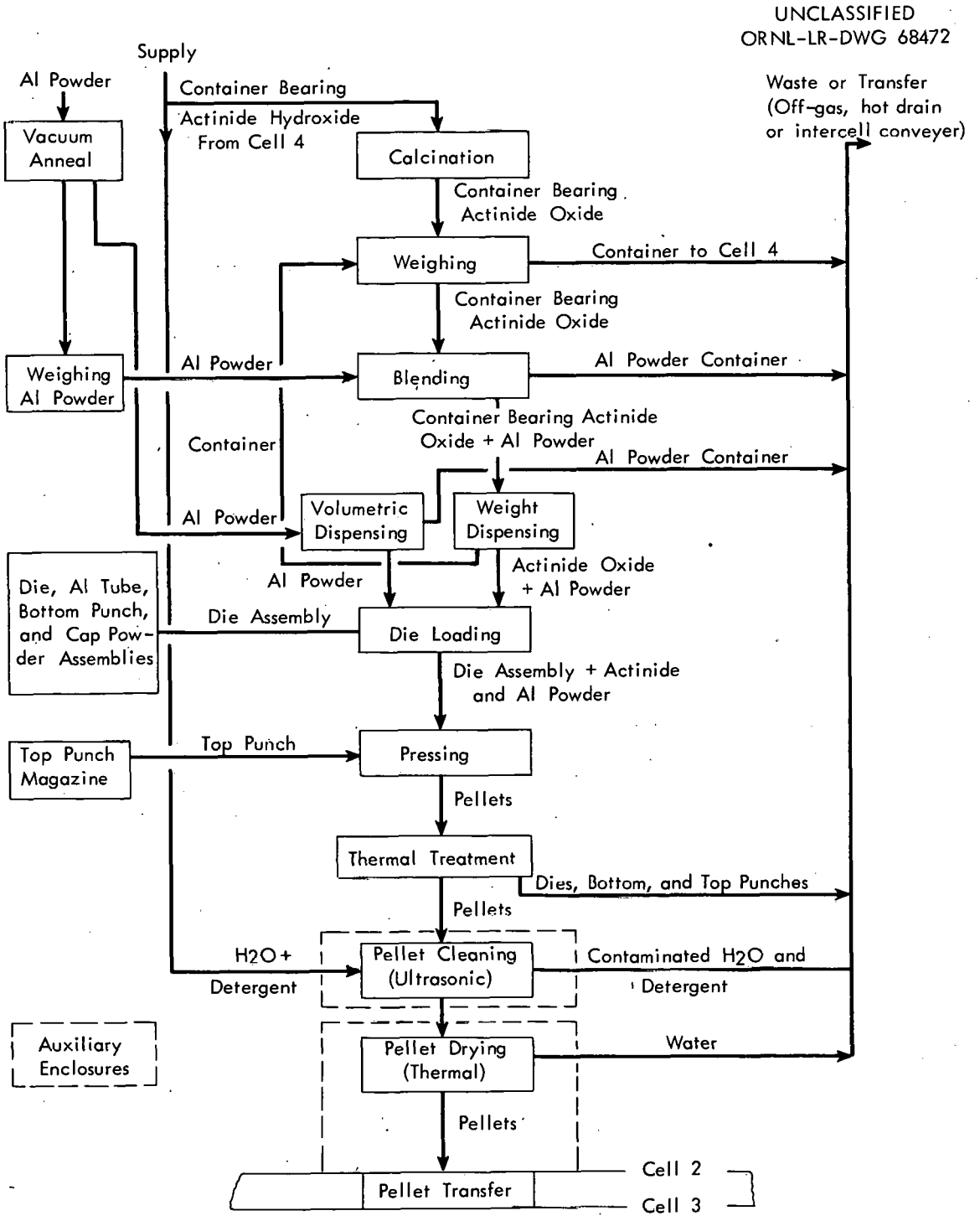

Fig. 4.6. Flowsheet fabrication, cell 3.

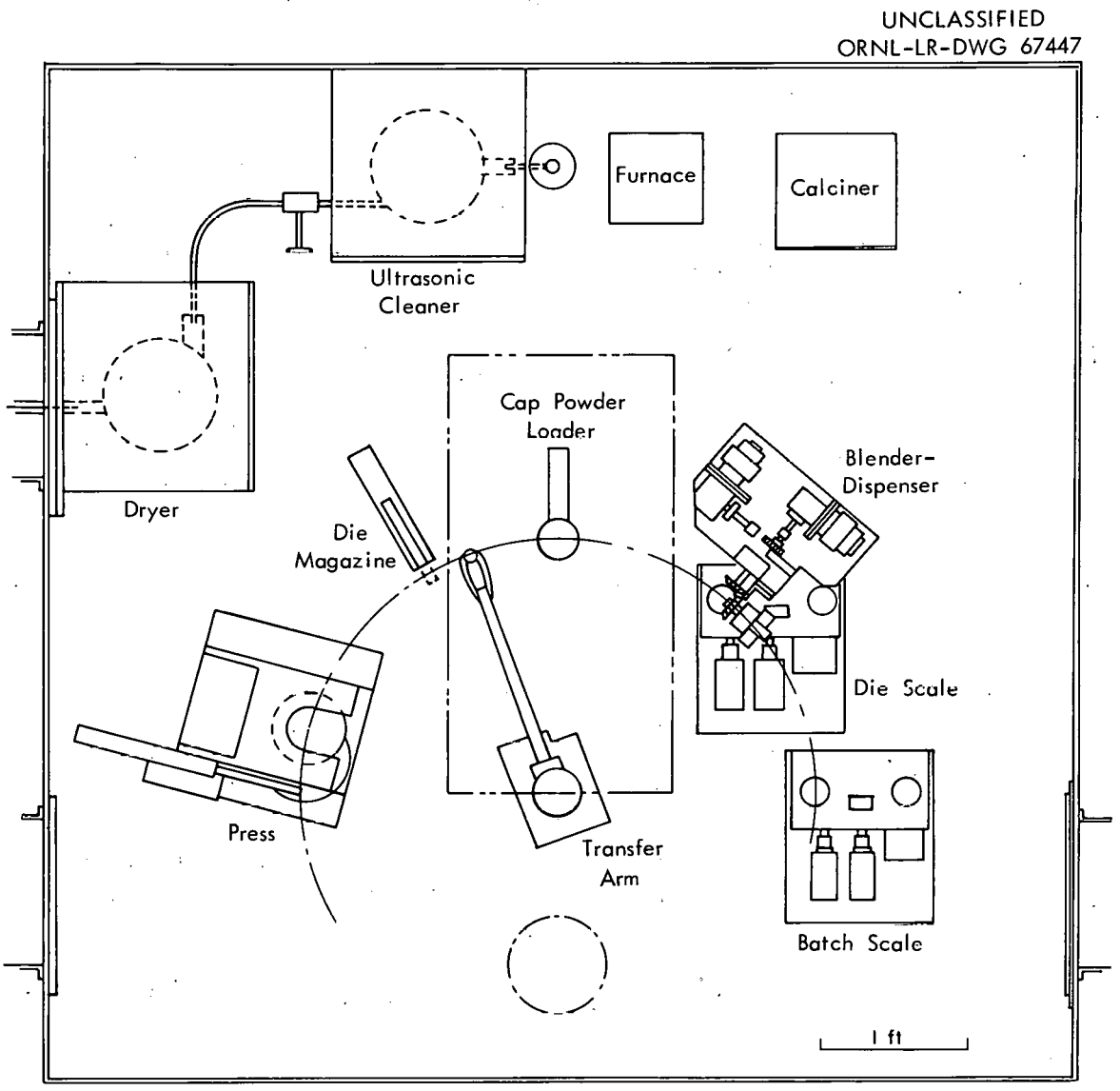

Fig. 4.7. Plan view of equipment, cubicle 3.

ferred to the ultrasonic cleaner by the manipulator.

Ultrasonic Cleaning and Drying. The pellets will be cleaned in either an aqueous detergent or sodium hydroxide solution, rinsed in the same equipment, and conducted by vibratory feeding to the drying chamber. They will be dried on a heated plate and then vibratorily fed through the wall to the tube-loading device in cell 2.

Cell 2 (Figs. 4.8 and 4.9)

All material except the target tubes will be conveyed to cell 2 by the intercell conveyor and transferred by the manipulator to the operations in which they will be used. Similarly, solid waste from the process will be conveyed by the manipulator to the intercell conveyor. The target tubes will be introduced through the equipment transfer hatch in the cubicle roof.

Pellet Measurement. Pellets, conveyed to the target tube loader by vibration, will be individually checked for diameter. On leaving the diameter gage, they will be stacked in a trough where, when the appropriate loading for a tube has been reached, the total length will be checked. Pellets not passing the diameter gage will be returned for reprocessing.

Tube Loading. Another pellet feeder will be used at the lower end of the trough to allow feeding the pellets singly to the tube with a stuffing rod.

Tube End Cleaning and Capping Placement. The target tube will be loaded horizontally, and the filled tube will be placed in an upright position. The end of the tube will then be cleaned, the end spacers inserted, the tube evacuated and backfilled with helium, and the end cap pressed into the tube.

End Cap Welding. The target tube will be welded closed by a Heliarc technique, and the closed tube will be removed to the helium-leak-test chamber by the transfer arm.

Helium-leak Test. The leak-test chamber will be evacuated to a helium-leak detector system, which will be located in the limited-access area of the facility.

Hydrostatic Pressure Collapse. After the leak test, the tube will be transported by the transfer arm to the hydrostatic pressure chamber, where the tube walls will be collapsed onto the pellets. To confirm that the tube has not been ruptured, another helium-leak test will be made.

Decontamination. By the transfer arm, the target element will be conveyed to the ultrasonic cleaning equipment, where it will be ultrasonically cleaned with water and a detergent and rinsed. A special device will be used to transfer the rod to the station where the element will be further rinsed and dried. For contamination

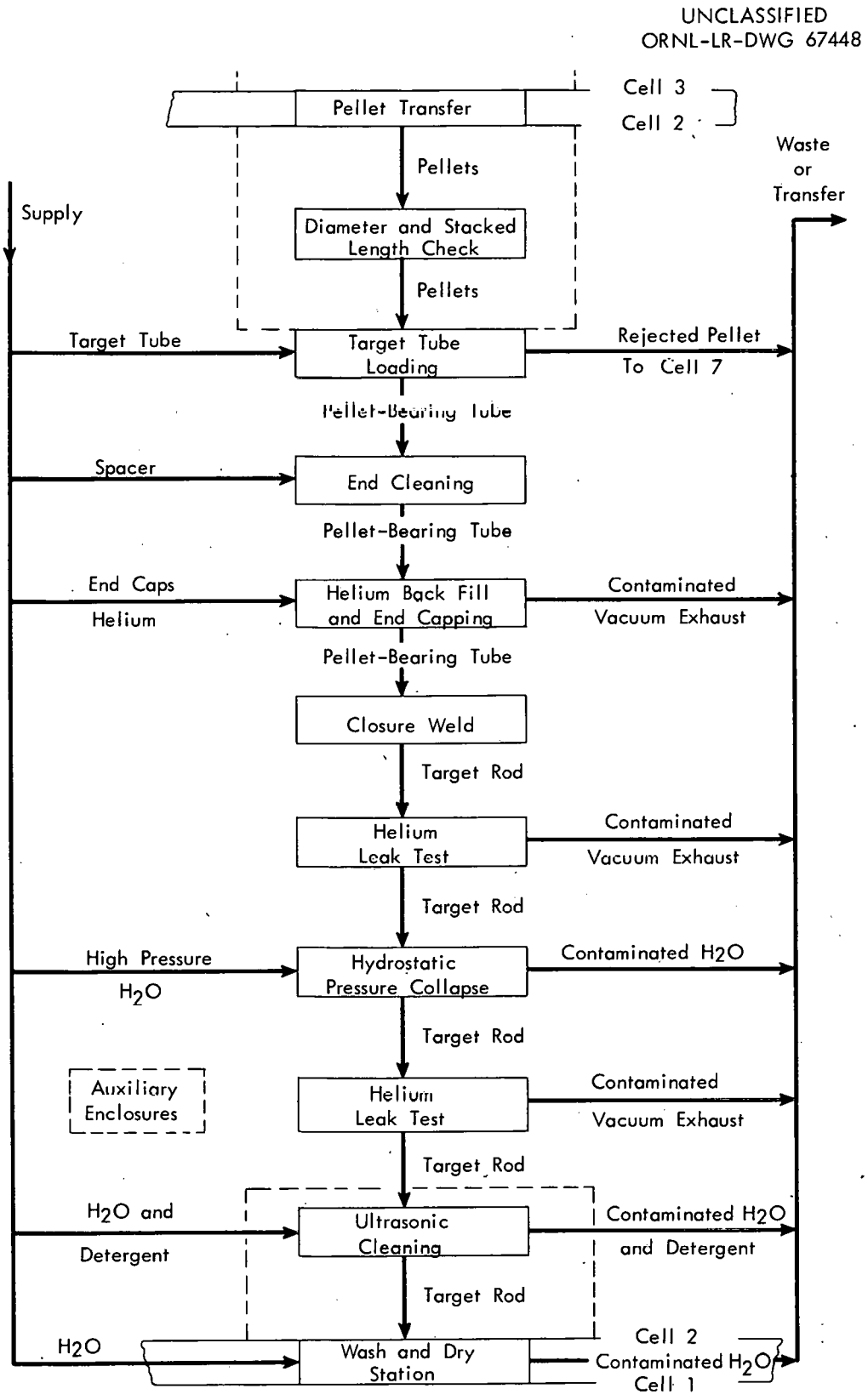

Fig. 4.8. Fabrication flowsheet, cell 2.

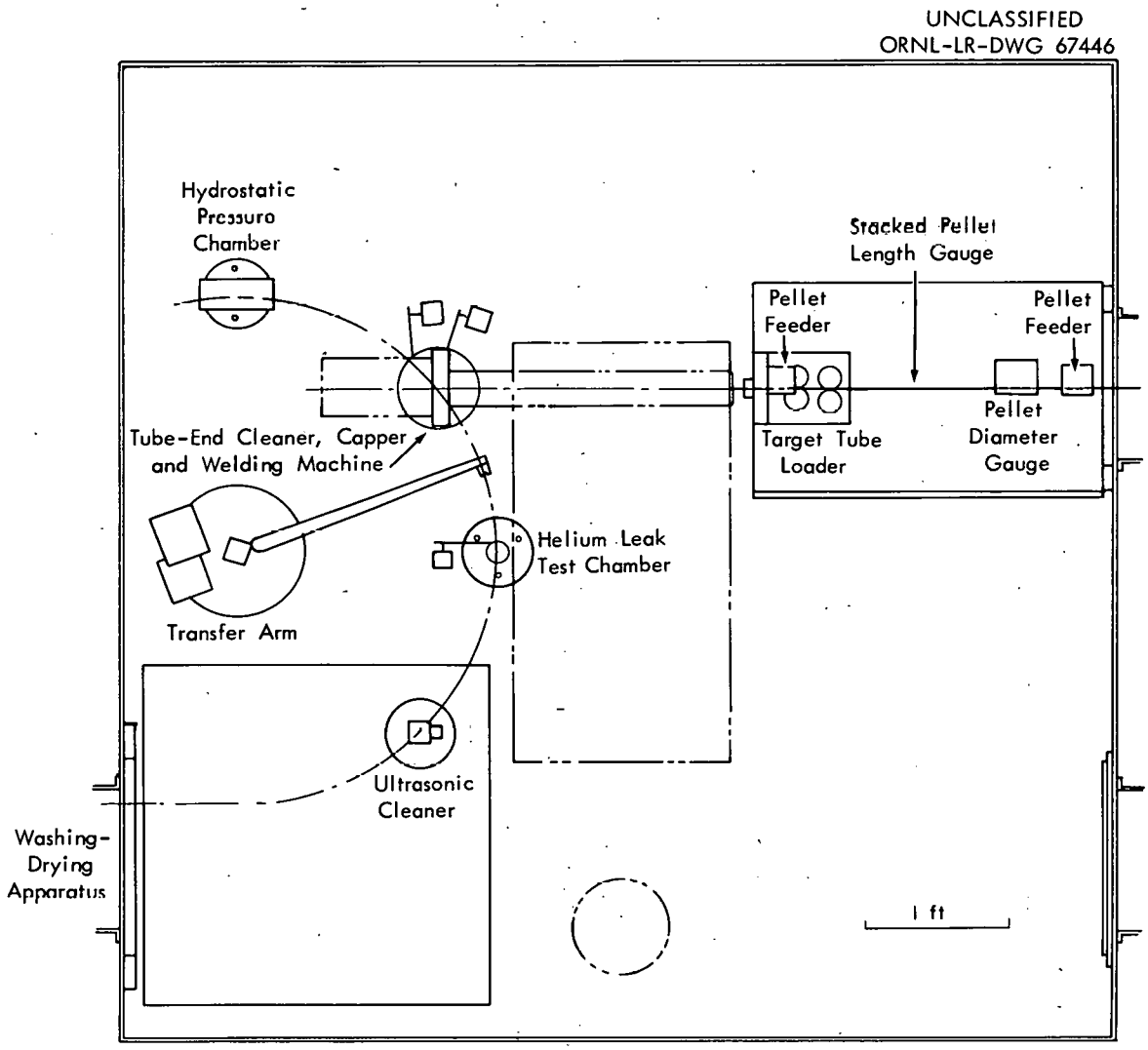

Fig. 4.9. Plan view of equipment, cubicle 2.

control, the equipment for washing and drying will be located in the wall between cells 2 and 1.

Cell 1 (Figs. 4.10 and 4.11)

All material required for the operations in this cell except the hexagonal can will be introduced by the intercell conveyor and transported to the specific operations by a manipulator. The hexagonal cans will be introduced through the equipment transfer hatch in the roof of the cubicle. The finished target element will be transported vertically through the cell ceiling to a carrier located on top of the cell bank. Solid waste will be removed by the intercell conveyor system.

Surface Smear. On being introduced to cell 1, the target element will be checked for transferable contamination on the surface by means of a foam rubber smear pad, which will travel the length of the rod and be taken from the cell by the intercell conveyor for Health Physics survey. When the target rod is proved clean, it will be moved by the transfer arm to the radiographic film and tube holder.

Weld Radiography. The weld will be radiographed, tube and film holders being used, by an x-ray tube located at the rear of the cell. After radiography, the target element will be conveyed to the dye-penetrant tanks by both transfer arms.

Dye-Penetrant Inspection. By means of the transfer arm, the target element will be dipped into the penetrant chemicals and then taken to the front of the cubicle by the transfer arm where the weld will be inspected through a periscope. The rod will then be conveyed to the dimensional inspection equipment by the left transfer arm.

Dimensional Inspection. The rod diameter will be measured in several places by special equipment, the degree of bowing will be determined, and the length measured.

Hexagonal Can Placement and Welding. The element will be inserted into a hexagonal can by special equipment, and the can will be welded to the target rod fins.

Final Cleaning and Surface Smear. The element will then be admitted to the vertical ultrasonic cleaning tank by the right transfer arm. After being cleaned and rinsed, the rod will be transported back to the surface smear device for final smearing. The target element will then be removed to the vertical transfer device, from which it will be transported to the target carrier.

4.2.3 Equipment Design

Cell 3

Calciner. The calciner has not yet been conceptually designed because

UNCLASSIFIED
ORNL-LR-DWG 67449

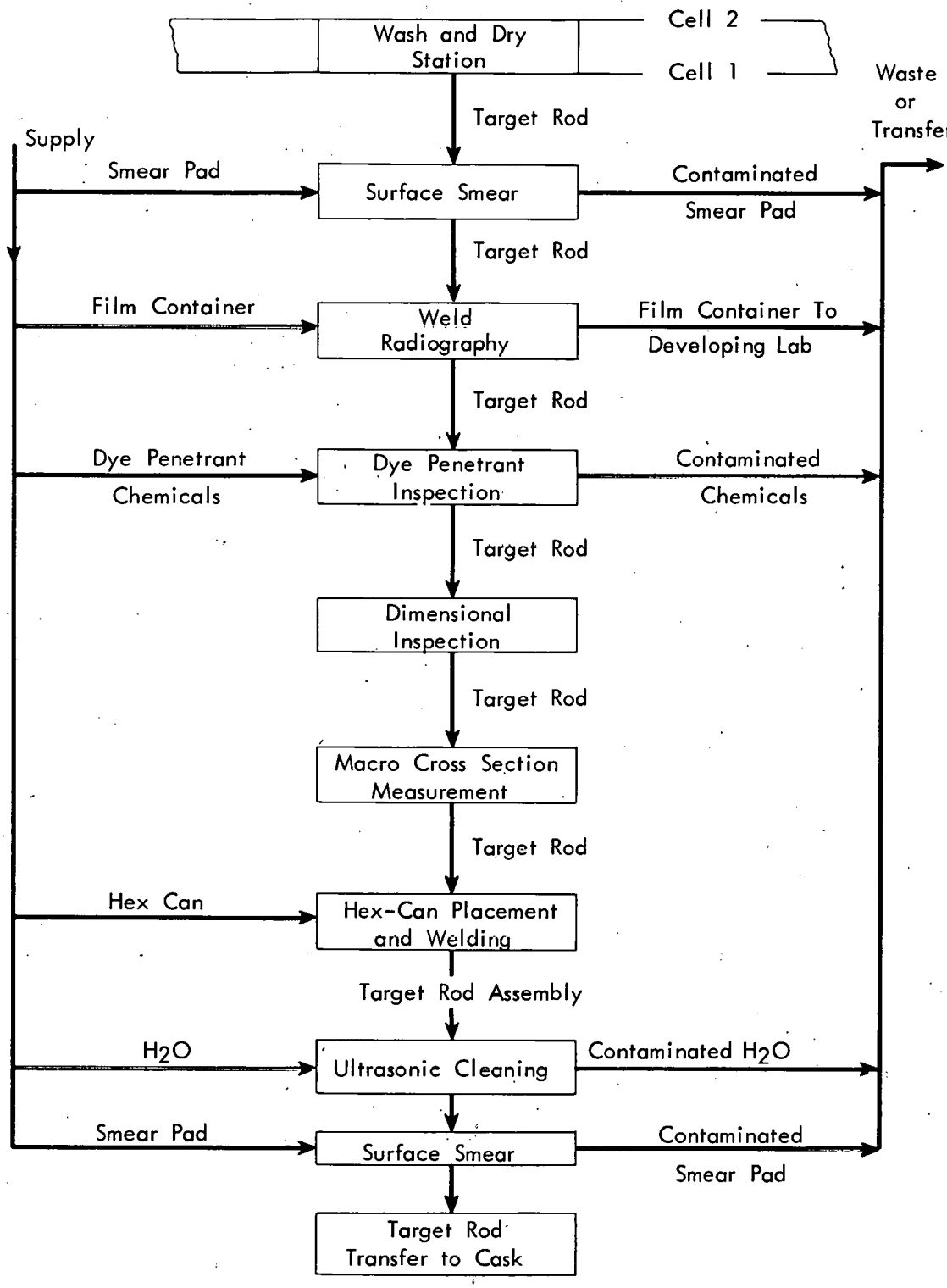

Fig. 4.10. Fabrication flowsheet, cell 1.

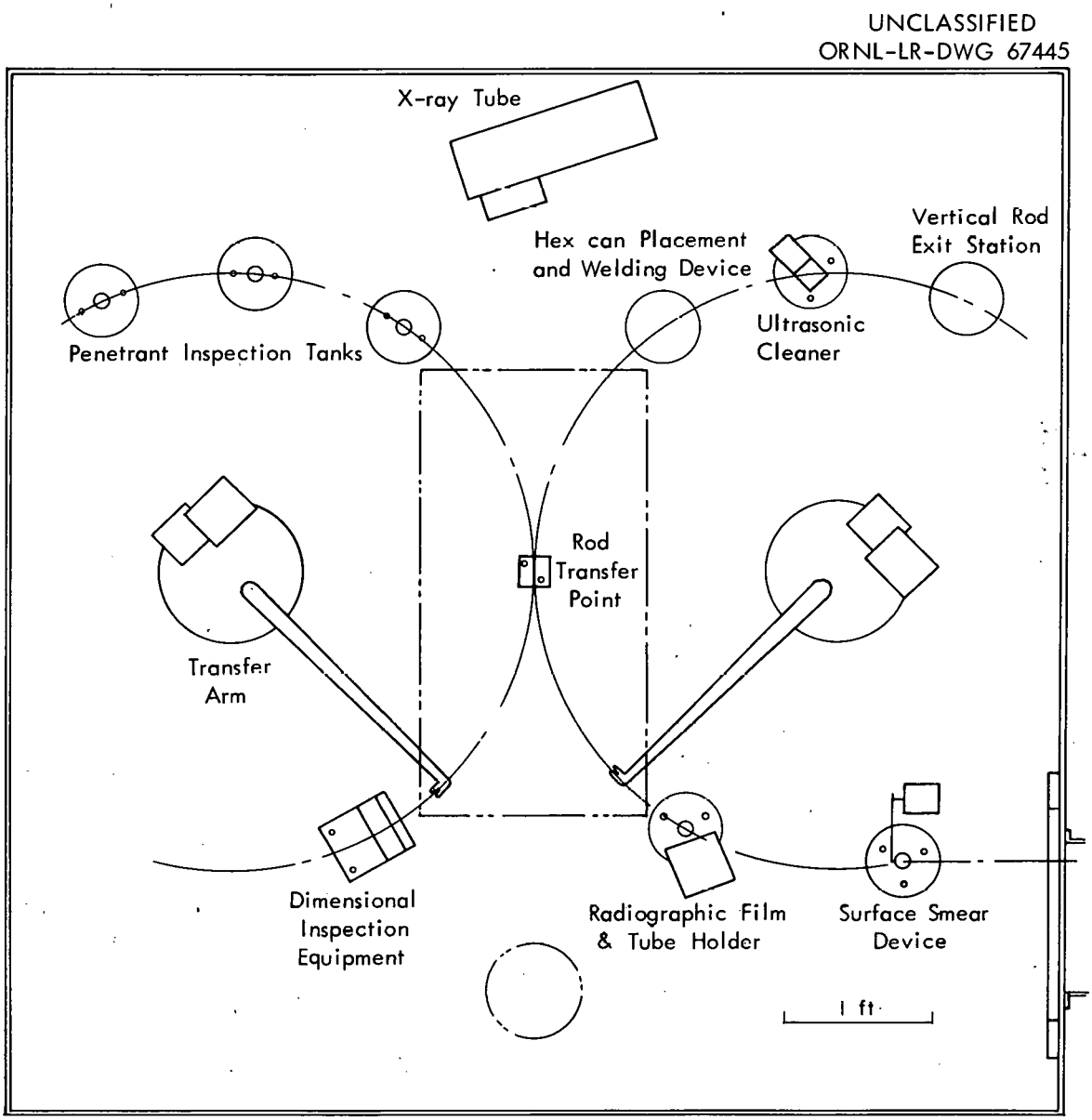

Fig. 4.11. Plan view of equipment, cubicle 1.

research has not progressed to a point where the criteria can be established.

Batch Scale. Preliminary inquiries have been made for procurement of a batch scale. Very little design will be required for use of the commercially available equipment.

Blender-Dispenser. A blending and metering device has been conceptually designed, but additional study is underway to establish the container geometry. Because of the anticipated particle size of the actinide oxide, 0.01 μ, the same container will be used for conveying the hydroxide from cell 4 and for the calcining, blending, and metering steps to eliminate material losses and contamination.

Die Scale. Preliminary inquiries have been sent to scale manufacturers for a top-loading scale with 100 g capacity. On order for test and evaluations is a torsion balance and automatic readout equipment that should weigh with an accuracy of ±5 mg.

Cap-Powder Loader. The aluminum cap-powder loader, which uses volumetric dispensing, has been conceptually designed.

Die Magazine. The die magazine, which has been conceptually designed, will hold 15 dies and will convey the loaded dies from outside the cell to the pellet press.

Press. Conceptual design of the pellet press is complete and approved. Detailing is under way, and fabrication will start in March 1962. The pressing force is furnished by a single-acting spring-return cylinder operated by 100-150 psi water medium.

Ultrasonic Cleaner and Dryer. The pellet-cleaning conceptual design is 50% complete, and preliminary inquiries have been made for equipment needed: an ultrasonic cleaning tank, rotary vibrator feeders, and a heating element in the drying station. The vibratory transfer devices will be used to transfer the pellets from one operation to the next. The cleaning stations are to be enclosed in auxiliary enclosures to decrease the possibility of pellet recontamination.

Transfer Arm. Conceptual design of the transfer arm is 85% complete. The arm, which has horizontal and vertical motions, will be powered with electric motors and will be positioned with positive stops for the various operations.

Cell 2

Pellet Inspection and Loading Equipment. Pellet inspection and loading equipment will consist of the pellet diameter gage, the stacked-pellet length gage, the pellet feeders, and the target tube loader. Conceptual design of this equipment is complete and design details are now being prepared.

Target End Cleaning, Capping, and Welding Equipment. Preliminary studies have been made of a tube and cleaner, a tube end capper which will incorporate devices for evacuation, backfilling with helium for pressing the end cap to the tube, and a fixture for holding the tube. Conceptual design has not been completed, primarily because of the lack of a suitable welding procedure for the end cap.

Helium-leak-test System. A commercial leak detector is being modified to compensate for the long suction and discharge lines and for the absolute filters that must be used. The leak-test chamber has been conceptually designed.

Hydrostatic Pressure System. The pressure chamber has been conceptually designed, and a preliminary inquiry has been issued for an air-powered hydraulic booster pump to deliver 15,000 psi pressure. The pressure chamber will be located in the cubicle and will be connected to the hydraulic booster pump located in the limited-access area of the building.

Ultrasonic Cleaner. No specific equipment has been designed for ultrasonic cleaning of the target tubes. However, other methods tested and found unsatisfactory on target tubes contaminated with UF_4 were dry abrasive metal removal with a centrifugal wheel and wet and dry abrasive removal by a nozzle, both of which used too much abrasive; and steam cleaning with and without an added reagent, which did decrease the tube surface contamination appreciably. The smallest commercially available centrifugal wheel using dry abrasive was 8 in. dia and 3/4 in. thick, and delivered 60 lb of abrasive per minute. Steam cleaning with and without the addition of trisodium phosphate changed the contamination count only very slightly in 5 min, as did a commercial steam jet booster pump, borrowed for evaluation, in 2.5 min operation in which 5 gal of Turco Decon 4513, an acidic detergent solution, 25 gal of water, and 5 gal of condensed steam were used.

Target Transfer Arm. This device will have characteristics similar to the one being designed for cell 3; conceptual design is 75% complete.

Cell 1

Surface Smear Device. Of various materials—white lens tissue (wet and dry), paper wipers, dacron felt, and white foam rubber—investigated for smearing for transferable activity over the entire target rod length, foam rubber gave the best results when UF_4 was the contaminant. Design of the fixture for holding the target rod and smear material will be started shortly.

Radiographic Film and Rod Holder. Conceptual designs have not started on the radiographic film and rod holder; however, it will consist of a shielded container for the target rod and a film magazine holder containing two or four film packs.

X-ray Tube. Vendors have been contacted to obtain information on an x-ray unit capable of operating with power in the range 25-150 kvp at a current of 20 ma.

The tube will have a beryllium window for low filtration.

Penetrant Inspection Tanks. The penetrant inspection tanks have been conceptually designed.

Dimensional Inspection Equipment. Conceptual design of a fixture to check the length, diameter, and bow of the completed target rod is approximately 50% complete.

Transfer Arm. Conceptual design for this arm, which will be similar to that for cell 3, is 75% complete.

4.3 Plutonium Target Fabrication Equipment Development (A. L. Lotts)

Plans are being made for the installation in Bldg. 3508 of a line of equipment to fabricate the HFIR target rods that contain Pu-242. Operations involving Pu-242 must be carried out in glove boxes, but a shielded facility will not be required. The flowsheet for the process and the general description and location of equipment have been established. Some of the equipment has been selected, but no procurement has been initiated. The present schedule specifies that the plutonium target fabrication line will be in operation by January 1963 and the first target of 31 rods will be completed by July 1963.

The criteria that have been established are: (1) the process should, insofar as possible, duplicate the steps of the fabrication scheme planned for the Transuranium Processing Plant; (2) the process should be simple and reliable, and the spread of contamination should be controlled; (3) the equipment should be capable of fabricating approximately 60 target assemblies per year; (4) the equipment must fit into existing laboratory space and, where possible, in existing containment (fume hoods or glove boxes); (5) the equipment should be inexpensive.

4.3.1 Process Flowsheet (Fig. 4.12)

The procedure for fabrication and inspection of plutonium-bearing HFIR target rods starts with the introduction of PuO_2 which, by techniques of powder metallurgy, welding, and inspection, will be finally contained in a finished target element.

4.3.2 Equipment Design

The glove boxes will be standard commercial models made of steel and glass. Most of the boxes will probably be located in Laboratory 5 of Bldg. 3508 and will use existing drains as well as off-gas, electrical, and water services.

Target element components will be transferred between boxes by a bagging technique or by simply connecting the boxes with a polyethylene sleeve lined with a metal protection sleeve. For loading pellets into the tubes, a special interbox

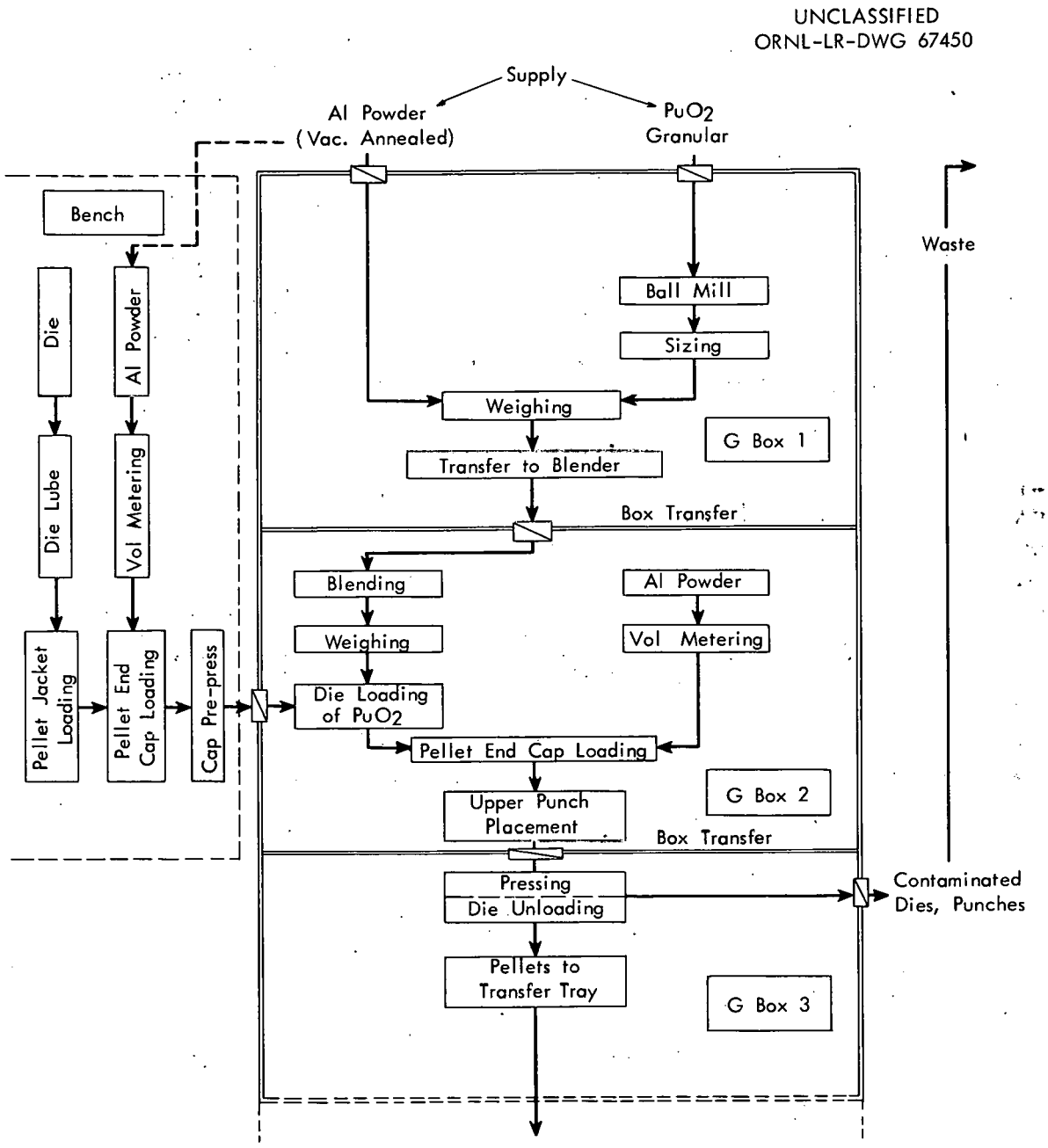

Fig. 4.12. Fabrication diagram for Pu-242 target rods (sheet 1).

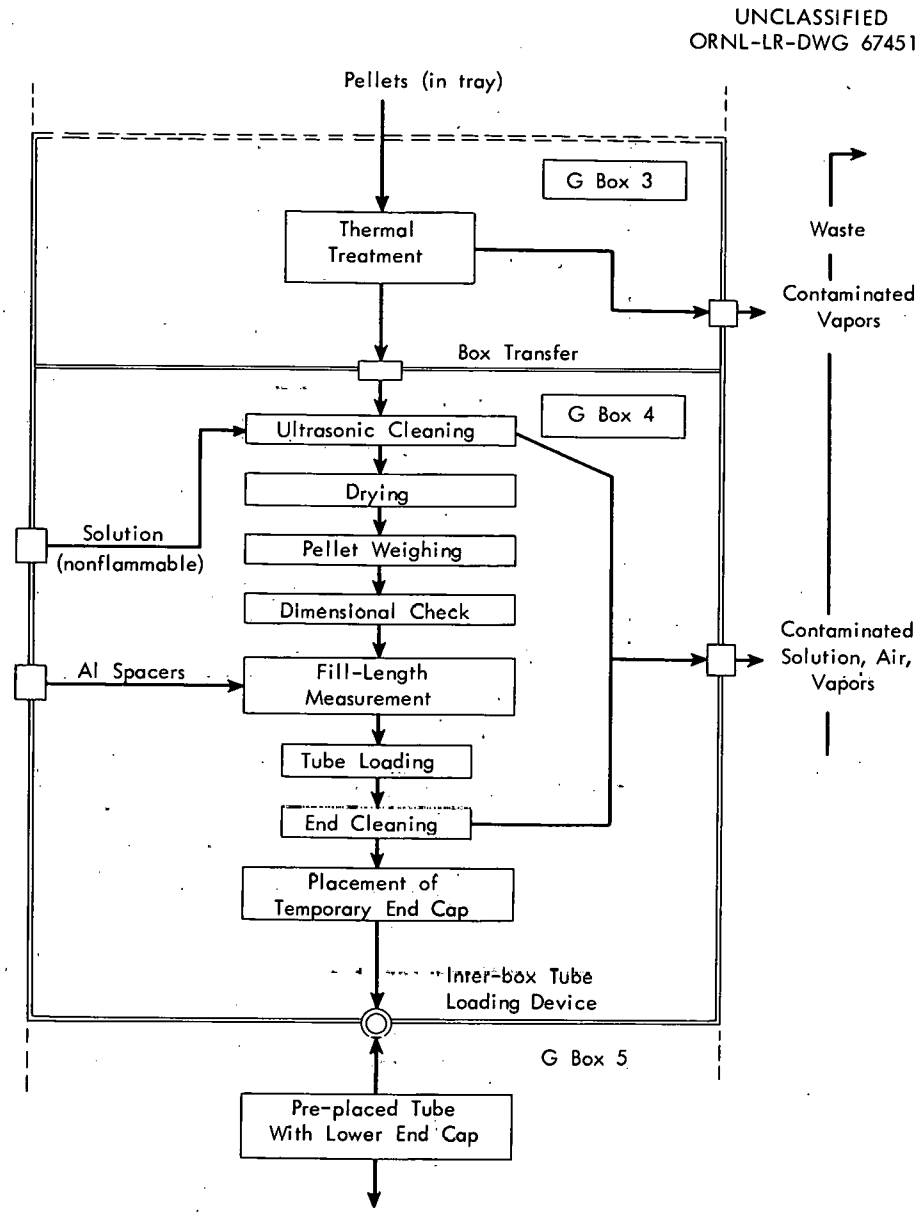

Fig. 4.12. Fabrication diagram for Pu-242 target rods (sheet 2).

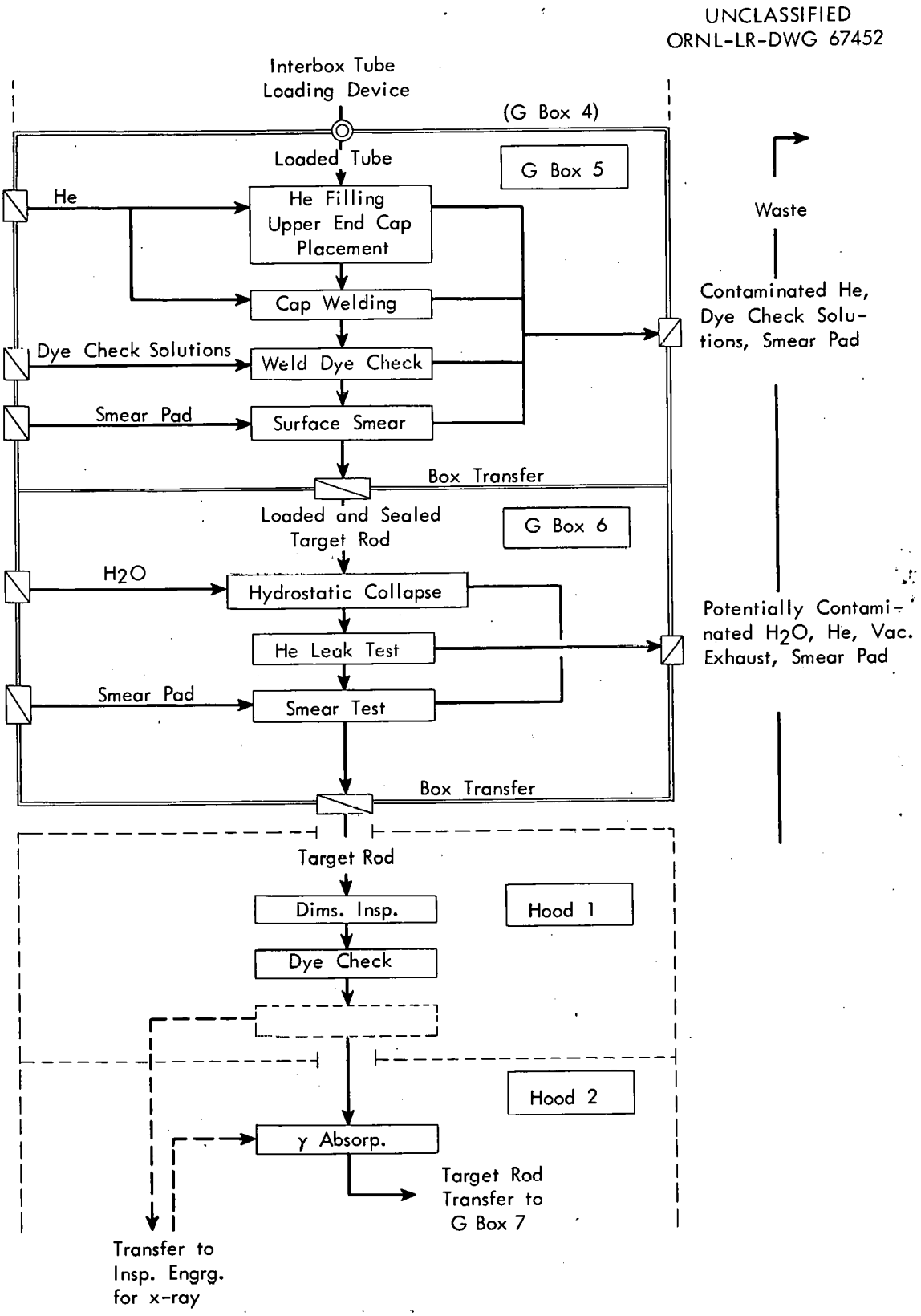

Fig. 4.12. Fabrication diagram for Pu-242 target rods (sheet 3).

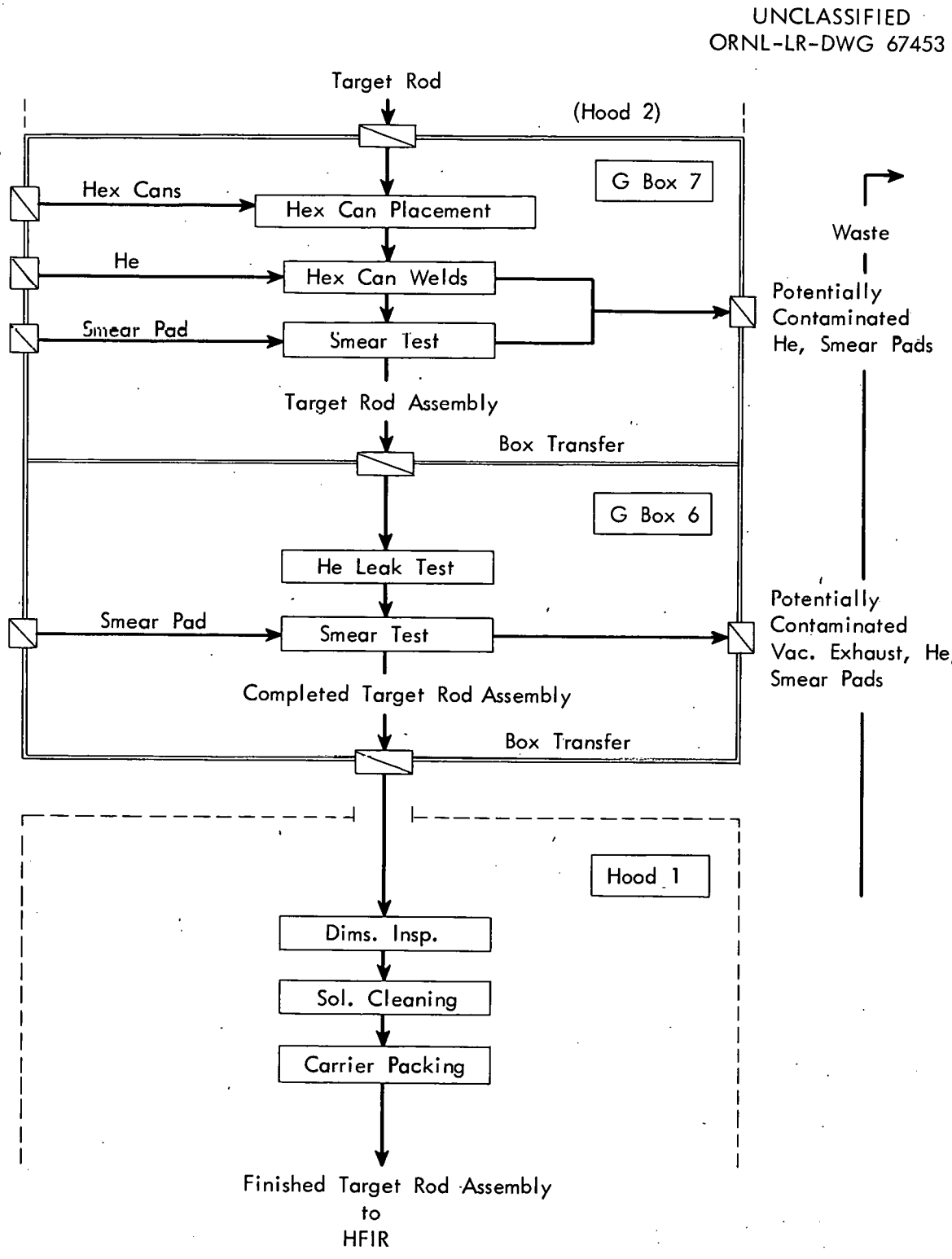

Fig. 4.12. Fabrication diagram for Pu-242 target rods (sheet 4).

tube loading port will be used between boxes 4 and 5. It will be designed so that the bare pellets are not exposed to the atmosphere of box 5.

Operations involving sealed, externally clean elements will be conducted in existing fume hoods except for the radiography of end closure welds, which will probably be done in an existing unhooded facility. To ensure that there is no contamination of this equipment or its environs, the target elements will be wrapped and sealed with a polyethylene bag.

As now planned, the various steps will be largely hand operations. A few steps will be automatic or power-assisted to ensure that the operations are reliably done or that they are not excessively laborious.

Wherever possible, inexpensive, commercially available equipment has been selected for the various operations. This approach was satisfactory for most of the operations through the pellet preparation. For many of the subsequent steps in the process, modifications of equipment designed for the Transuranium Process Facility can be used, but a few pieces must be specially designed and constructed. The commercially available glove boxes must be modified somewhat to accommodate maneuvers that must be made with the target rods.

5.0 TRANSURANIUM FACILITY DESIGN
(W. E. Unger)

5.1 Target Processing (J. E. Bigelow)

5.1.1 Dissolution of Aluminum

The dissolution rate of the aluminum targets must be kept below 1 $mg/cm^2 \cdot min$ to control the rate of evolution of hydrogen, the volume of which plus purge gas to dilute it below the explosive level could otherwise exceed the design capacity of the off-gas system. Calculations have shown that this can be done by temperature control of the dissolver. Measurements of the heat transfer from dissolving aluminum showed effective heat transfer coefficients for a vertical rod varying from 500 to 1300 $Btu/hr \cdot ft^2 \cdot °F$, depending on the dissolution rate. Calculated coefficients were of the order of 50 for natural convection and 500 for forced convection with a draft tube. Evidently the strong evolution of hydrogen from the aluminum surface creates as much circulation of the bulk liquid as a draft tube. Heat transfer is probably further improved by the scouring action of the hydrogen bubbles as they agitate the stagnant surface film.

A momentary increase in the dissolution rate will cause a rise in the metal temperature, which in turn will further increase the dissolution rate. However, the larger temperature difference between the metal and the dissolver solution and the increased heat-transfer coefficient increase the rate of heat transfer to the solution

sufficiently to bring the rod back to the original temperature and restore the dissolution rate.

5.1.2 Solvent Extraction Studies

Three of the main chemical separation steps in the TRU chemical processing flowsheet are solvent extraction processes, two of which require multistage contactors. A code was written in Algol for the Oracle to carry out calculations with the equations describing the distribution of various components between the two streams leaving the contactor. This code, called KREMSER-MURPHREE, can be used to calculate either the number of stages required for a specified degree of separation or the separation attained for a given number of stages. The distribution coefficients and the stage efficiencies may be different for the scrubbing and extraction sections, but must be constant within each section. Two to 12 components can be considered at once.

The code was used to calculate the distribution of five actinide elements in the second solvent extraction cycle of the TRU flowsheet (Dwg. E-34610). Partial results of four calculations (Fig. 5.1) showed that if the normalities of the feed and scrub are <1.55, berkelium will be preferentially extracted and can be separated from curium (and americium). At an acid normality of 1.0, berkelium recovery would be >99.9% with curium contamination reduced by a factor of $>10^5$. At higher acidities the berkelium will remain in the raffinate and hence can be separated from californium, which tends to remain in the extract. This separation is less clean because of the smaller difference in distribution coefficients. For example, at 1.9 N HCl, berkelium recovery in the raffinate is ~95% with reduction of californium contamination by a factor of only 10^2.

These calculations were made for americium, curium, berkelium, and californium feed concentrations as given by the flowsheet for 1-year irradiated Pu-242. An arbitrary value of 1 was taken as the einsteinium feed concentration. Distribution coefficients as a function of aqueous phase acidity were obtained from laboratory studies. Eight stages with a Murphree efficiency of 70% were assumed for both scrub and extraction sections. The feed/scrub/extractant flow ratios were taken as 1/1/2.

A further set of calculations was made for the same feed except that the feed acidity was constant at 0.5 M and the scrub acidity was varied. The results (Fig. 5.2) indicate an increase in overall performance, with both an increase in berkelium recovery and a decrease in curium contamination of the berkelium product. With a high-acid scrub and low-acid feed, curium can reflux in the column and build up to a concentration much higher than that in the feed. This causes a long equilibrium time, with startup and shutdown problems, and may even accelerate solvent radiation damage. The actual concentrations reached in such a refluxing system have not yet been calculated. However, the 16-stage separation appears to make an adequate separation even without refluxing.

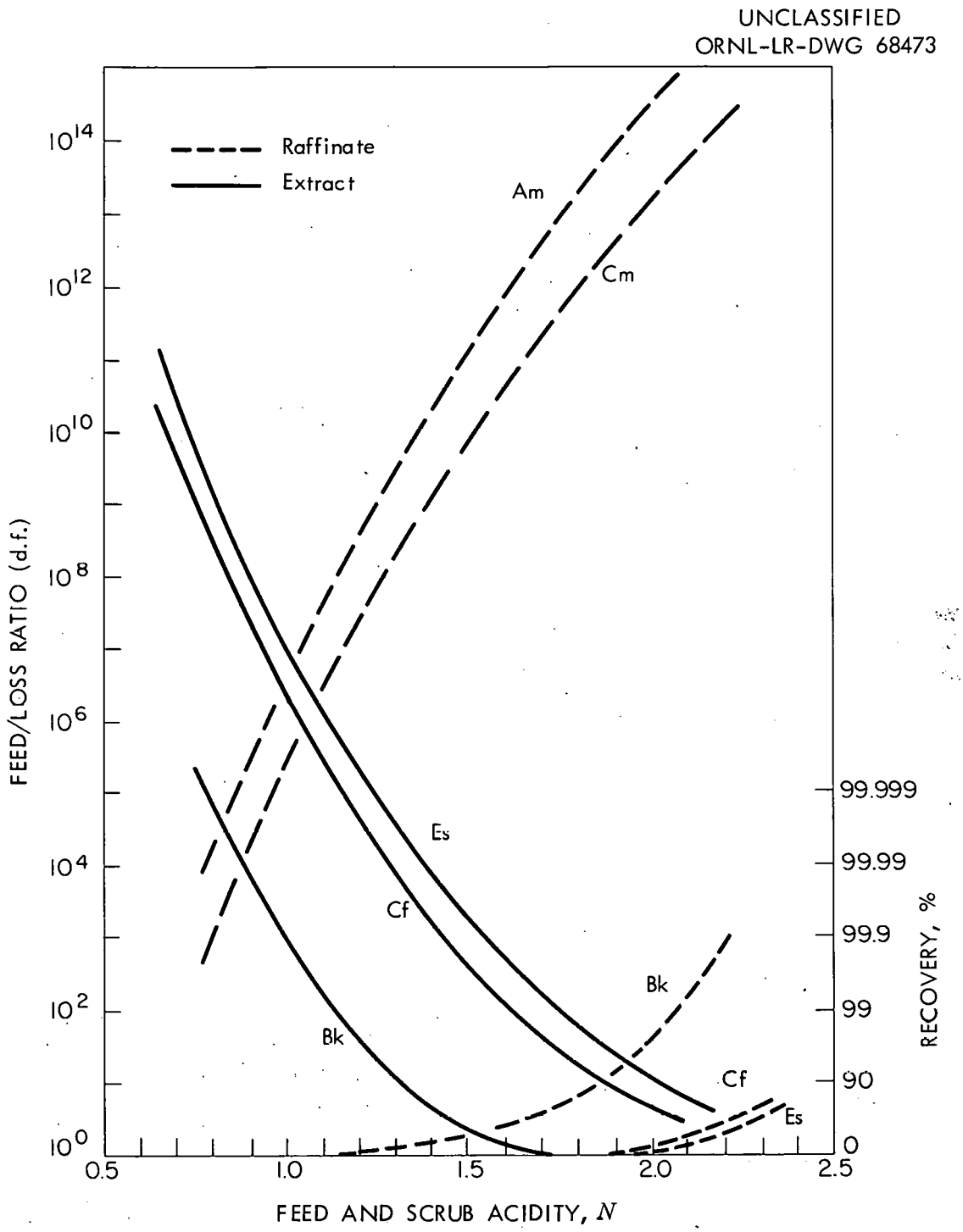

Fig. 5.1. Calculated actinide recovery and decontamination in phosphonate extraction from HCl solution by 0.8 *M* 2-EH(ØP)A in DEB. HCl concentration in scrub same as that in feed. Extraction section: 8 stages, 70% Murphree efficiency; scrubbing section: 8 stages, 70% Murphree efficiency; scrub/feed flow ratio = 1; extractant/feed flow ratio = 2; data from Baybarz (ORNL), personal communication. See note on Fig. 5.2.

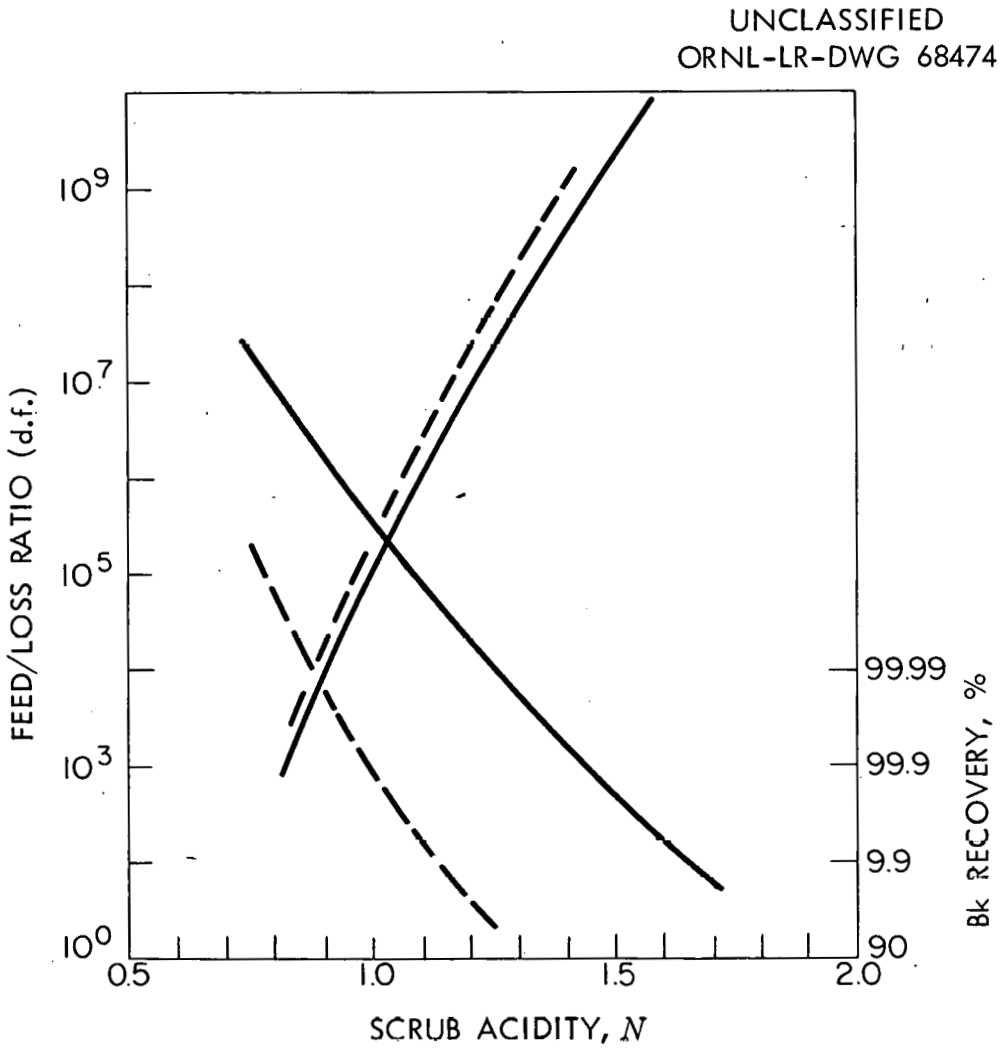

Fig. 5.2. Effect of feed acidity on distribution of berkelium and curium between raffinate and extractant (see Fig. 5.1). —— 0.5 M acid feed, scrub acidity varied. —— feed acidity = scrub acidity. The curves of Figs. 5.1 and 5.2 can be read on either ordinate. The right-hand one gives the percentage recovery of the component in the indicated phase. Decontamination factors for the stated element based on another component that is recovered in the other phase are read on the left-hand ordinate.

The partitioning of berkelium from californium was examined in more detail. A partitioning solution with an acidity of 1.9 N and a feed of berkelium and californium in the organic phase from the curium separation discussed above were assumed. A berkelium recovery of 95% with the californium contamination decreased by a factor of 100 was specified. The scrub and extractant flow ratios were varied and the number of stages required to achieve the specified separation were computed. The calculations (Fig. 5.3) showed that separation of berkelium and californium by this system is very marginal. Figure 5.4 is a plot of the minima of the curves in Fig. 5.3. Since the highest practical ratio of scrub to feed is about 2, some 22 stages (70% efficiency) would be required for the specified separation. Figure 5.5 shows how this number is affected by the required berkelium recovery.

A single calculation on the possibility of separating americium from curium indicated that this is not practical. Conditions were probably not optimum, but 32 stages (70% efficiency) gave 99.6% curium recovery with only half the americium removed.

5.1.3 Preparation of Actinide Oxide

Two common methods of preparing the oxides of the transuranium elements are (1) precipitation as the oxalate followed by calcination at ~800°C and (2) slow neutralization (such as by the controlled hydrolysis of urea) and precipitation as the hydroxide. The hydroxide can be converted to the oxide at 500°C or lower. The much lower temperature of calcination for the hydroxide leads to a number of simplifications in subsequent processing. Less expensive materials may be used for the calcination vessel, which may then be processed to recover residual product. The rods used to break up agglomerates could be made of aluminum to eliminate contamination of the powder, and the chance of forming low-melting glasses which would cause the oxide to form clinkers is decreased. The advantages of the hydroxide route appear to outweigh the necessity for installing an extra purification step before the precipitation. However, the design should be such as to permit a changeover to the oxalate system because if plutonium is ever to be fabricated in the TRU Facility, the oxalate precipitation must be used to avoid the gel-like polymer formed on hydrolysis of plutonium.

5.2 Chemical Processing Equipment Design (W. D. Burch and O. O. Yarbro)

Conceptual studies which will ultimately determine the criteria to be followed in the detailed design of the chemical processing equipment were largely completed. Included were the establishment of tentative irradiation and processing schedules, equipment flowsheets, equipment sizes, and throughput rates. Initial conceptual layouts of all equipment in cubicles and tank pits and the methods of installing this equipment were completed. Detailed design of service line penetrations into both the tank pits and the cubicles and of the hot disconnect well in the cubicles was started.

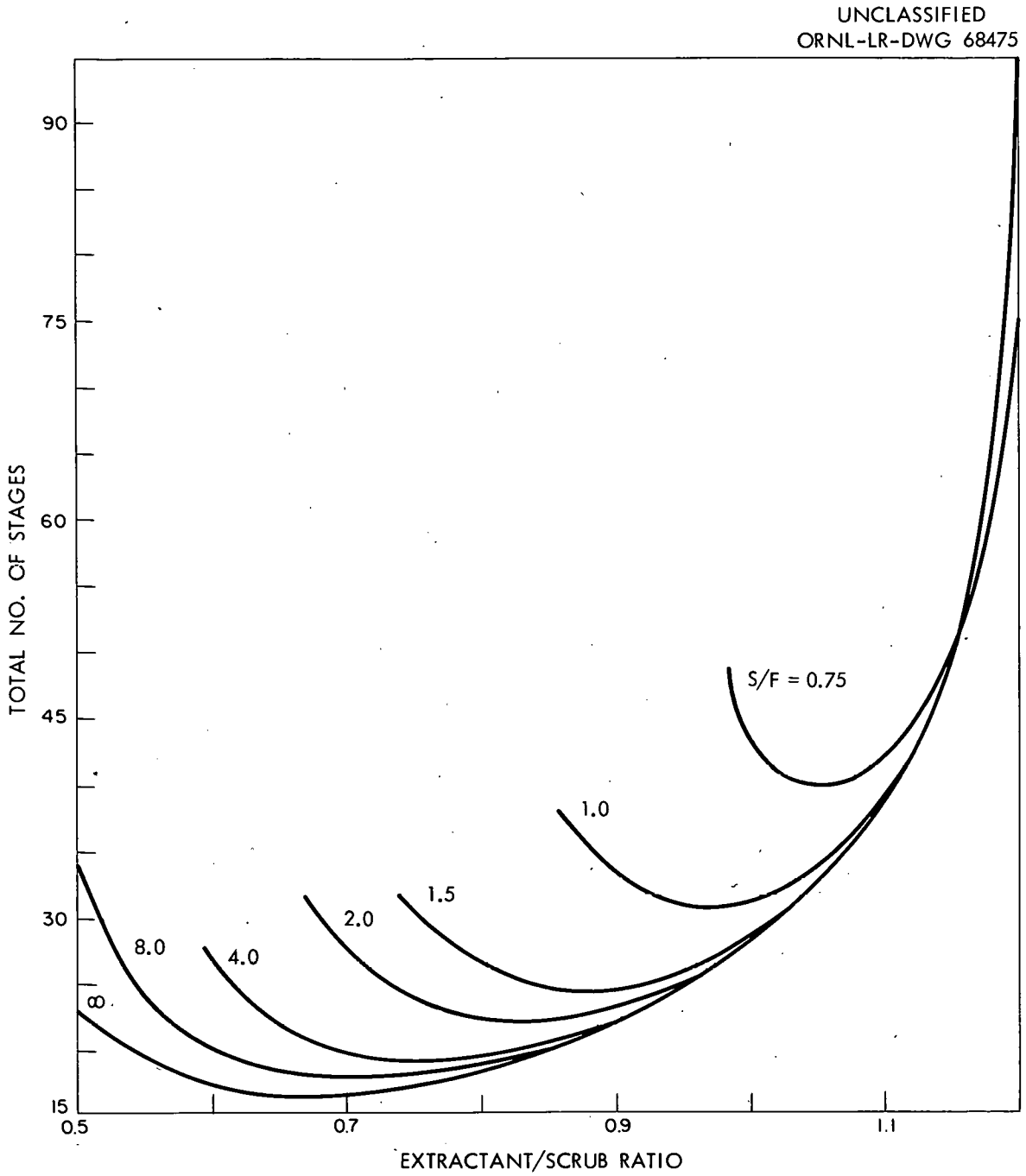

Fig. 5.3. Number of stages required to partition berkelium from californium as a function of extractant/scrub ratio with varying scrub/feed ratio. Specifications: 95% berkelium recovery, californium decontamination factor of 100.

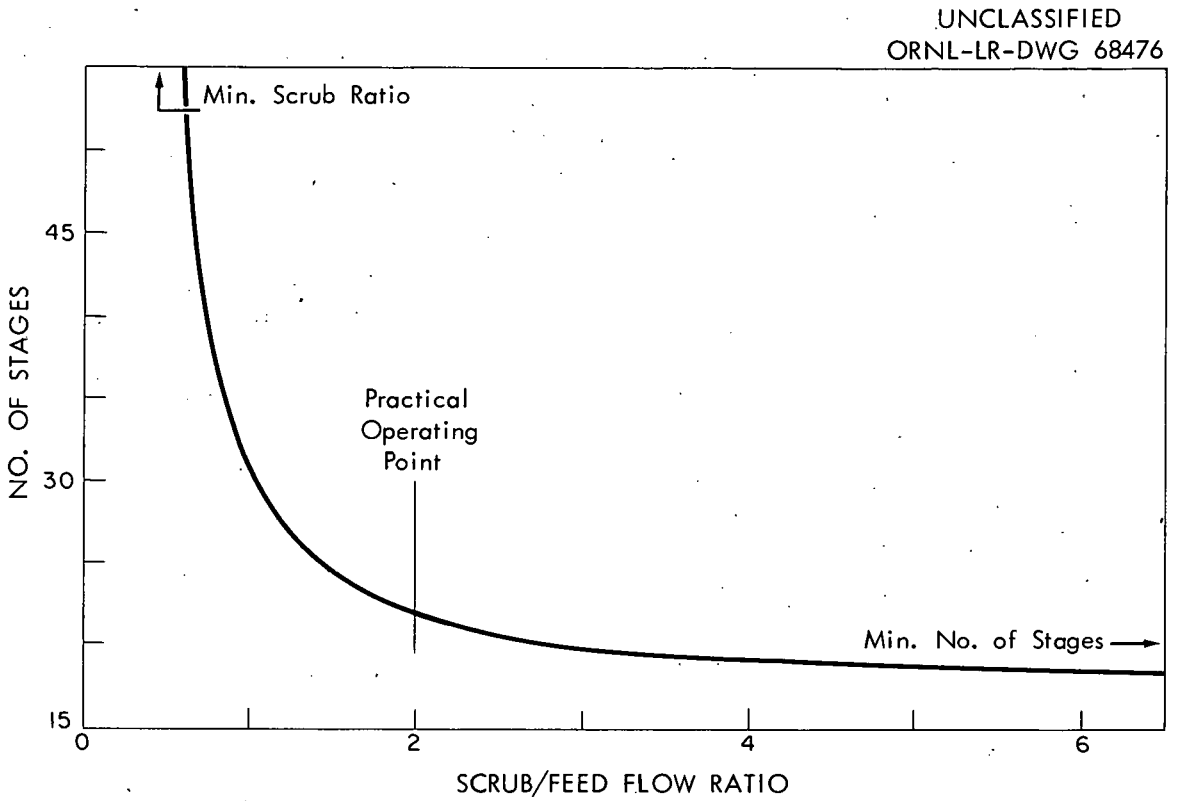

Fig. 5.4. Cross plot of minima of Fig. 5.3. Berkelium recovery of 95%, californium decontaimination factor of 100.

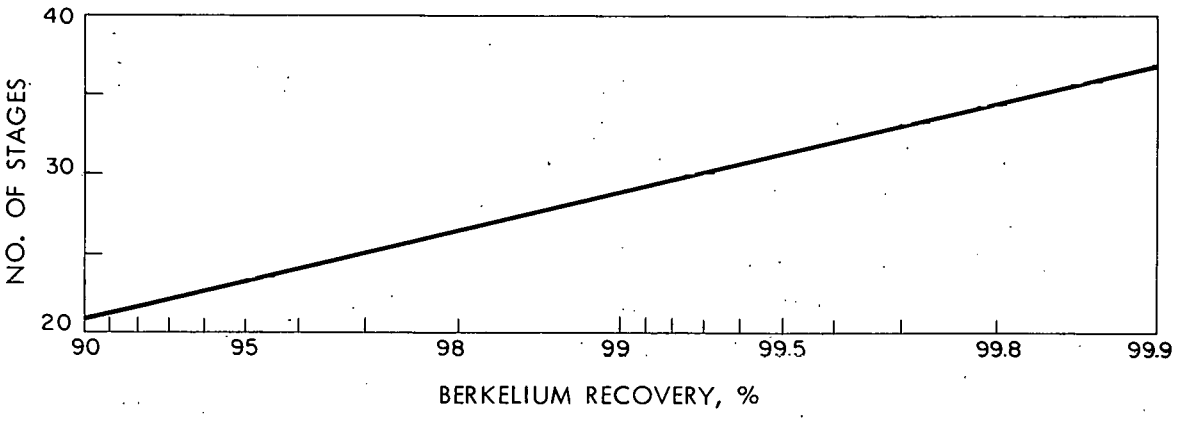

Fig. 5.5. Effect of required berkelium recovery on number of stages. S/F = 2.0; E/S = 0.9. Californium decontaimination factor = 100.

5.2.1 Plastic Materials of Construction

The decrease in the expected radiation levels in the TRU Processing Facility, due to the lower values of Cf-253 capture cross-section now assumed, permits consideration of organic compounds for certain applications in the cells and cubicles. A literature survey showed the following compounds to have the best probability of combining radiation resistance and resistance to chemicals used in the TRU chemical processing flowsheet:

	Exposure Resulting in Significant Damage, whr/g
Container and Tubing Materials	
Glass-fiber reinforced epoxy resins	20
Acrylic butadiene styrene	>0.25
Allyl diglycol carbonate	0.25
Polyethylene	0.25
Chlorinated polyether	~0.1
Gasket and Booting Materials	
Acrylic nitriles	0.4
Hypalon	0.1
Neoprene	0.1

5.2.2 Irradiation and Processing Schedules

When the TRU Facility is ready for full-scale operation in January 1966, the first HFIR loading of 31 rods will have been irradiated for about 16 months, discharged from the reactor, and be awaiting processing. The chemical processing system is designed for a throughput rate of one target per day, which will permit processing 10 first-cycle plutonium rods per month on a semicontinuous basis; thus approximately three months will be required to process the first loading and fabricate the curium isotopes into recycle rods for further irradiation. At the design capacity, no more than 50% of the time will be required for main-line processing. The remainder is reserved for special separations, equipment modifications, and maintenance. On a long-term basis, approximately 40 target rods will be processed per year, one-half of which are first-cycle and the remainder recycle rods. One hundred milligrams of californium will be recovered from the initial HFIR loading, and two years after startup of the TRU Facility the californium inventory should reach 1 g.

5.2.3 Equipment Flowsheets

Schematic flowsheets developed from chemical flowsheets for the main-line processing (Figs. 5.6 and 5.7) provide for dissolution, feed adjustment, and first cycle solvent extraction to be done in cell 7. Americium and curium will be

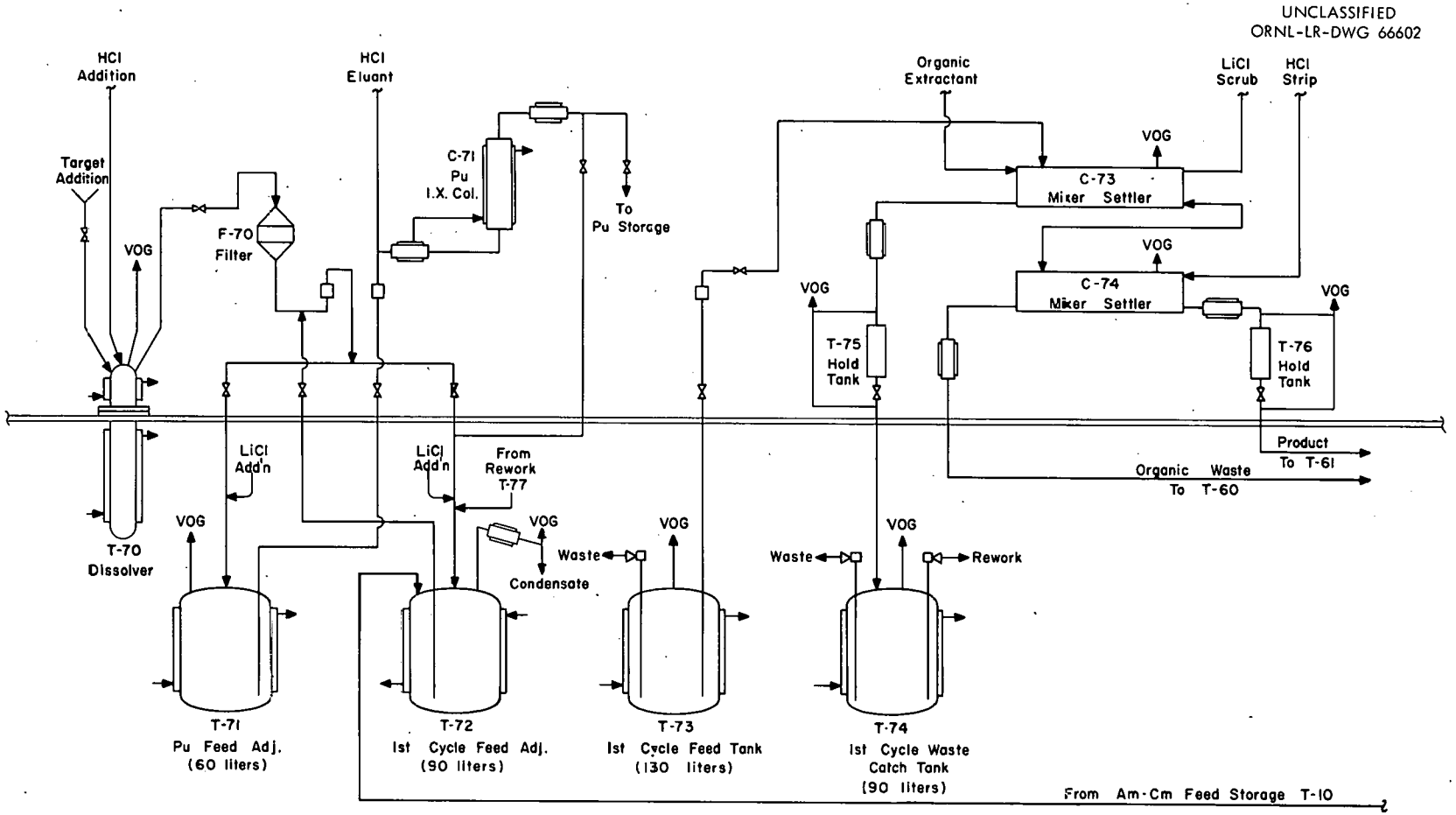

Fig. 5.6. Target processing equipment flowsheet, cell 7.

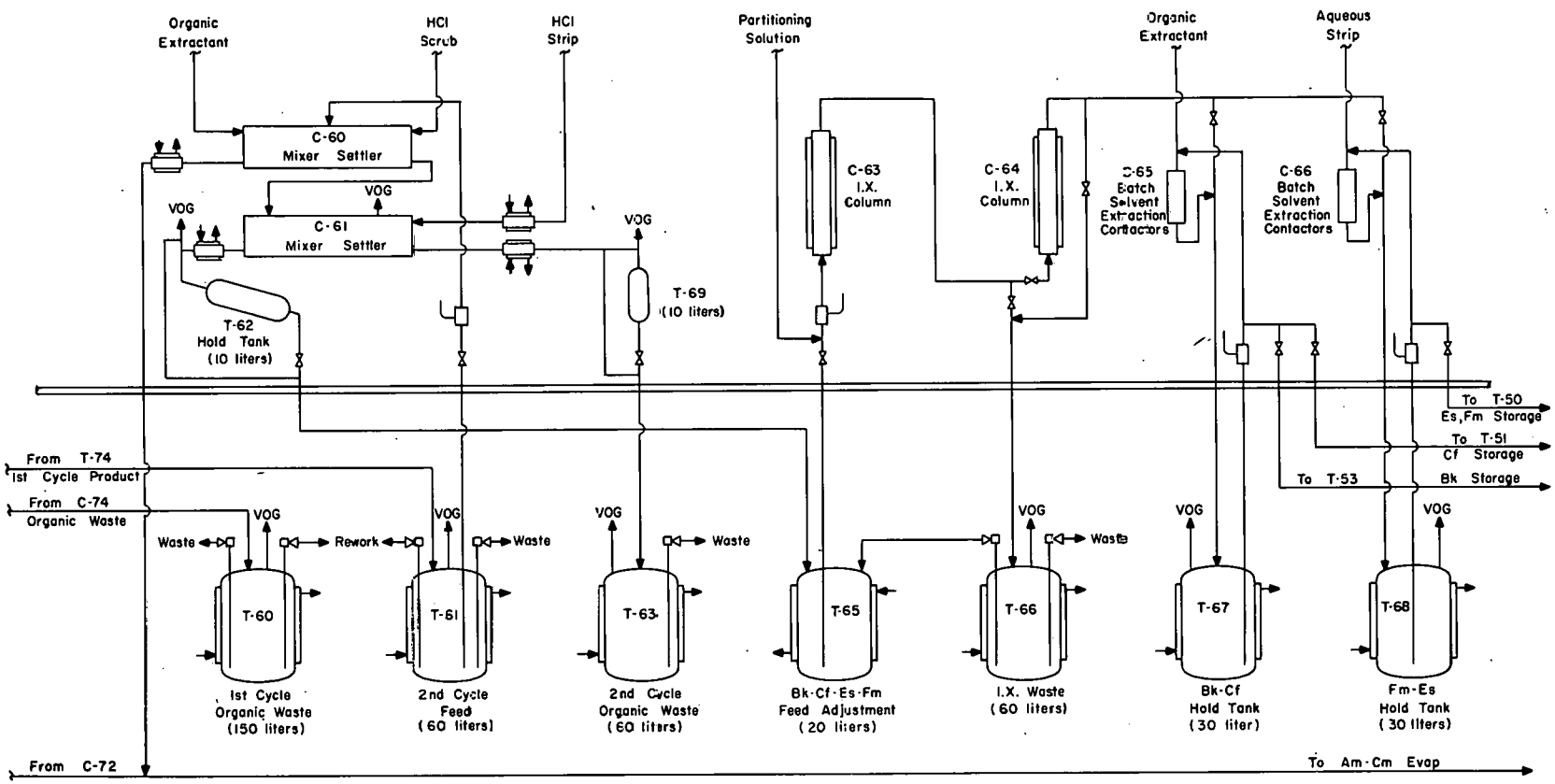

Fig. 5.7. TRU equipment flowsheet, Cell 6.

separated from the higher actinides by solvent extraction, and berkelium, californium, einsteinium, and fermium will be separated by ion exchange in cell 6. Flowsheets for product purification and special product separations, to be done in cell 5, have not been developed.

In cell 4, curium will be purified and precipitated for subsequent calcination and fabrication into recycle rods. Tankage for the various processes is located, where possible, in tank pits of the respective cells where the solvent contactors or ion exchange columns are located. At least part of the tank pit space in cells 1, 2, and 3 behind the target fabrication cubicles must be used for product storage tanks and rework systems.

5.2.4 Conceptual Layouts

Typical Cubicle. All vulnerable process equipment will be located on removable racks in the cubicles. Three such racks, approximately 36 in. long, 18 in. wide, and 6 ft high are located in each cubicle (see Fig. 5.8). Incorporated into the lower half of the back rack is a sampler system containing diaphragm pumps to pump solutions through the needle block assembly and mechanisms for handling sample bottles. Service lines enter through the cubicle ceiling and are joined to the equipment at the rear of each rack with a standard TRU disconnect (see Fig. 5.9). Process jumper

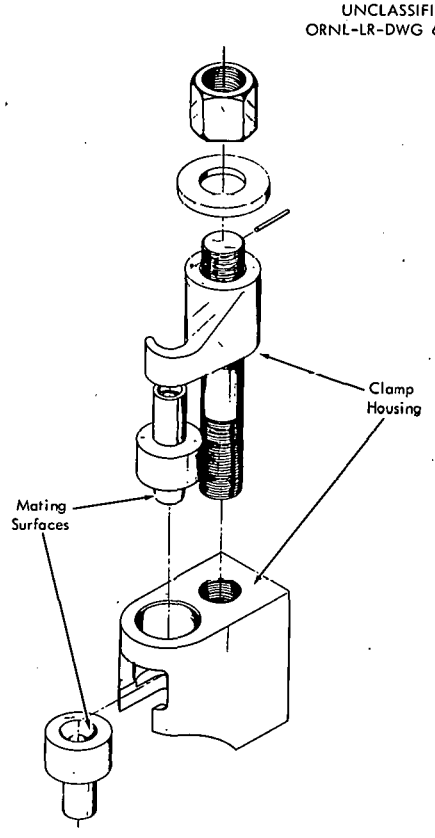

Fig. 5.9. TRU process disconnect.

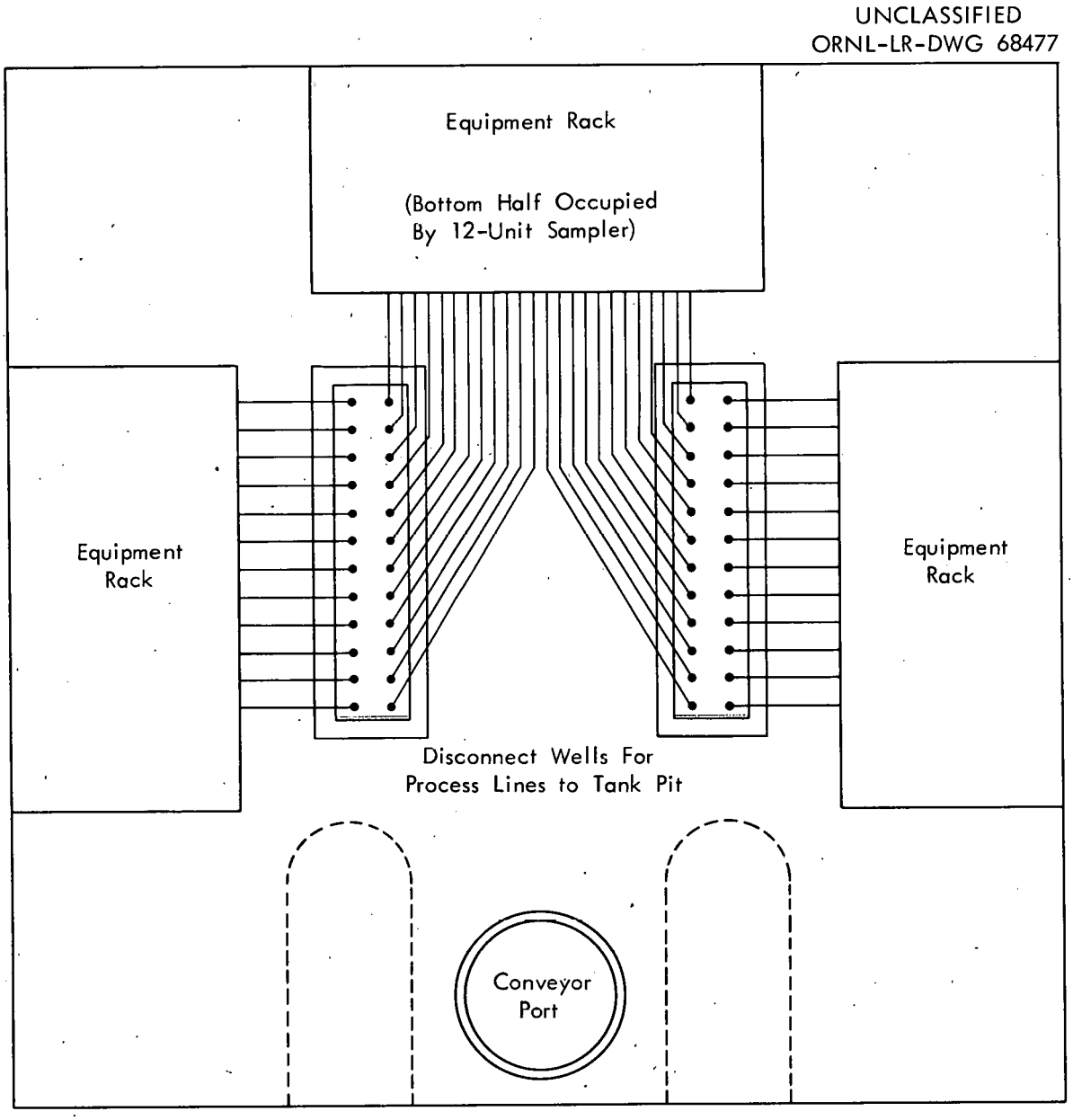

Fig. 5.8. Typical cubicle layout plan.

lines, provided with similar disconnects, join the various equipment racks, samplers and the hot disconnect wells through which solutions are routed to the tank pits behind the cubicles. Maintenance to be performed by the in-cell master-slave manipulators includes replacement of individual components such as pumps, valves, and sample needle blocks, and installation of entirely new equipment racks. Conceptual layouts (e.g. Fig. 5.10) of all main-line process equipment were made to ensure that adequate space was available for all required operations.

Typical Tank Pit. All tanks, which should require only infrequent maintenance, are located in the tank pits. Because of the high probability of corrosion failures and the necessity for designing a flexible system which can be modified if desired, all tanks and piping in the tank pits are designed to be replaceable with the use of water shielding and overhead maintenance techniques. A typical layout and an elevation view of a typical tank and its connecting lines are shown in Figs. 5.11 and 5.12. Service lines penetrate the rear wall and contain a disconnect at the inner cell wall. Process jumper lines, which connect the various tanks, waste and off-gas headers, and cubicle hot well, may be replaced or rerouted as required. Tank elevations are such that a minimum of 3 ft of water shielding covers all tanks when the pit is flooded to the maximum level. All disconnects are located above this water level so that the tanks will not fill when the cell is flooded.

5.2.5 Detailed Design Features

Hot Disconnect Well. Spare lines will be incorporated into the two line bundles connecting cubicles and tank pits, but complete reliance on a permanent nonreplaceable installation does not appear logical. Therefore these line bundles with their hot disconnect well in the cubicle floor and disconnect terminal block on the tank pit were designed for replacement (Fig. 5.13). After removal of all process jumper lines connected to both ends of this bundle, the well in the floor of the cubicle is unbolted from the cubicle and the assembly dropped onto tracks suspended from the cubicle floor. The entire unit is then withdrawn into the tank pit by a cable and pulley arrangement. A new bundle is installed by reversing these operations.

Tank Pit Service Plug. Service lines to the tank pits will be brought in through stepped concrete plugs (Fig. 5.14). All lines to any given tank will be brought through the same plug. Present plans call for only one disconnect in each service line, to be located as shown at the cell side of the plug. The female half of the disconnects on the tank end of the service lines will be mounted in a support bracket which bolts to the face of the plug and at the same time aligns both halves of the disconnects. The 0.5-in.-dia lines are offset 1.5 in. in the plug to minimize streaming.

Vents on Steam Supply Lines to Process Jets. A system designed to vent steam supply lines to process jets and thus prevent solution from being drawn back into the line by condensing steam functioned properly in engineering tests. A continuous air

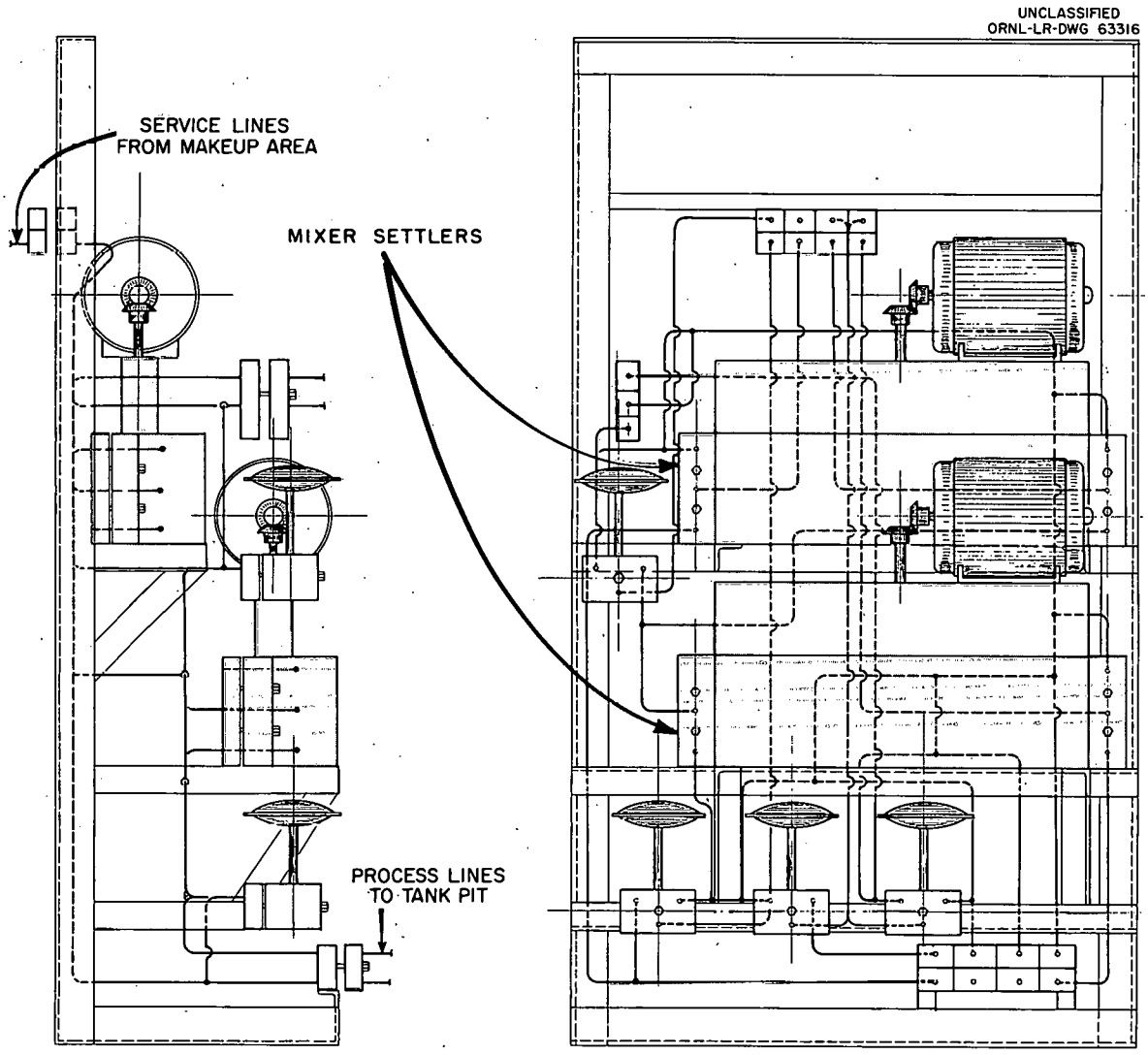

Fig. 5.10. TRU process cubicle typical equipment rack.

UNCLASSIFIED
ORNL-LR-DWG 63314 R 1

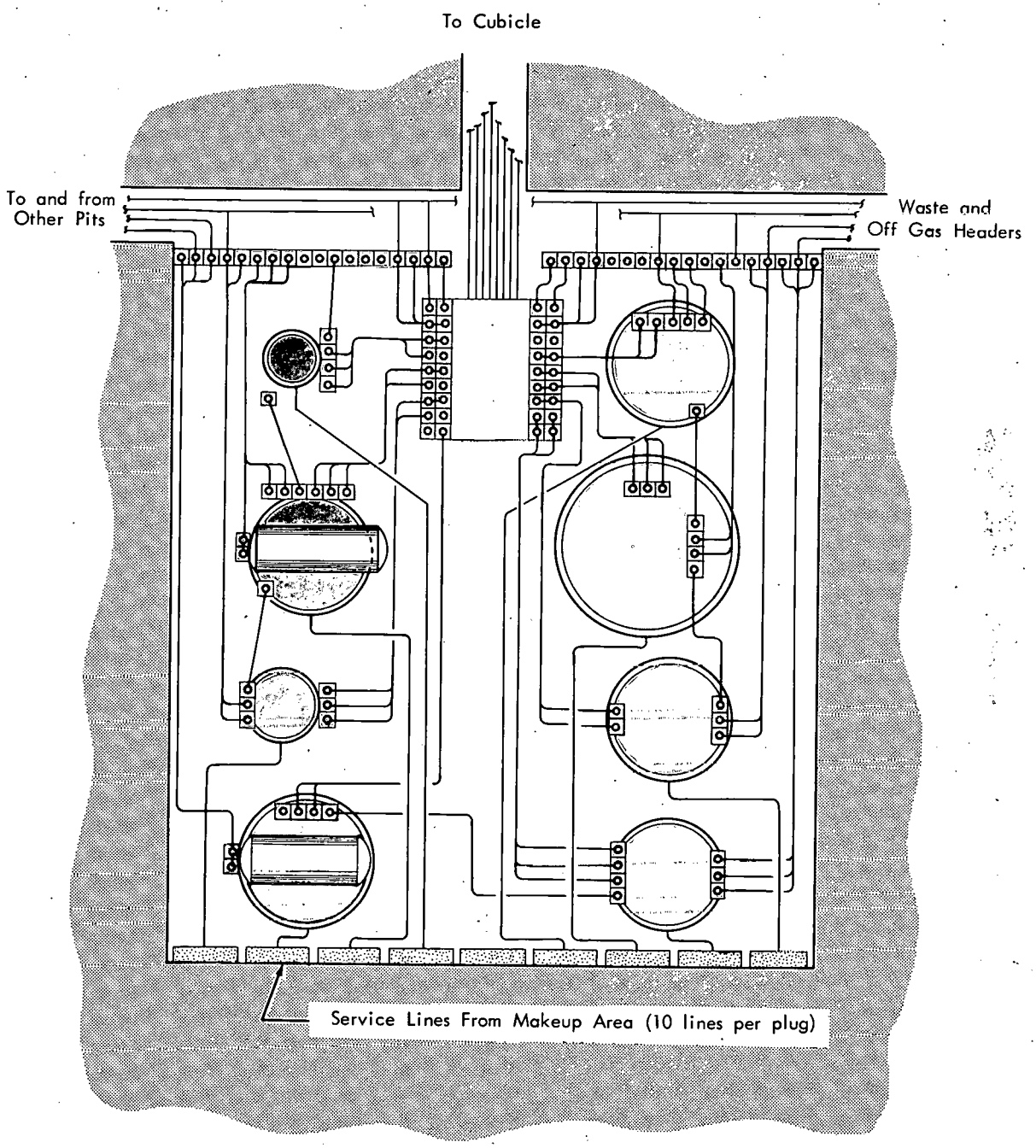

Fig. 5.11. Typical tank pit piping layout plan.

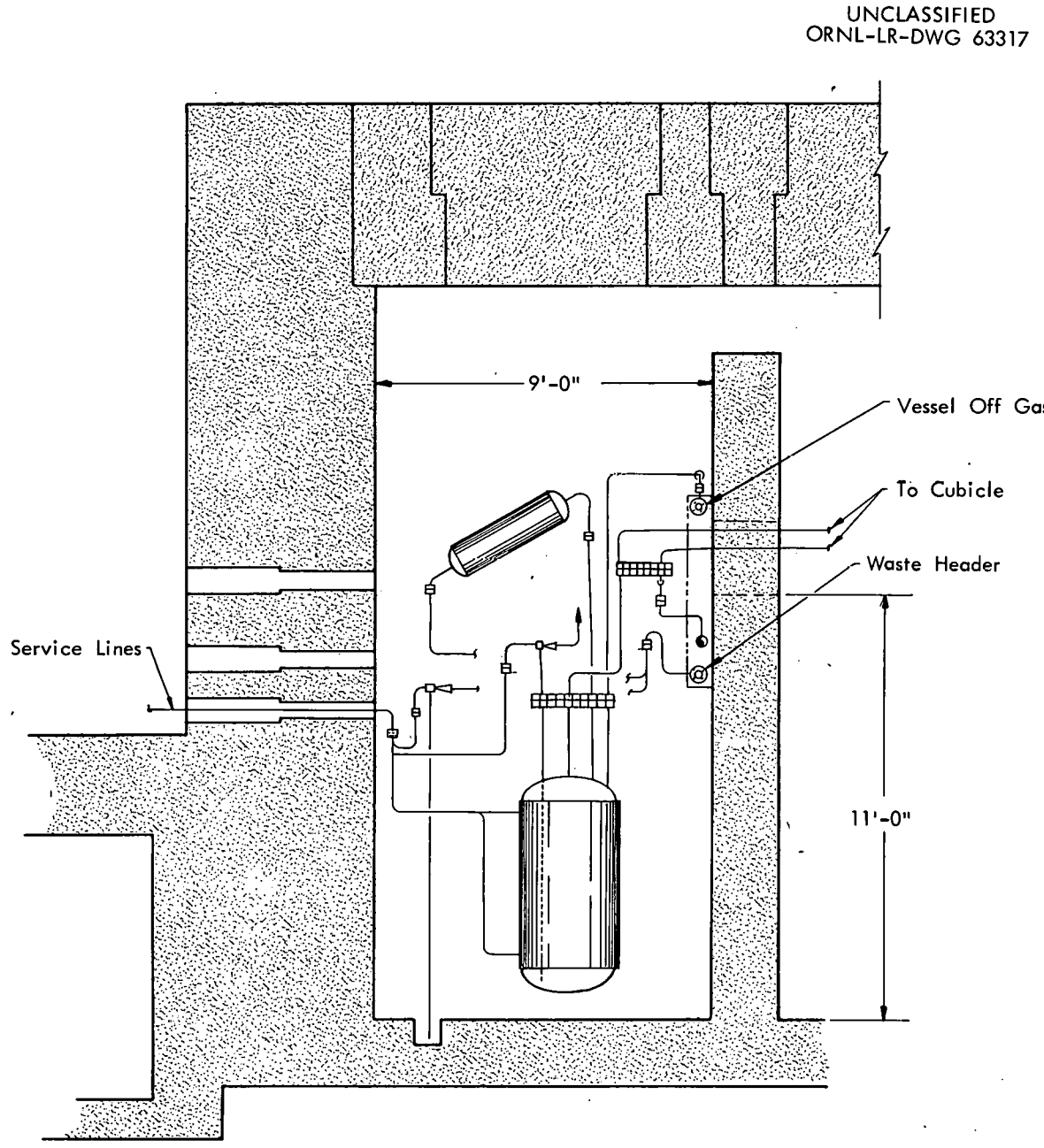

Fig. 5.12. Typical tank pit piping layout, elevation.

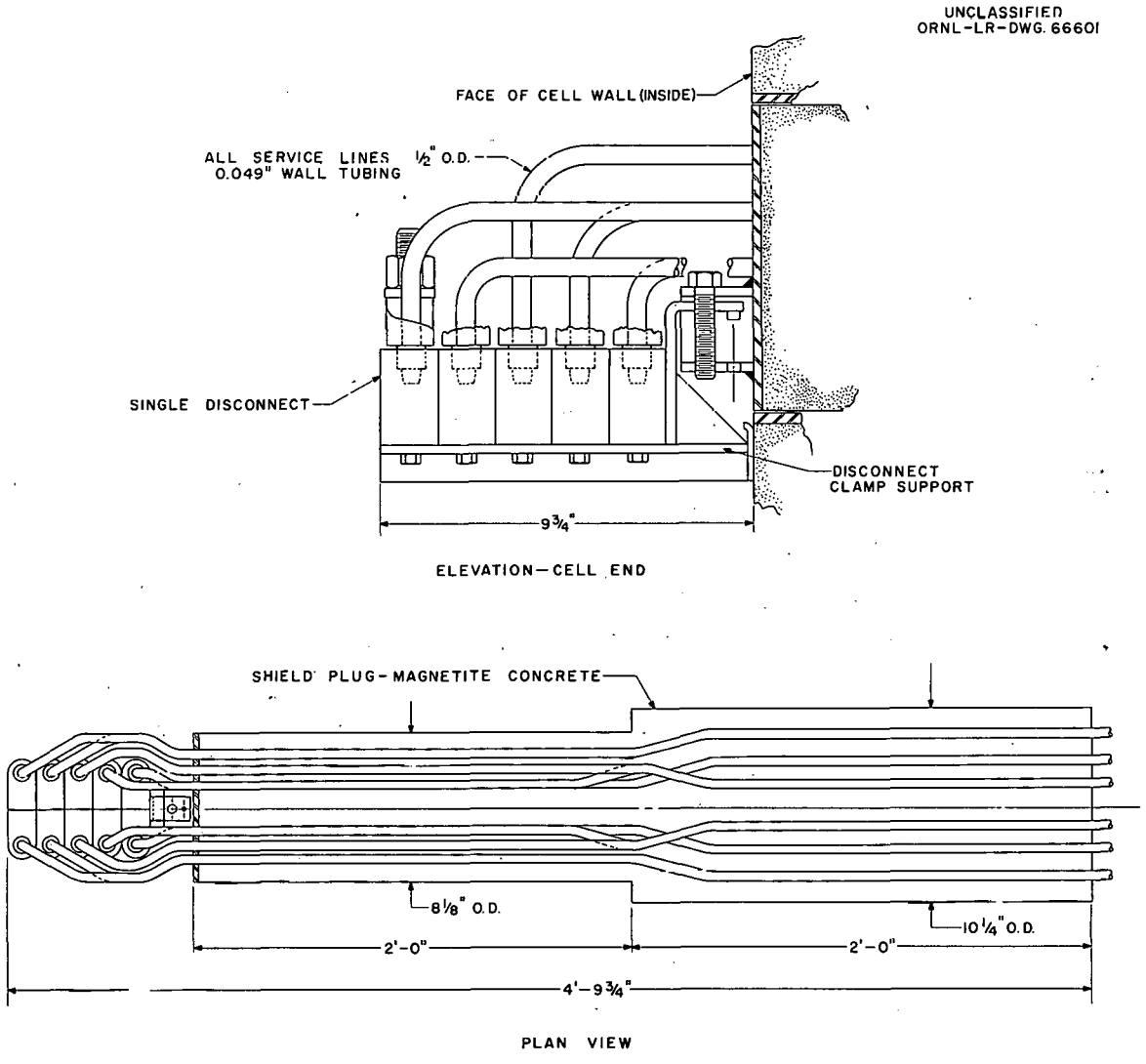

Fig. 5.14. Tank pit service plug.

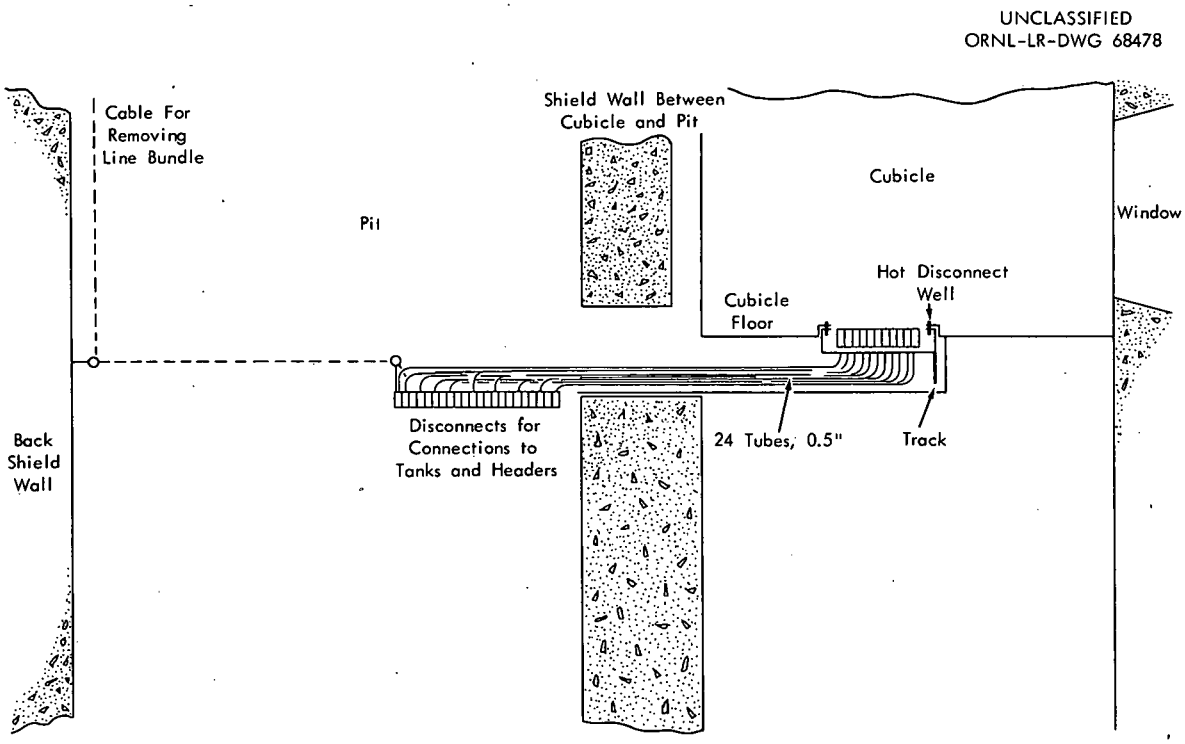

Fig. 5.13. Hot disconnect well replacement method.

purge of 200 cc/min is discharged into the steam line from a 100-psi air header through a 500-cc accumulator. Following a jetting operation, residual steam is purged from the line before sufficient condensation occurs to suck solution more than a few inches up the steam line. Such a system is cheap, requires no elaborate instrumentation, and thus should be essentially foolproof. The total purge rate through all jets (about 10 liters/min) will not tax the capacity of the off-gas system. Optimum purge rates and accumulator size were determined in the tests.

5.3 Shielding, Hazards, and Target Calculations (J. E. Bigelow, J. P. Nichols)

5.3.1 Shielding Studies

TRU shielding design is based on sources constituted by a solution containing 2×10^5 curies of Ce-144-Pr-144 from burnup of 10 kg of Pu-239 and by a fifth cycle target, composed of residual actinides from successive High Flux Isotope Reactor irradiations, which contains 305 mg of californium and spontaneously emits 3×10^{12} fission neutrons per second. During the processing of these sources the radiation dose rate in normally occupied areas is to be no greater than 0.75 mrem/hr with permissible hot spots around penetrations no greater than 2.5 mrem/hr.

Using Renupak, a code for moments method solution of the neutron transport equation, and SDC, a gamma penetration code, it has been determined that a cell shielding wall of 54 in. of magnetite concrete, of water content, 12.2 lb/cu ft,

satisfies the dose rate criteria. The dose rate is controlled by fast neutrons from the fission source and is increased by factors of 5 and 50 for water contents of 6.1 and 3.0 lb/cu ft, respectively.

A 54-in.-thick cell shielding window, consisting of laminations of oil, 2.7 g/cc glass, 3.3 g/cc glass, and 6.2 g/cc glass, was developed in an experimental program at the ORNL Lid Tank Shielding Facility. Fission neutron removal cross sections of window components were determined to be 0.076, 0.080, and 0.095 $\pm$ 0.004 cm^{-1} for PPG 4966, Corning 8362, and Corning 8363 glasses, respectively. The effects of thickness and arrangements of laminations on neutron and gamma attenuation were studied. Dose rates measured through a full length mockup of the window and calculated with Niobe, a code for numerical integration of the Boltzmann equation, indicate that the window is equivalent to magnetite concrete for fission source attenuation and has slightly less attenuation for pure, hard gamma sources.

Renupak and SDC were used to evaluate fission source carrier shields composed of concrete or combinations of lead or iron with borated paraffin.

5.3.2 Neutron Activation Studies

A computer program was prepared to determine the neutron activation of TRU components as a function of flux, exposure time, and decay time. Multigroup transport and diffusion codes were used to determine the neutron flux spectrum within cells. Concrete walls, windows, manipulators, and process vessels will survey <1 r/hr 10 days after credible exposure to TRU fission sources.

5.3.3 Maximum Permissible Concentrations

The relative hazard of the various nuclides produced by long-term irradiation of plutonium must be known for use in preparing hazards summary reports, evaluating waste treatment and disposal schemes, computing necessary decontamination of various components from each other, and finally, at the time of operation, for guides to allowable exposures and for judging whether operating practices are safe. The Health Physics Handbook does not list a number of important isotopes that will be encountered by the Transuranium Project, and the Health Physics Division has undertaken the evaluation of hazards from these other isotopes and review of the various assumptions made about internal radiological hazards to see how they might be extended to include spontaneous fission hazards. In the meantime, some new assumptions have been made and a set of unofficial MPC's has been calculated for use in planning.

These MPC's (Table 5.1) were calculated by the exact rules given in ICRP Publication 2, "Report of Committee II on Permissible Dose for Internal Radiation (1959)." The results differ from those presented in Publication 2 in the following respects:

Table 5.1. Maximum Permissible Concentrations (Unofficial)

Nuclide	Water		Air		Body Burden		Sp. Act., curies/g
	Crit. Organ	$MPC_{w'}$ $\mu c/cm^3$	Crit. Organ	$MPC_{a'}$ $\mu c/cm^3$	Crit. Organ	Value, μc	
Pu-238	Bone	1.53×10^{-4}	Bone	2.02×10^{-12}	Bone	0.046	17.4
Pu-239	Bone	1.35×10^{-4}	Bone	1.79×10^{-12}	Bone	0.045	0.061
Pu-240	Bone	1.35×10^{-4}	Bone	1.79×10^{-12}	Bone	0.045	0.227
Pu-241	Bone	7.14×10^{-3}	Bone	9.42×10^{-11}	Bone	0.990	112
Pu-242	Bone	1.42×10^{-4}	Bone	1.88×10^{-12}	Bone	0.048	3.90×10^{-3}
Pu-243	GI Tract	1.21×10^{-2}	GI Tract	2.14×10^{-6}	Bone	7.23	2.59×10^{6}
Pu-244	Bone	1.27×10^{-4}	Bone	1.68×10^{-12}	Bone	0.043	1.93×10^{-5}
Pu-245	GI Tract	1.35×10^{-3}	GI Tract	2.39×10^{-7}	Bone	3.04	1.21×10^{6}
Am-241	Bone	1.27×10^{-4}	Bone	5.57×10^{-12}	Bone	0.054	3.24
Am-242m	Bone	1.27×10^{-4}	Bone	5.57×10^{-12}	Bone	0.067	9.73
Am-242	GI Tract	2.73×10^{-3}	Liver	3.93×10^{-8}	Liver	0.064	8.10×10^{5}
Am-243	Bone	1.26×10^{-4}	Bone	5.56×10^{-12}	Bone	0.044	0.192
Am-244m	GI Tract	5.08×10^{-2}	Bone	3.99×10^{-6}	Bone	0.179	2.97×10^{7}
Am-244	GI Tract	9.10×10^{-3}	Bone	1.73×10^{-7}	Bone	0.180	1.27×10^{6}
Am-245	GI Tract	1.67×10^{-2}	GI Tract	2.96×10^{-6}	Liver	11.6	6.40×10^{6}
Cm-242	GI Tract	7.05×10^{-4}	Liver	1.19×10^{-10}	Liver	0.047	3.32×10^{3}
Cm-243	Bone	1.57×10^{-4}	Bone	6.88×10^{-12}	Bone	0.092	52.6
Cm-244	Bone	2.14×10^{-4}	Bone	9.40×10^{-12}	Bone	0.104	83.3
Cm-245	Bone	1.02×10^{-4}	Bone	4.50×10^{-12}	Bone	0.043	0.157
Cm-246	Bone	1.02×10^{-4}	Bone	4.49×10^{-12}	Bone	0.043	0.265
Cm-247	Bone	1.07×10^{-4}	Bone	4.71×10^{-12}	Bone	0.044	3.62×10^{-5}
Cm-248	Bone	1.32×10^{-5}	Bone	5.81×10^{-13}	Bone	0.005	3.07×10^{-3}
Cm-249	GI Tract	8.25×10^{-2}	Liver	7.51×10^{-6}	Liver	0.827	1.18×10^{7}

Table 5.1 (Continued)

Nuclide	Water		Air		Body Burden		
	Crit. Organ	$MPC_{w'}$ $\mu c/cm^3$	Crit. Organ	$MPC_{a'}$ $\mu c/cm^3$	Crit. Organ	Value, μc	Sp. Act., curies/g
Bk-249	GI Tract	0.140	Bone	7.76×10^{-10}	Bone	0.600	1.67×10^{3}
Bk-250	GI Tract	9.62×10^{-3}	Bone	1.37×10^{-7}	Bone	0.045	3.89×10^{6}
Cf-249	Bone	1.24×10^{-4}	Bone	1.64×10^{-12}	Bone	0.041	3.59
Cf-250	Bone	3.53×10^{-4}	Bone	4.66×10^{-12}	Bone	0.041	1.31×10^{2}
Cf-251	Bone	1.17×10^{-4}	Bone	1.55×10^{-12}	Bone	0.039	1.78
Cf-252	GI Tract	2.53×10^{-4}	Bone	6.83×10^{-12}	Bone	0.015	5.57×10^{2}
Cf-253	GI Tract	4.14×10^{-3}	Bone	8.24×10^{-10}	Bone	0.036	2.87×10^{4}
Cf-254	GI Tract	1.22×10^{-5}	Bone	5.42×10^{-12}	Bone	0.00075	9.19×10^{3}
Es-253	GI Tract	6.35×10^{-4}	Bone	7.44×10^{-10}	Bone	0.0368	2.58×10^{4}
Es-254m	GI Tract	5.40×10^{-4}	Bone	4.87×10^{-9}	Bone	0.0196	3.17×10^{5}
Es-254	GI Tract	6.70×10^{-4}	Bone	1.84×10^{-11}	Bone	0.0217	1.07×10^{3}
Es-255	GI Tract	6.91×10^{-4}	Bone	6.07×10^{-10}	Bone	0.0361	2.14×10^{4}
Fm-254	GI Tract	1.70×10^{-4}	Bone	6.03×10^{-8}	Bone	0.0202	3.81×10^{6}
Fm-255	GI Tract	7.72×10^{-4}	Bone	1.63×10^{-8}	Bone	0.0362	5.72×10^{5}
Fm-256	GI Tract	1.25×10^{-5}	GI Tract	2.21×10^{-9}	Bone	0.00076	4.59×10^{6}

1. Rounding off between various steps in the calculation was not done except for one parameter which was rounded to 3 significant digits.

2. The latest information on half lives and decay schemes was taken from Landolt-Bornstein, "Numerical Data and Functional Relationships in Science and Technology, New Series (Group 1, Nuclear Physics and Technology, Vol. 1, Energy Levels of Nucleii A = 5 to A = 257)."

3. Some even more recent data on half lives were taken from ANL publications.

4. No account was taken of photon absorption. This is a good assumption except where it may interact with 6, below.

In addition, the following new assumptions about the spontaneous fission process were made:

5. The relative biological effectiveness (RBE) was assumed to be 20 for spontaneous fission fragments, and a weighting factor (n) equal to 4 was used for absorption in bone.

6. The total energy absorbed in the walls of the gastrointestinal tract is assumed to be 1% of the fission fragment kinetic energy. This same assumption is usually made for a particles because experiments have shown that they do not penetrate the mucosa appreciably.

5.3.4 Hazards Evaluation

Hazards evaluation studies indicate that downwind personnel exposures and fallout levels arising from the maximum credible accidents in TRU will be acceptable. Since the secondary containment region, which surrounds the alpha laboratories and cells, is to be maintained at a vacuum of -0.3 in. w.g. at all times, there is essentially no mechanism for release of activity to the atmosphere except through filtered ventilation streams, even in the maximum credible glove box or cell cubicle rupture. The filter removal efficiency and atmospheric dilution factors are adequate to protect the environment in these maximum credible accidents.

Although the hazard presented to the environment by TRU is small, the hazard to TRU operating personnel is large. Alpha laboratory personnel could inhale a lethal quantity of actinides in a single breath in the event of the maximum credible glove box rupture or a spill from a carrier rupture. This hazard will be minimized by limiting glove box and transfer operations to those which have an adequately low probability for dispersing activity in the building.

During normal operation of the facility, rare gases, I-131, and a-emitting actinides will be released at average rates of less than 22, 0.07, and 10^{-5} curies/day, respectively. These releases will cause maximum downwind air concentrations

equivalent to 0.25 mrem/hr and maximum β and α ground deposits of 1000 and 4.5 d/min per 100 cm^2, respectively.

5.3.5 HFIR Target Design

A preliminary target design has been developed as a result of studies of fabrication techniques, heat transfer, gas release, corrosion, radiation damage, and allowable surface contamination. The active portion of the target consists of a 20-in.-long column of 0.25-in.-dia x 0.50-in.-long pellets, which is fabricated by pressing ~18 vol % actinide oxide-82 vol % aluminum powder inside an aluminum can to a density 89 ± 3% of theoretical. The 35-in.-long target is fabricated by hydrostatically collapsing a finned, X-8001 aluminum tube, sealed by welded end caps, onto the pellet column and tack-welding a hexagonal X-8001 aluminum can to the fins.

The target is to be designed for irradiation to a total nvt of 1.5×10^{23} (1.5 years at 3×10^{15} flux) with hot-spot heat fluxes of 10^6 Btu/hr·ft^2. Fission gas release in the target is to be accommodated by providing a reinforced void at each end of the pellet column.

The allowable transferable α contamination on the target surface was calculated to be approximately 10^4 d/min per 100 cm^2 by considering the allowable fission product and actinide concentration in the HFIR coolant and the possible effects of an accident during transfer of the target from TRU to HFIR.

5.4 TRU Facility Building Design (G. B. Berry, B. F. Bottenfield, E. J. Breeding, F. L. Hannon)

The scope of the Transuranium Processing Facility was changed from a $14,000,000 project to $8,700,000 in late September, and criteria intended to define this scope were transmitted to the Architect-engineer, Catalytic Construction Company, on Oct. 4 and 5, 1961. Catalytic made a brief re-estimate and determined that the new scope and the new criteria were compatible and they immediately proceeded with the next phase of the conceptual design study.

In early November it was found necessary to modify the cell configuration at the west end of the cell bank to allow entry to the analytical cells (Nos. 8 and 9) directly through the rear of the cell. Both cells were decreased to 7 by 7.5 ft and a 4 by 7 ft shield access door was added in the rear wall. The pit area behind these cells is covered with 4-ft-thick shielding plugs. The current building layout is shown in Fig. 5.15.

During December and January, the 42 drawings, 12 criteria specifications, and numerous narrative sections of the conceptual design report were reviewed by Chemical Technology Division and other interested parties at the Laboratory, and a preliminary issue of the conceptual report was made on March 2, 1962. Following

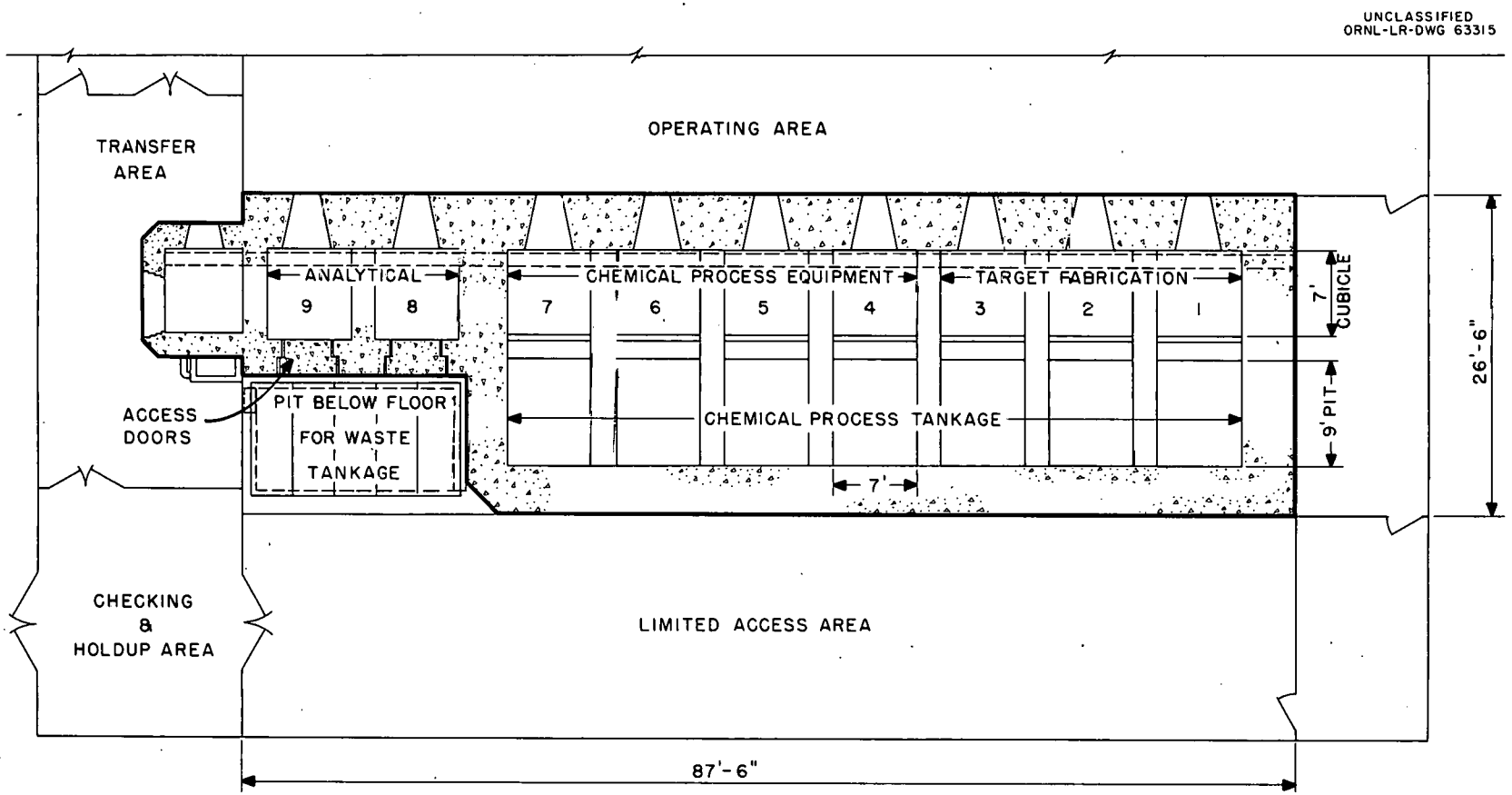

Fig. 5.15. Space allocation in TRU cell bank.

the preparation of the final cost estimate by Catalytic and review of the preliminary conceptual report by AEC-ORO, a final issue will be made during the early part of April.

During November advanced design funds in the amount of $300,000 were made available to AEC-ORO for Title I engineering. A directive was issued for $200,000 of this money to cover the participation of the Architect-engineer in the Title I engineering, which was initiated late in December, 1961.

All Title I drawings are scheduled for completion by the Architect-engineer by the last week in May for final review by ORNL. It is estimated that 105 drawings will be required. The schedule for the Title I design calls for completion by July 1, 1962, with Title II engineering being initiated at that time and completed in mid-April, 1963. The schedule as currently proposed by AEC-ORO is shown in Fig. 5.16.

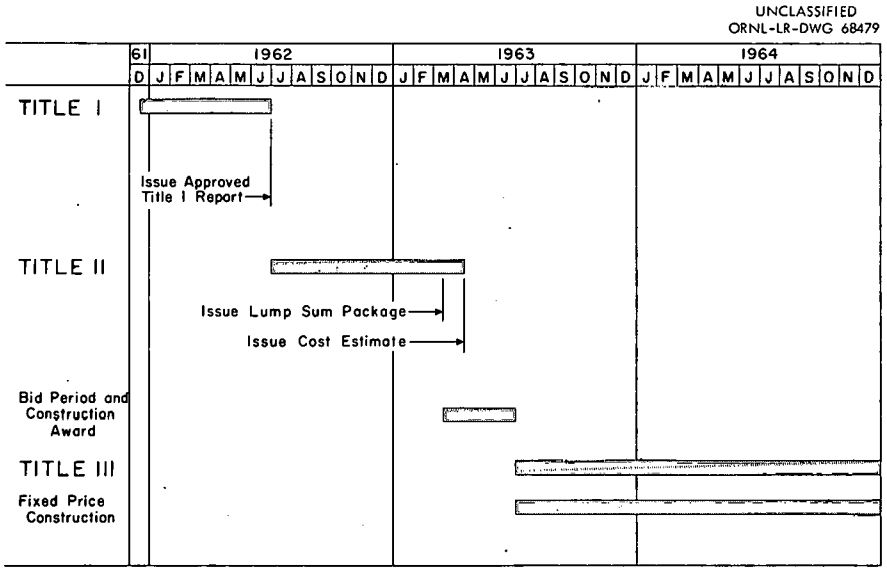

Fig. 5.16. TRU engineering and construction schedule.

5.5 Cells 3 and 4, Bldg. 4507 (J. P. Nichols, F. L. Peishel, R. A. Schmidt, W. R. Whitson)

5.5.1 Flowsheet

The TRU Processing Plant chemical flowsheets developed during the past few years have been tested at radiation levels limited by the containment standards and shielding available in the laboratory. Installation of equipment in cells 3 and 4 of Bldg. 4507 will meet the need to test these flowsheets at or near radiation levels to be encountered in the final processing plant. Americium-curium will be separated from rare earth fission products and irradiated materials processed to isolate californium in these cells. The chemical flowsheets shown in Fig. 5.17 and Fig. 5.18 were used as the basis for design.

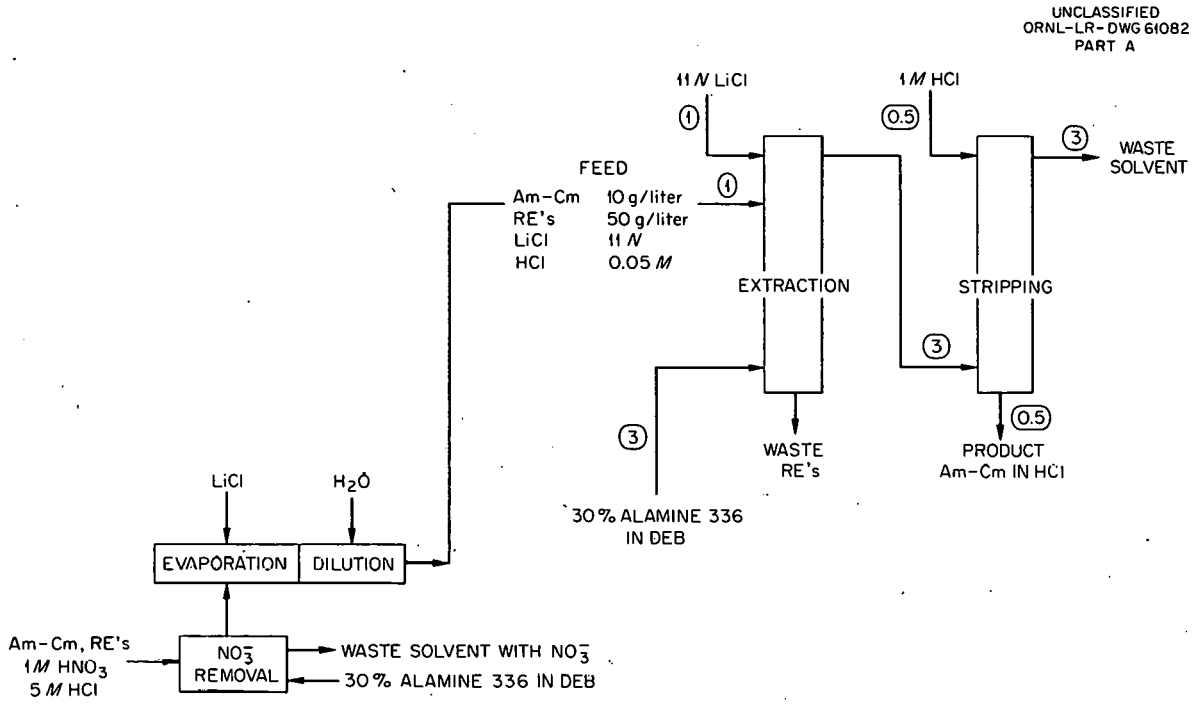

Fig. 5.17. Flowsheet of tertiary amine extraction processes for separating americium and curium from rare earths. Circled numbers are flow ratios.

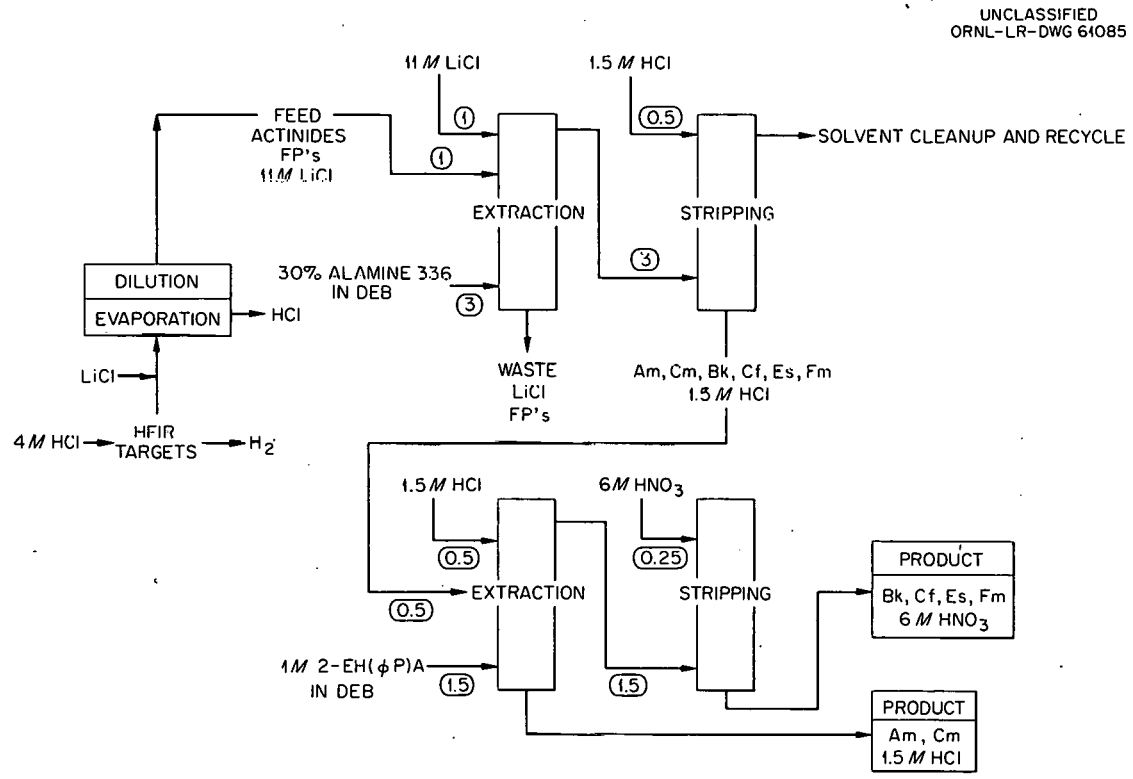

Fig. 5.18. Flowsheet for processing of HFIR targets. Circled numbers are flow ratios.

Figures 5.17 and 5.19 illustrate the chemistry and equipment to be used for the isolation of americium and curium from highly irradiated plutonium, which will be processed in cell 1, Bldg. 4507, for plutonium isolation. This material will have been processed in cell 1 by an additional ion exchange step to remove the bulk of the aluminum and fission products other than the rare earths. The product solution from the ion exchange step will be evaporated to approximately 100 liters and stored in T416, one of two new tanks to be installed beneath the floor of cell 4.

Design and installation of head-end equipment for dissolution of a 6-month-irradiated HFIR target and other large targets will be started immediately after the design of the cell 4 equipment. This dissolution equipment and the equipment required for separation of berkelium from californium and higher isotopes will be installed in cell 3.

Figures 5.18 and 5.20 are the chemical and equipment flowsheets for the cells 3 and 4 complex. Item numbers of equipment with a "3" or "4" prefix indicate cell 3 or 4 locations. The cell 4 equipment for target processing is basically the same as that shown in Fig. 5.19 for americium-curium recovery with the exception of the addition of T407.

5.5.2 Equipment Description and Arrangement

The desire to keep the cell as simple and as uncluttered as possible led to a decision to install only enough equipment to perform one cycle of solvent extraction, a 16-stage extraction mixer-settler, and an 8-stage scrub mixer-settler. After cleanup of the mixer settlers, subsequent cycles of solvent extraction will be carried out in the same contactors. The jeopardy in convenience and run-time is off-set by the advantage of decreasing congestion in the working area of the cell.

The materials of construction selected are a compromise between corrosion resistance and time of procurement. The modest total radiation to which the equipment will be subjected makes the extensive use of plastic and glass or glass-lined materials acceptable. This will permit flexibility and will simplify materials problems. Tantalum-lined equipment is being investigated.

The equipment will be installed so that it may be removed by heavy duty manipulators, an impact wrench, and a crane mounted in the large equipment-removal cubicle located on the top of the cell bank. The equipment will be in a modular arrangement to allow relocation or replacement of all cell tanks in a standard support frame (Fig. 5.21). The piping between tanks and racks will be joined with disconnects similar to that shown in Fig. 5.22, which will be operable with a manipulator. The solvent extraction equipment and other miscellaneous items will be located in racks supported on top of the tankage framework. These racks will also be removable through the roof hatch.

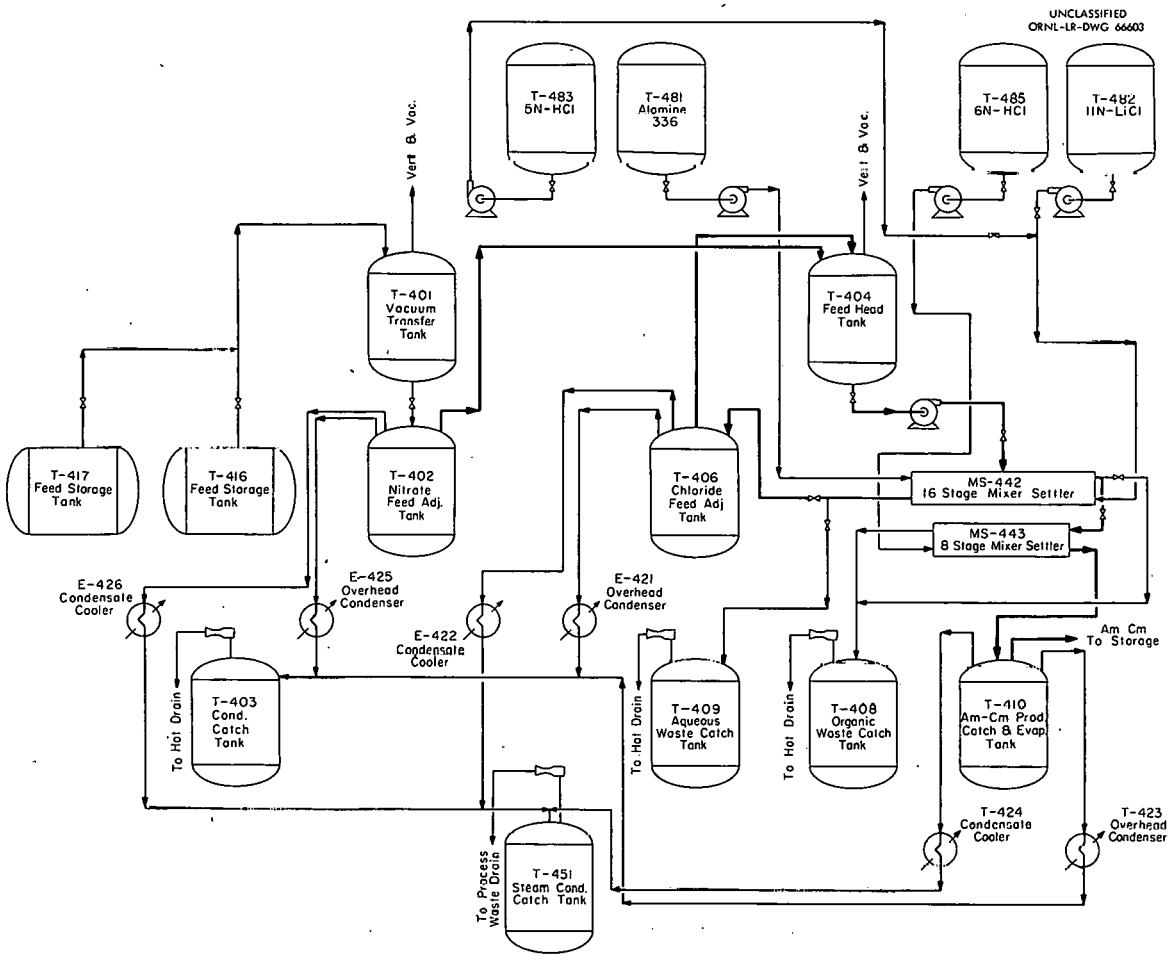

Fig. 5.19. Americium-curium recovery equipment flowsheet.

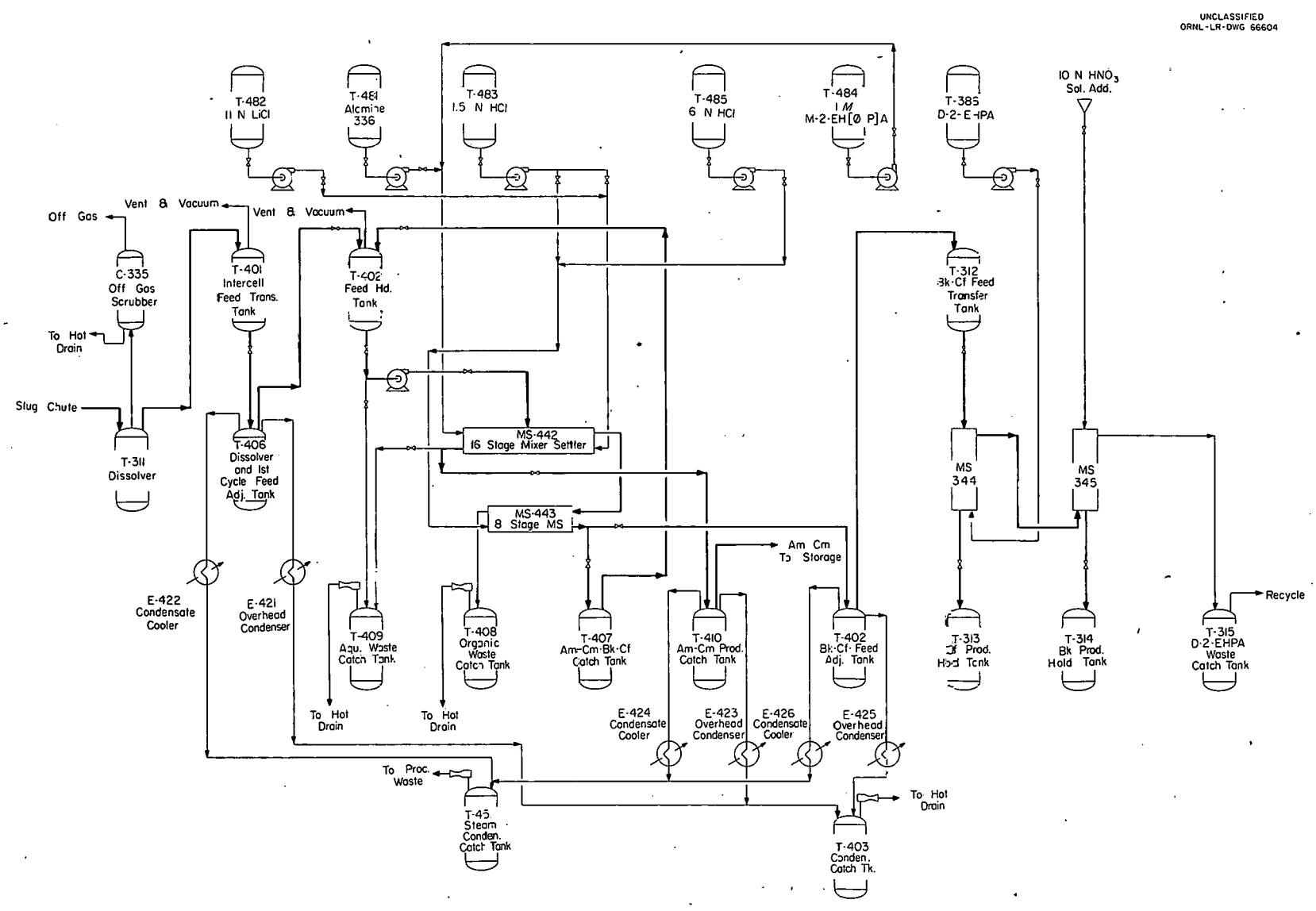

Fig. 5.20. Target processing equipment flowsheet.

UNCLASSIFIED
ORNL-LR-DWG 67112

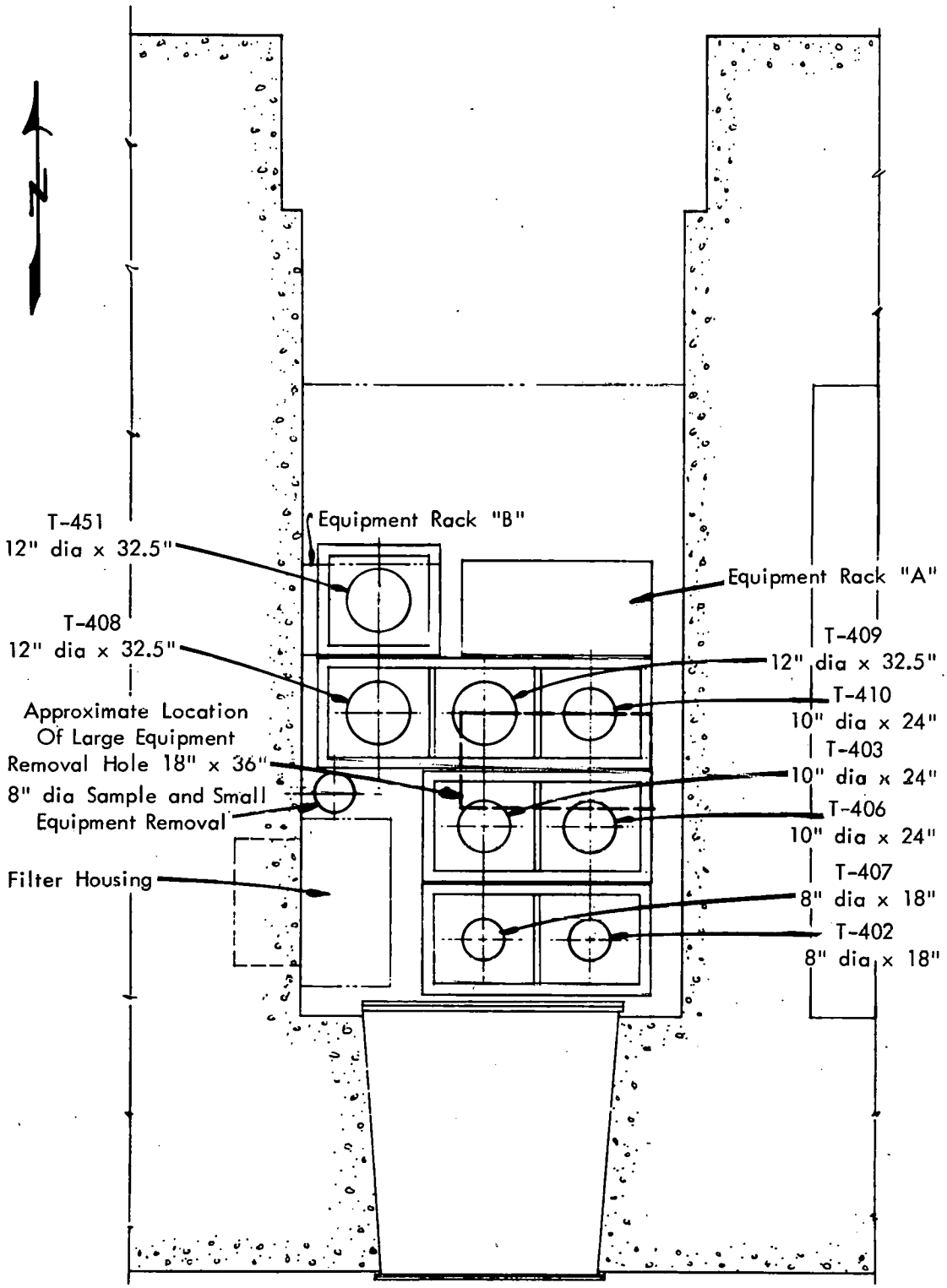

Fig. 5.21. Cell equipment plan.

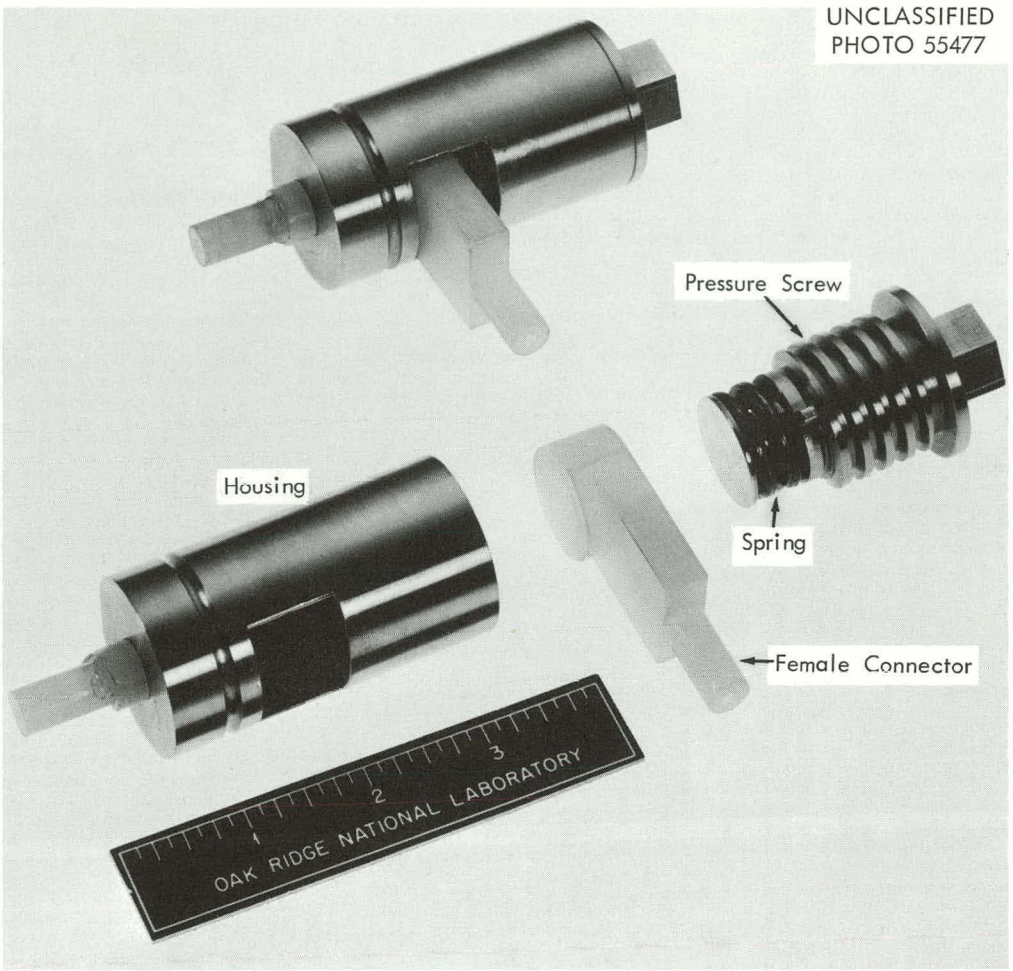

Fig. 5.22. Single unit disconnect.

Figure 5.23 illustrates the cell and support areas arrangement and Fig. 5.24 illustrates a typical tank top.

5.5.3 Shielding

The shielding of the concrete and viewing windows of cells 3 and 4 in Bldg. 4507 is adequate for the work to be performed. The calculations were based on a cell wall of 48 in. of barytes and a window of 48 in. of Corning 8362 (3.27 g/cc density) glass and 2.5 in. of oil; this combination is very effective for attenuation of gamma radiation but is poor for neutrons.

The highest neutron sources proposed for use in the cells will be in a 6-month-irradiated HFIR target; the properties of this target are given in Table 5.2. The neutron dose rate values given in Table 5.3 are expected to be accurate within a factor of 2, assuming that the neutron source strengths are correct.

The fission product gamma attenuation through the wall and window and

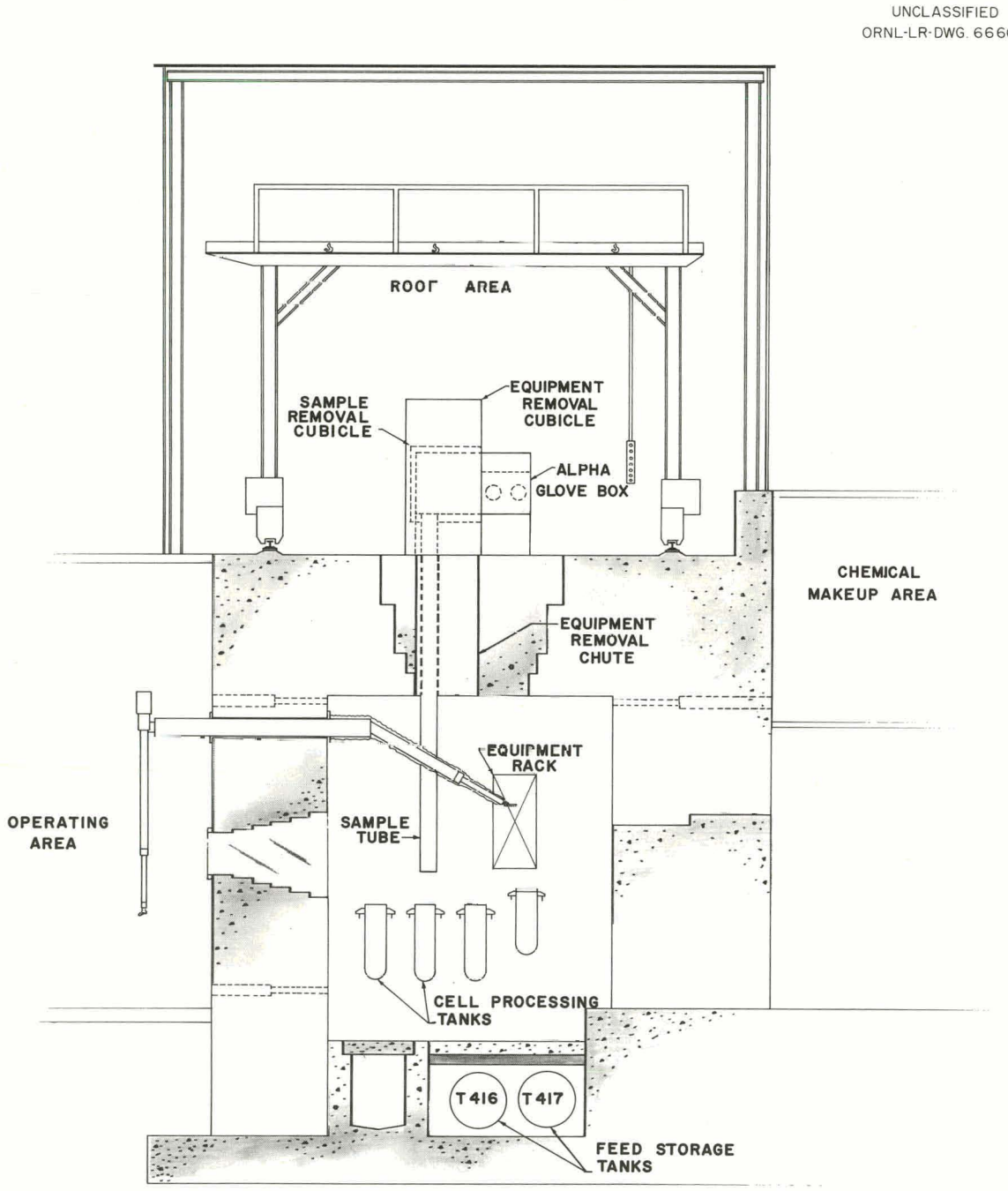

Fig. 5.23. Sectional view of Cell 4 in Bldg. 4507.

UNCLASSIFIED
ORNL-LR-DWG 66607

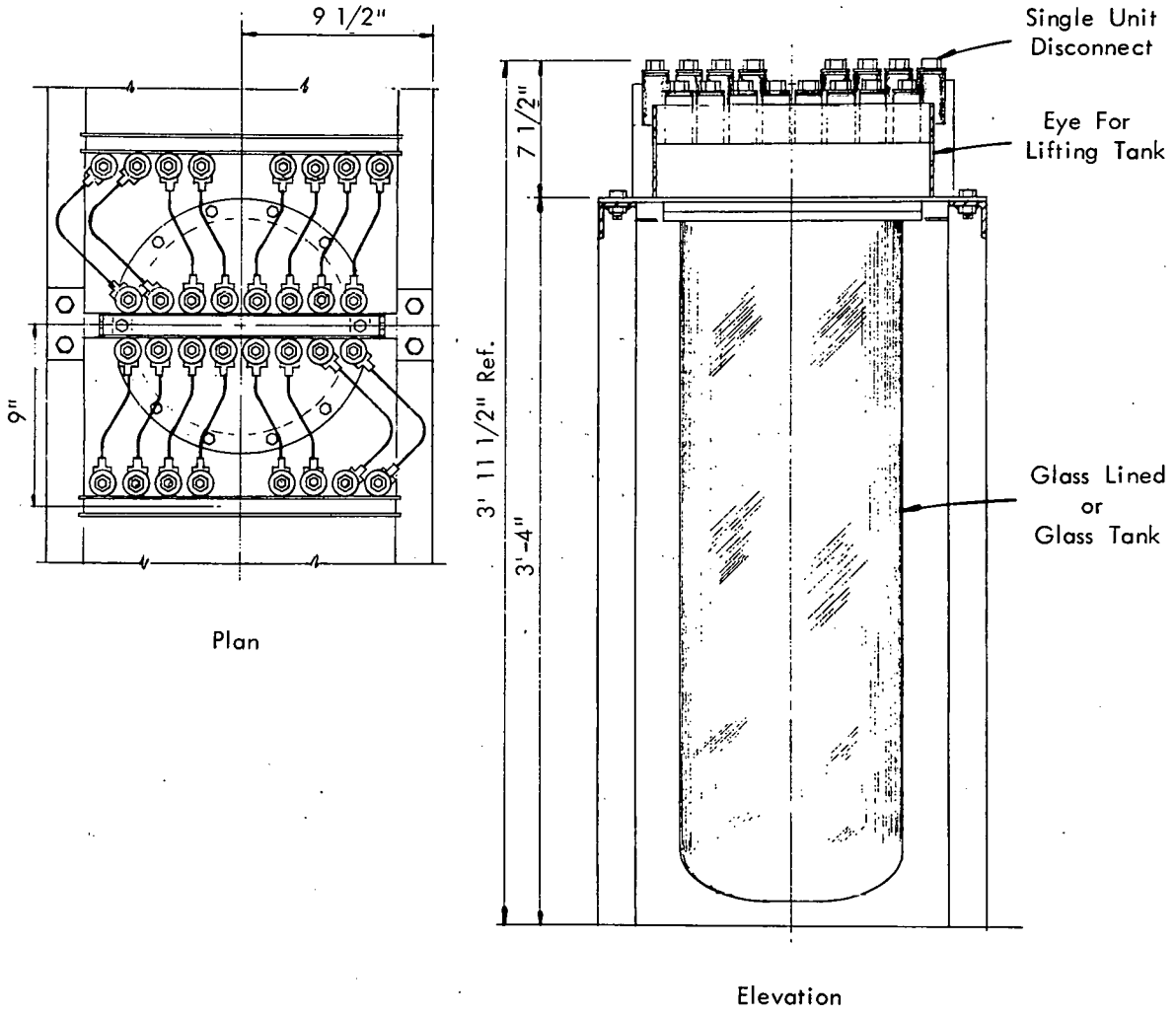

Fig. 5.24. Typical cell tank piping arrangement.

Table 5.2. Properties of a 6-month-irradiated HFIR Target

(30 days' decay)

Cf-252 content, μg	350
Cf-254 content, % of Cf-252	0.52
Cf neutron source, n/sec	3.5×10^9
1.7-Mev γ source, Mev/sec	$\sim 2 \times 10^{13}$

Table 5.3. The Dose Rate[a] at the Surface of 4507 Cell Wall and Window from a 6 Months' Irradiated Target Located 1 ft from the Inside of the Shield

Fission product γ dose rate through window or wall, mr/hr	<0.01
Neutron dose rate through barytes wall, mrem/hr	0.026
Neutron dose rate through window, mrem/hr	3.3

[a]The Cf-252 content of a 6-month-irradiated HFIR target was taken from ORNL-CF-59-8-125. The Cf-254 content of the HFIR rod was calculated using a Cf-253 capture cross-section of 3 barns.

neutron attenuation through the wall were calculated from measured attenuation coefficients and removal cross sections. The neutron attenuation through the window was determined with the Renupak neutron transport code on the IBM-7090.

5.5.4 Containment

The containment effectiveness of cell 4 in Bldg. 4507 must be increased consistent with the rest of the building. This will include the addition of roughing and absolute filters on the present cell exhaust duct opening, improvement of seals on all existing sleeves and penetrations, and modification of the manipulator booting to provide reliable α-tight seals. All materials must be introduced to or removed from the cell by bag-out techniques, and a large equipment-removal cubicle and a small sample-removal cubicle will be provided for this purpose in the roof area over cells 3 and 4.

5.5.5 Schedule

The time planned between the first two and the last program is ~1 year (Fig. 5.25). The MTR-irradiated Am-241 or Cm-244 targets, to be dissolved in T-406 because of their small size, 0.5 in. dia by 4 in. long, may be processed during this hiatus.

The cells will accommodate tankage of twice the size required for americium-curium processing (Fig. 5.21). The larger tanks would provide capacity sufficient for processing Cm-242 produced by irradiation of Am-241. Curium-242 processing would not conflict with the present schedule for americium-curium recovery and the 6-month-irradiated HFIR target processing.

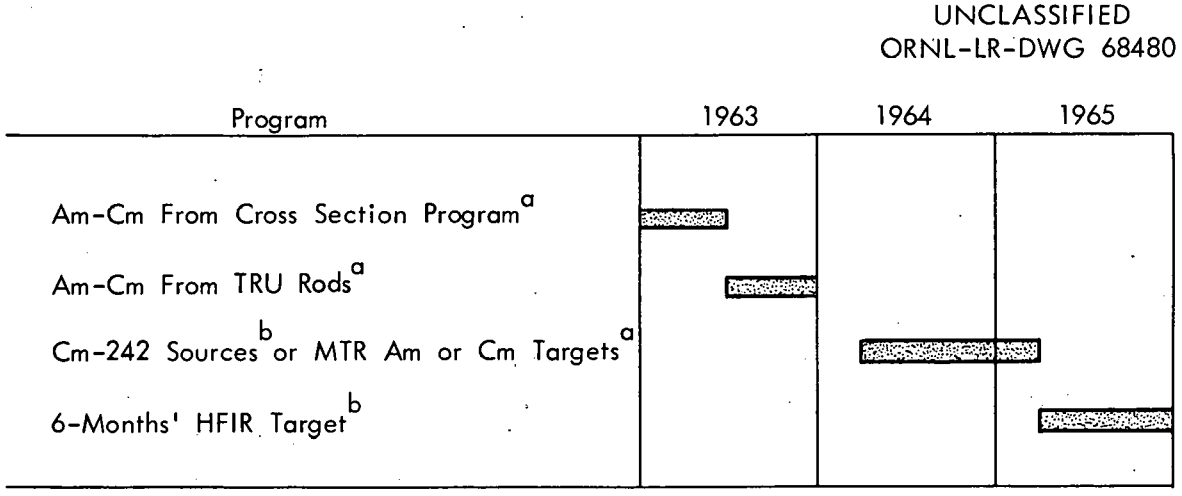

[a]Solvent extraction equipment.

[b]Cell 3 head-end; cell 4 solvent extraction.

Fig. 5.25. TRU processing schedule.

6.0 TRU CORROSION STUDIES

(J. L. English, J. C. Griess, P. D. Neumann)

In the exploratory corrosion-test program to select materials of construction for the transuranium separation facility, specimens of 25 metals and alloys which offered varying degrees of promise for use in chloride-containing solutions were exposed in the solution, solution-vapor, and vapor phases of a number of simulated process solutions to be handled in the separation facility. From the results of these tests six potential container materials were selected: Hastelloys B and C, niobium, tantalum, titanium, and Zircaloy-2. The corrosion rates of these metals are shown in Table 6.1, the reported values being the highest values observed (usually for solution specimens) for a particular environment, regardless of specimen position.

In current more intensive tests in chloride-containing solutions initial results are not encouraging. Hastelloy B was corroded at 5 to 7 mils/mo in oxygen-aerated 6 M HCl at 43°C; these rates were doubled when hydrogen peroxide was substituted for the oxygen. Rates were 2-4 mils/mo in oxygen-aerated 3 M HCl at 43°C. In oxygenated 10 M LiCl-0.1 M HCl at atmospheric boiling, resistance was good, with rates of 2 mils/mo. Attack on weld specimens in all environments was uniform.

Corrosion rates for welded Hastelloy C specimens in oxygen-aerated 3 and 6 M HCl solutions at 43°C ranged from 6 to 14 mils/mo; specimens in the vapor were corroded at rates of <1 to 10 mils/mo, depending on the particular environment. In general, observed rates increased with increased exposure times, and on all specimens there were varying degrees of preferential attack in heat-affected zones. This type of attack was eliminated by the use of a post-weld heat treatment at 2250°F, but the overall corrosion resistance was not improved. Resistance was excellent at 43°C in an oxygenated acid or neutralized waste solution, with rates of <1 mil/mo in waste solution containing 0.3 M HCl, 0.6 M HNO_3, 0.6 M $Al(NO_3)_3$, 3.6 M LiCl, and 0.003 M $RuCl_3$. Corrosion resistance was extremely poor with Hastelloy C in all chloride-containing solutions at elevated temperatures.

In oxygen-aerated 6 M HCl and 10 M LiCl-0.5 M HCl solutions at 105 and 128°C, respectively, niobium was corroded uniformly at rates of 0.6 mil/mo or less. In flow tests with 6 M HCl solution containing 0.0041 M $LaCl_3$ and different amounts of hydrogen peroxide rates were from <1 to 5 mils/mo. There was evidence that the presence of either hydrogen peroxide and/or lanthanum accelerated the rates, but additional testing will be required to resolve this observation. In tests in which niobium coupled between two pieces of aluminum was exposed to hot 6 M HCl solution, the aluminum dissolved rapidly with copious quantities of hydrogen gas evolution. After seven such exposures, the niobium fractured during a bend test. A hydrogen determination showed 960 ppm in the exposed specimen as compared with 4 ppm in an unexposed control specimen.

Tantalum was chemically inert in the chloride-containing solutions at all temperatures. Some evidence of hydrogen pickup was obtained in a dissolving test

Table 6.1. Summary of Initial Corrosion-Test Data for Transuranium Separation Facility

Material	Medium	Temp, °C	Time, hr	Corrosion Rate, mils/mo
Hastelloy C	3 M HCl-O_2	43	336	13
Haynes 25			168	29
Zirconium			336	<0.1
Hastelloy C	3 M HCl-1 M HNO_3-O_2	43	336	1
Hastelloy C	8 M HNO_3-O_2	43	1008	3
Haynes 21			336	0.1
Haynes 25			336	0.1
Zirconium			336	nil
Tantalum	6 M HCl (no O_2)	105	168	nil
Titanium-55A			3	>100
Zircaloy-2			96	0.1
Zirconium			72	<0.1
Hastelloy C	6 M HCl-O_2	43	200	6.6
Hastelloy C	6 M HCl-H_2O_2	43	200	14
Hastelloy B	6 M HCl-H_2O_2	105	96	7[a]
Hastelloy C			24	125
Molybdenum			96	b
Titanium-0.1% Pd			24	>500
Zircaloy-2			96	1[a]
Zirconium			96	1
Niobium	6 M HCl-O_2	112	900	0.6
Zirconium		105	336	<0.1
Haynes 25	6 M HCl-8 M HNO_3-no O_2	105	96	3
Tantalum			168	nil
Titanium-55A			72	3
Zircaloy-2			24	14
Zirconium			24	165
Chlorimet-2	10 M LiCl-0.1 M HCl-O_2	128	168	5
Hastelloy A			168	3
Hastelloy B			168	3
Tantalum			24	nil
Titanium-75A			3	>900
Titanium-75A	10 M LiCl-0.1 M HCl-H_2O_2	85	120	<0.1
Hastelloy B		128	48	44
Tantalum			120	nil
Niobium	10 M LiCl-0.5 M HCl-O_2	128	900	0.3

[a]Flowing system.

[b]Specimens completely dissolved.

similar to the one described with niobium. After seven exposures, the specimen contained 54 ppm of hydrogen. The hydrogen content of an unexposed control specimen was 1 ppm. No cracking of the exposed specimen was observed during a 180° bend test, however.

The corrosion behavior of titanium was dependent on the presence of an oxidizing species in the chloride-containing solutions. With sufficient quantities of hydrogen peroxide or nitric acid present, resistance was acceptable. In the absence of an oxidant, corrosion was generally catastrophic.

Zircaloy-2 showed excellent resistance in flow tests with 6 M HCl at 105°C with or without the presence of hydrogen peroxide, with corrosion rates of 0.2 mil/mo or less. In similar tests in 6 M HCl containing 0.0041 M $LaCl_3$ and different amounts of hydrogen peroxide, rates increased to between 1 and 6 mils/mo. Corrosion was severe with the alloy in the mixed hydrochloric-nitric acid system at 105°C.

6.1 Effect of Alpha Radiation on Corrosion (R. D. Baybarz)

Scouting corrosion tests (7) were made on glass and welded specimens of tantalum, Hastelloys B and C, titanium 45A, and Zircaloy-2 exposed to chloride solutions containing 20 g/liter Am-241, which is 2 watts/liter. No direct effects of alpha radiation on corrosion were found. Secondary effects, which are attributed to the presence of H_2O_2 produced by radiolysis of water, were noted for Hastelloys B and C and for titanium 45A. Under conditions which allowed appreciable buildup of H_2O_2 concentration, corrosion rates of Hastelloys B and C were increased, and corrosion of titanium was drastically decreased. Corrosion rates of glass and tantalum were <1 mpy, and corrosion of Zircaloy-2 was <10 mpy for all conditions tested.

Tests were made by immersing corrosion specimens 1 cm x 2 cm x 1/32 to 1/8 in. thick in Pyrex glass test tubes containing 10 ml of solution. Other specimens were suspended in the vapor phase on a tantalum wire. Solutions used were 6 M HCl and 10 M LiCl-0.5 M HCl, each containing 20 g/liter Am-241. Control solutions were identical with the exception that nonradioactive lanthanum was substituted for Am-241. Tests were made at 45°C and at near boiling for 7 days. Corrosion rates were determined by weighing the specimens both before and after exposure to the chloride solution.

7.0 ANALYTICAL RADIOCHEMICAL METHODS DEVELOPMENT (L. T. Corbin, F. L. Moore)

Eight tentative radiochemical methods have been developed and tested for application in the TRU program. These methods are as follows:

---

(7) R. D. Baybarz, "The Effect of High Alpha Radiation on the Corrosion of Metals Exposed to Chloride Solutions," ORNL-3265, Mar. 27, 1962.

1. Gross alpha, direct method
2. Gross alpha, LaF_3 method
3. Gross alpha, amine extraction method
4. Plutonium alpha, LaF_3 method
5. Plutonium alpha, TTA method
6. Transplutonium alpha, LaF_3 method
7. Transplutonium alpha, amine extraction method
8. Alpha spectrometry, silicon diode detector

Development of analytical radiochemical methods for berkelium and californium isotopes are in progress. Preliminary work indicates that the method of Peppard (8) for berkelium may be adapted for the TRU program. This method involves the oxidation and extraction of berkelium with a hexane solution of di(2-ethylhexyl)-orthophosphoric acid. Essentially quantitative recovery of the berkelium is possible with excellent separation from all other actinides and lanthanides except cerium.

Radiometric Determination of Fluoride. Work has been initiated on the possibility of the determination of fluoride ion by a radiometric technique. Briefly, the principle to be evaluated involves the highly selective extraction of a radioactive metal tracer as a fluoride complex. The radioactivity extracted will be proportional to the fluoride ion concentration. A literature survey has been completed recently.

8.0 URANIUM-232 PREPARATION

(R. E. Leuze, S. D. Clinton, J. M. Chilton, V. C. A. Vaughen)

Two samples of U-232, 20 mg of U-232 containing <150 ppm of U-233 and 1 g of U-232 containing <1% U-233, are being prepared by irradiating 50 g of Pa-231 oxide in the ORR, followed by anion exchange isolation of uranium and protactinium (9).

8.1 Flowsheet Testing

Three irradiations of Pa_2O_5 clad in aluminum were made, and the material

(8) D. F. Peppard, J. W. Moline, G. W. Mason, J. Inorg. Nucl. Chem. 4, 344-8 (1957).

(9) J. M. Chilton and N. Jackson, "Preparation of U-232 from Pa-231, Part 1. Preliminary Work," AERE-R3727, 1961.

was processed to test the flowsheet (9) for U-232 and Pa-231 recovery. Two smaller irradiations, 77.9 and 208 mg of Pa-231, were made first. The irradiated targets were allowed to decay 30 days to decrease the activity to a level such that processing could be carried out in gloveboxes with only unit shielding. The third irradiated target containing 7.36 g of Pa-231 was allowed to decay only 45 hr before the first U-232 isolation in order to limit the amount of U-233 growth from Pa-233. A second U-232 recovery was made 48 hr later, after a total of 93 hr decay. The larger amount of irradiated protactinium was processed in cell 3, Bldg. 4507, to test both the chemical flowsheet and the full-scale process equipment.

For this processing, the aluminum is dissolved in 7 M HCl (Fig. 8.1). The solution, which contains only small amounts of dissolved protactinium and uranium, is decanted through a filter and fed to a column of 50-100 mesh Dowex 1-4X resin. Both protactinium and uranium are sorbed on the resin under these conditions. The Pa_2O_5 containing the U-232 is dissolved in 8 M HCl-6 M HF and diluted with 8 M HCl to 8 M HCl-0.6 M HF and 5 to 10 g of protactinium per liter. When this solution passes through the resin, uranium is sorbed but protactinium, which is complexed with fluoride, is not. Any protactinium sorbed from the aluminum chloride dissolver solution is also eluted. After the column has been washed with 8 M HCl-0.6 M HF, the uranium is eluted quantitatively in about 3 column displacement volumes of 0.5 M HCl. The 77.9- and 208-mg Pa-231 runs were made with a 2- to 4-ml resin column and the 7.36-g Pa-231 run with a 400-ml resin column.

The U-232 and Pa-231 determinations for these runs are only approximate since they were made by a combination of gross α and α-pulse height analysis. The higher energy U-232 α radiation interferes with Pa-231 determination, and the high-energy daughters interfere with both U-232 and Pa-231 determinations. Because of this interference, the data in Table 8.1 indicate poorer protactinium-uranium separation than was actually obtained.

Mass analysis of U-232 product from the 208-mg protactinium irradiation was used to determine the natural-uranium contamination in the original Pa_2O_5. The 80-μg U-232 product from this run contained 1.994% U-238 and 0.0173% U-235. If there was no external contamination during processing, it can be calculated that the Pa_2O_5 contained about 7 ppm of natural uranium. This product also contained 281 ppm of U-233. Uranium-232 yields from both the 77.9- and the 208-mg protactinium runs were used to calculate the optimum irradiation time for the 7.36-g protactinium run. The U-232 product of ~5 mg from this run, which was separated from protactinium after 45 hr decay, contained 1.195% U-238 and 0.0080% U-235, which indicated ~8 ppm uranium in the original Pa_2O_5. Product from the 7.36-g protactinium run also contained 129 ppm of U-233. The second uranium product of 1.88 mg obtained by reprocessing the protactinium after 93 hr decay has not yet been analyzed for isotopic composition.

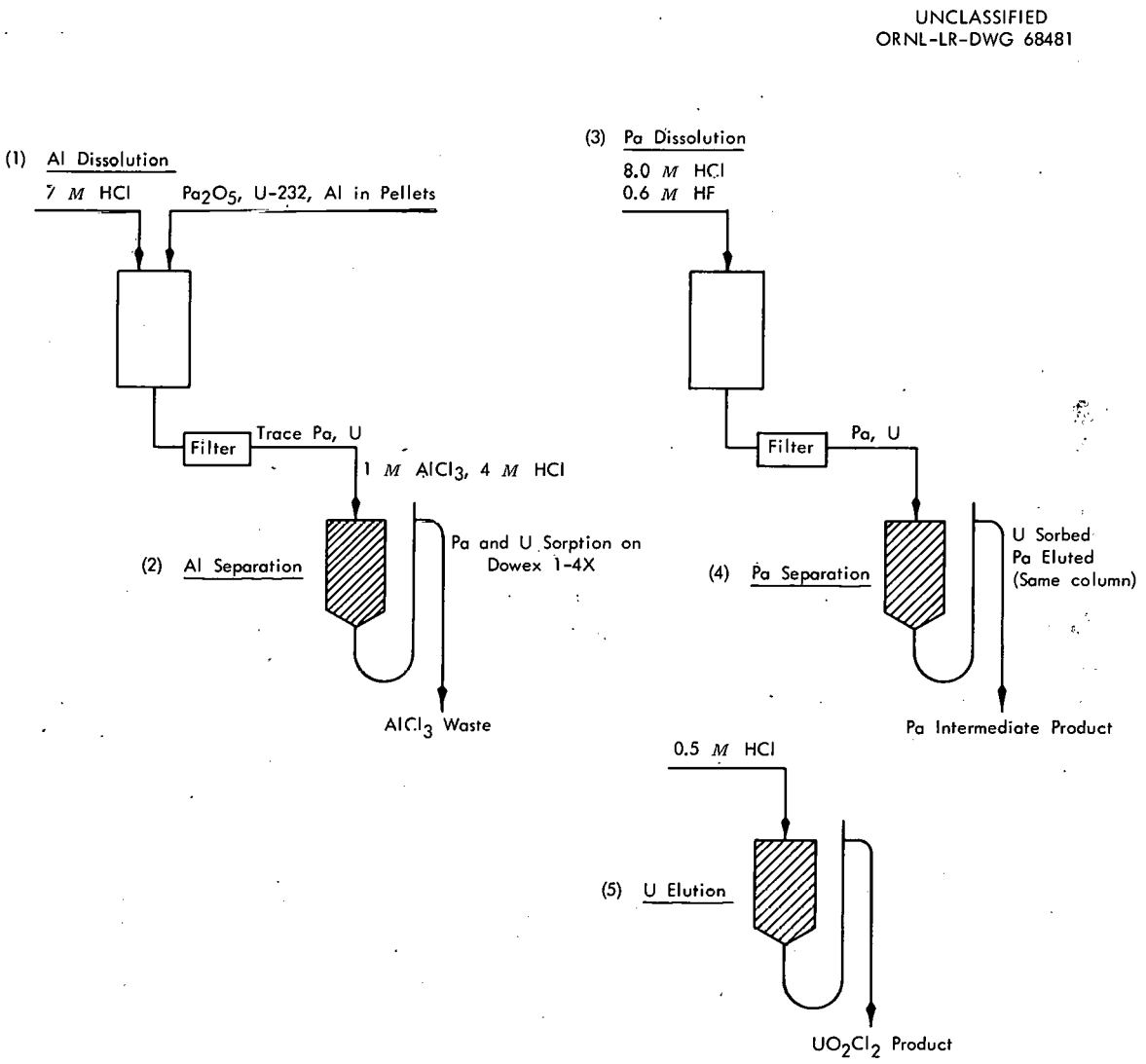

Fig. 8.1. Chemical flowsheet for protactinium-uranium separation.

8.2 Uranium Purification

Ion exchange and solvent extraction methods were investigated for final purification of the uranium product.

Ion Exchange. The uranium decontamination factor from protactinium was 22 when 40 ml of a synthetic feed containing 1 part of U-232 in 4000 parts of protactinium was passed through a 4-ml bed of Dowex 1-4X resin. The uranium was eluted from the column with 20 ml of 0.5 N HCl to give a product containing 1 part of uranium in 190 parts of protactinium.

Solvent Extraction (10). An HF concentration of 0.8-0.9 appeared to give maximum separation of protactinium from uranium in extraction by 0.1 N trilauryl amine from 8 M HCl containing HF. Uranium distribution coefficients increased from 40 to 100 as the HF concentration increased from 0.3 to 0.9, but decreased at higher HF concentrations (Fig. 8.2). Results were not entirely reproducible, but were fairly consistent from dilute uranium solutions containing no large amounts of other ions. Protactinium distribution coefficients from the same solutions decreased from 0.05 to 0.005, with still smaller values for higher HF concentrations, but were very erratic. In one run with three extraction stages and a scrub stage after each extraction stage, protactinium distribution coefficients were 0.014, 0.071, and 0.25 for the extractions and 0.11, 0.48, and 1.38 for the scrubs. In another run with 0.4 N HF, distribution coefficients were 0.092, 1.8, and 0.55. Some of the variability in protactinium results is due to the difficulty of obtaining accurate protactinium determinations in the presence of other α emitters.

In stripping, uranium distribution coefficients (o/a) between 0.1 N Alamine and HCl of various concentrations increased regularly from 0.09 with no acid to 90 with 3 M HCl, 530 with 4 N HCl, 3200 with 6 N HCl, but no further increase with 9 N HCl.

A synthetic solution containing U-232 and Pa-231 was adjusted to 8.0 M HCl-0.8 M HF and the U-232 was extracted with 1/5 volume of 4% Alamine 336 in diethyl benzene. The organic phase was scrubbed with 1/2 volume of 8.0 M HCl-0.8 M HF and stripped with 1/5 volume of 0.1 N HCl. The U-232 product showed an overall decontamination factor from protactinium of ~100.

8.3 Cell 3, Bldg. 4507, Equipment Installation and Cold Testing

Because of persistent leaks at the welds in the inner core of the original polyethylene dissolver, a one-piece plutonium product bottle was cut to size and placed inside the original cooling jacket. The humped bottom of this bottle made it necessary to stir from the top rather than use a magnetic stirrer. The equipment rack was further

(10) D. O. Campbell, ORNL, personal communication, January, 1962.

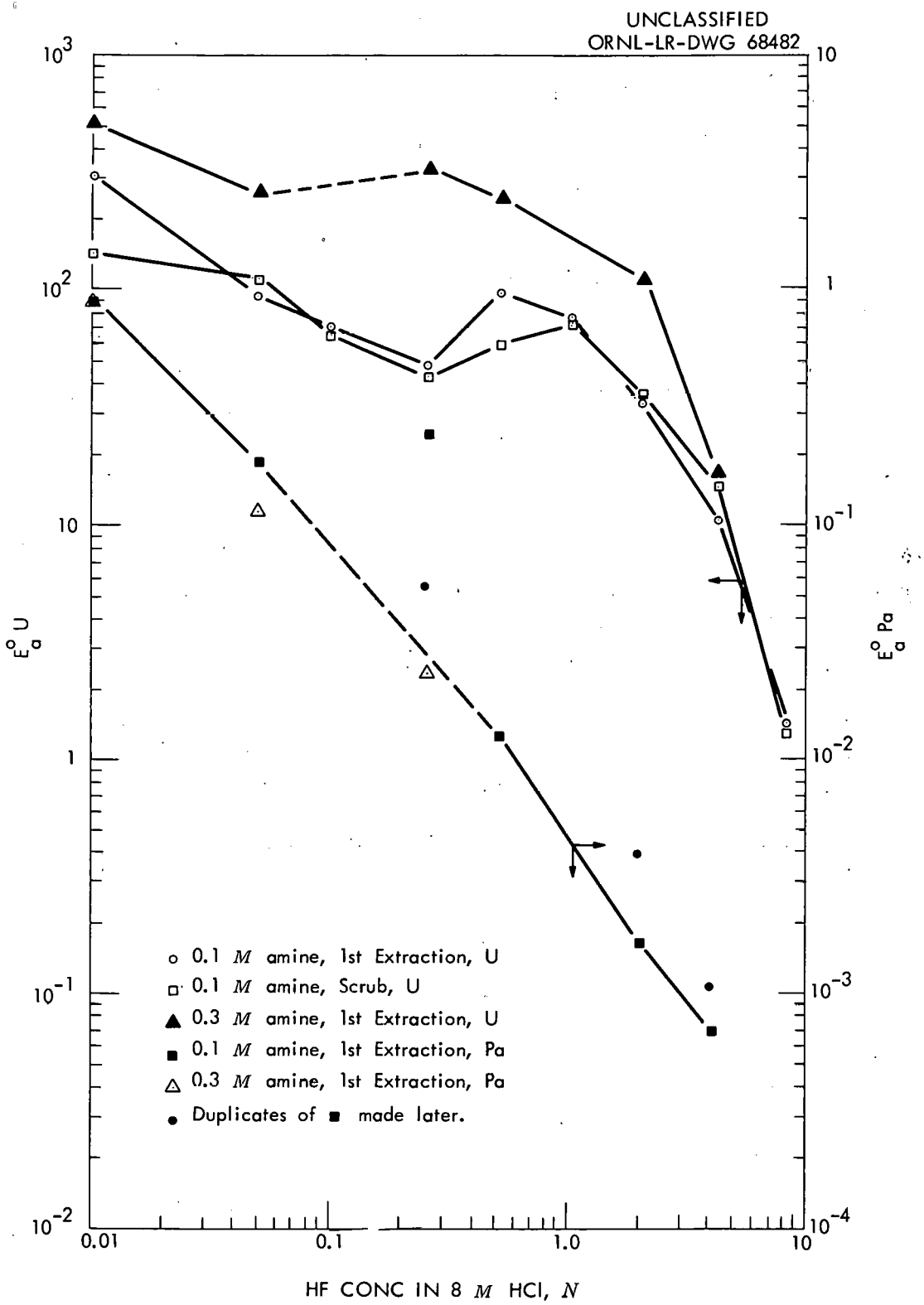

Fig. 8.2. Extraction of uranium and protactinium from HCl-HF solutions by tertiary amine.

modified so that three single-unit disconnects on the processing box wall could be used rather than the original twelve-unit gang disconnect on the rack. A second set of thermocouples was put in the jacket and dissolver as spares.

Figure 8.3 is a picture taken through the front window of cell 3 in Bldg. 4507 after equipment installation was complete. Notice the cell walls and side mercury lights visible through the side windows of the processing box. The polyethylene dissolver with cooling jacket, stirrer, filters, and off-gas scrubber is located on the left equipment rack on the back wall of the processing box. The ion exchange column equipment rack is located to the right of the dissolver. Also shown are the slug chute connecting the penthouse to the interior of the cell (top left); the drill chuck for holding the can during decladding (middle, left wall); single-unit process services disconnects mounted behind the chuck; modified T-8 finger pump (behind bottle on floor); sampler line and diaphragm with micropipette (on ringstand, left front); sample bottle capper (front center); manipulator detonger (front center); and sample bottle holders (right rear corner).

Two full-scale nonradioactive tests of the final system were made with aluminum rods and Nb_2O_5 powder. In the first there was some difficulty from foaming during the aluminum dissolution. The niobium oxide was allowed to dissolve overnight. In the second test there was no trouble with foaming but the niobium oxide did not dissolve in several hours.

With the exception of an air-line break on the off-gas condensate valve and difficulty in separating the aluminum and protactinium oxide by washing the equipment, the process performed as expected. The air-line break removed the off-gas scrubber from the system. The slug radiation level (mainly β-γ) may have given the bottom of the dissolver a dose close to its limit (10^8 rads) and necessitated its replacement. The Teflon stirrer blade became brittle and broke and was replaced with a polyethylene stirrer blade. The flowsheet will be modified in the next run to facilitate aluminum dissolution by heating and stirring for a longer time before rinsing.

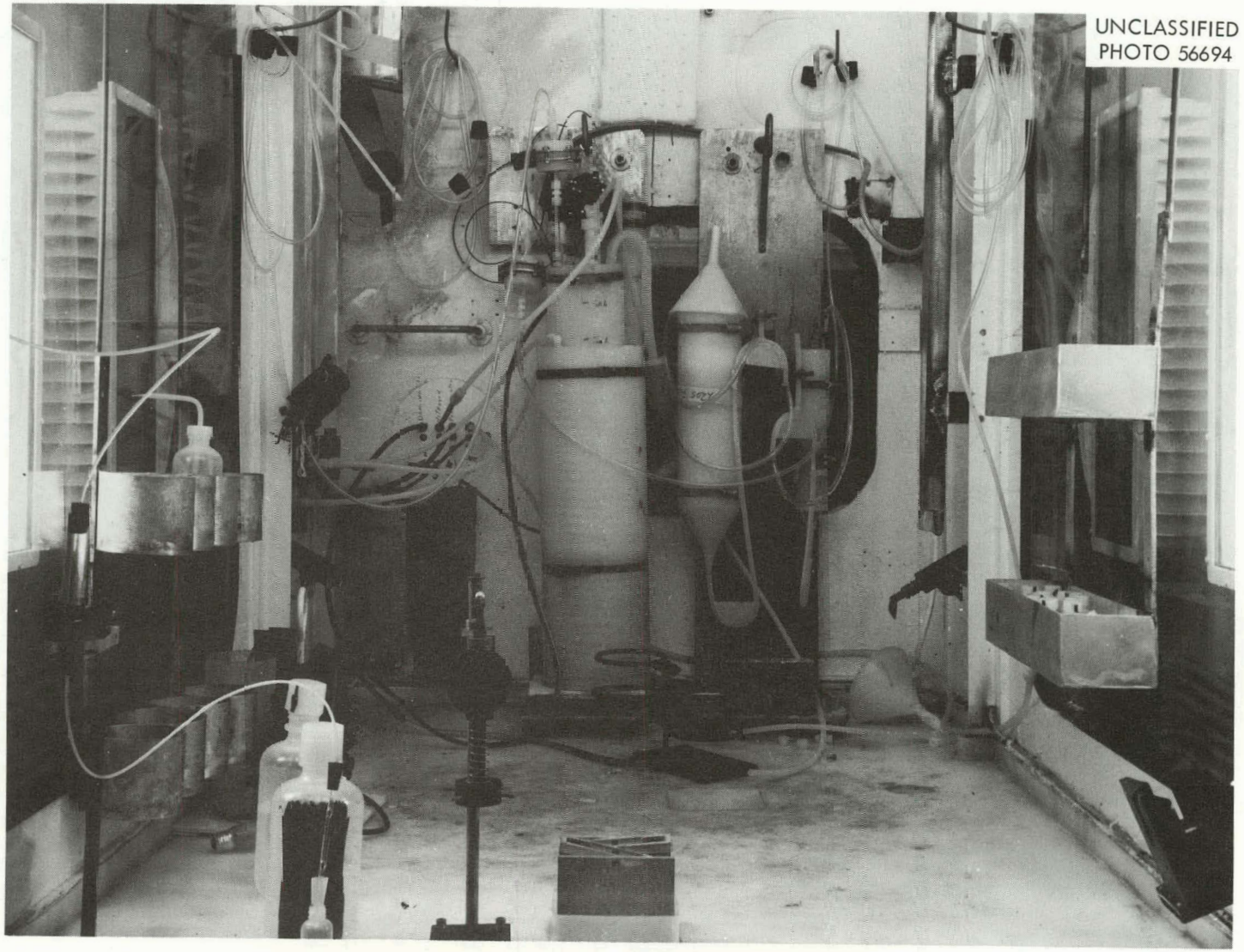

Fig. 8.3. U-232 process equipment, cell 3 Bldg. 4507.

THIS PAGE

WAS INTENTIONALLY

LEFT BLANK

ORNL-3290
UC-10 – Chemical Separations Processes
for Plutonium and Uranium
TID-4500 (17th ed.)

INTERNAL DISTRIBUTION

1. C. E. Larson
2. Biology Library
3-4. Central Research Library
5. ORNL - Y-12 Technical Library, Document Reference Section
6. Reactor Division Library
7. Laboratory Shift Supervisor
8-27. Laboratory Records Department
28. Laboratory Records, ORNL R.C.
29. A. M. Weinberg
30. J. A. Swartout
31. M. J. Skinner
32. J. P. Murray (K-25)
33. R. G. Jordan (Y-12)
34. E. H. Acree
35. G. M. Adamson
36. E. D. Arnold
37. P. S. Baker
38. R. D. Baybarz
39. C. E. Bettis
40. G. B. Berry
41. J. E. Bigelow
42. R. E. Biggers
43. R. E. Blanco
44. A. L. Boch
45. E. G. Bohlmann
46. B. F. Bottenfield
47. E. J. Breeding
48. J. C. Bresee
49. K. B. Brown
50. P. E. Brown
51. W. D. Burch
52. T. A. Butler
53. A. E. Cameron
54. W. L. Carter
55. A. Chetham-Strode
56. J. M. Chilton
57. J. H. Cooper
58. L. T. Corbin
59. G. A. Cristy
60-61. F. L. Culler
62. J. E. Cunningham
63. F. L. Daley
64. J. L. English
65. D. E. Ferguson
66. R. G. Gilliland
67. H. E. Goeller
68. H. B. Graham
69. J. C. Griess
70. W. R. Grimes
71. P. A. Haas
72. J. P. Hammond
73. F. L. Hannon
74. J. C. Hart
75. D. M. Hewett
76. P. R. Kasten
77. M. T. Kelley
78. C. E. Lamb
79. R. E. Leuze
80. M. H. Lloyd
81. A. L. Lotts
82. T. S. Mackey
83. F. L. Moore
84. W. R. Musick
85. P. D. Neumann
86. J. P. Nichols
87. F. L. Peishel
88. M. K. Preston
89. S. A. Rabin
90. R. H. Rainey
91. S. J. Rimshaw
92. R. A. Robinson
93. H. T. Russell
94. A. D. Ryon
95. J. L. Scott
96. G. M. Slaughter
97. W. C. Thurber
98. T. L. Trent
99. W. E. Unger
100. V. C. A. Vaughen
101. C. D. Watson
102. Boyd Weaver
103. G. A. West
104. M. E. Whatley

105. J. C. White
106. W. R. Whitson
107. O. O. Yarbro
108. D. L. Katz (consultant)
109. J. J. Katz (consultant)
110. T. H. Pigford (consultant)
111. H. Worthington (consultant)

EXTERNAL DISTRIBUTION

112. R. I. Deaderick, Union Carbide Nuclear Company (ORGDP)
113. R. B. Martin, Oak Ridge Operations Office
114. D. R. Miller, U.S. Atomic Energy Commission, Washington
115. L. H. Jackson, Oak Ridge Operations Office
116. J. Vanderyn, U.S. Atomic Energy Commission, Washington
117. C. W. J. Wende, Savannah River Operations Office
118. Division of Research and Development, AEC, ORO
119-626. Given distribution as shown in TID-4500 (17th ed.) under Chemical Separations Processes for Plutonium and Uranium category (75 copies - OTS)